

The Texas Medical Center Library

DigitalCommons@TMC

---

The University of Texas MD Anderson Cancer  
Center UTHealth Graduate School of  
Biomedical Sciences Dissertations and Theses  
(Open Access)

The University of Texas MD Anderson Cancer  
Center UTHealth Graduate School of  
Biomedical Sciences

---

8-2017

## GSK3B regulates epithelial-mesenchymal transition and cancer stem cell properties and is a novel drug target for triple-negative breast cancer

Geraldine Vidhya Raja

Follow this and additional works at: [https://digitalcommons.library.tmc.edu/utgsbs\\_dissertations](https://digitalcommons.library.tmc.edu/utgsbs_dissertations)



Part of the [Life Sciences Commons](#), and the [Medicine and Health Sciences Commons](#)

---

### Recommended Citation

Raja, Geraldine Vidhya, "GSK3B regulates epithelial-mesenchymal transition and cancer stem cell properties and is a novel drug target for triple-negative breast cancer" (2017). *The University of Texas MD Anderson Cancer Center UTHealth Graduate School of Biomedical Sciences Dissertations and Theses (Open Access)*. 806.

[https://digitalcommons.library.tmc.edu/utgsbs\\_dissertations/806](https://digitalcommons.library.tmc.edu/utgsbs_dissertations/806)

This Dissertation (PhD) is brought to you for free and open access by the The University of Texas MD Anderson Cancer Center UTHealth Graduate School of Biomedical Sciences at DigitalCommons@TMC. It has been accepted for inclusion in The University of Texas MD Anderson Cancer Center UTHealth Graduate School of Biomedical Sciences Dissertations and Theses (Open Access) by an authorized administrator of DigitalCommons@TMC. For more information, please contact [digitalcommons@library.tmc.edu](mailto:digitalcommons@library.tmc.edu).

The  
**TMC LIBRARY**  
Health Sciences Resource Center

**GSK3 $\beta$  REGULATES EPITHELIAL-MESENCHYMAL  
TRANSITION AND CANCER STEM CELL PROPERTIES AND  
IS A NOVEL DRUG TARGET FOR TRIPLE-NEGATIVE  
BREAST CANCER.**

by

*Geraldine Vidhya Raja, MS.*

APPROVED:

-----  
Sendurai Mani, Ph.D.  
Advisory Professor

-----  
Joya Chandra, Ph.D.

-----  
Jonathan Kurie, MD.

-----  
Zahid Siddik, Ph.D.

-----  
Rama Soundararajan, Ph.D.

APPROVED:

-----  
Dean, The University of Texas  
MD Anderson Cancer Center UTHHealth Graduate School of Biomedical Sciences

**GSK3 $\beta$  REGULATES EPITHELIAL-MESENCHYMAL  
TRANSITION AND CANCER STEM CELL PROPERTIES AND  
IS A NOVEL DRUG TARGET FOR TRIPLE-NEGATIVE  
BREAST CANCER.**

A

DISSERTATION

Presented to the Faculty of

The University of Texas

MD Anderson Cancer Center UTHealth

Graduate School of Biomedical Sciences

in Partial Fulfillment

of the Requirements

for the Degree of

DOCTOR OF PHILOSOPHY

by

Geraldine Vidhya Raja, MS.  
Houston, Texas

August, 2017

Dedicated to my husband who has been my pillar of support, for his unwavering faith in me even when I did not and for seeing me through all my frustrations and without whom I could not have withstood the rigors of Ph.D.

## Acknowledgement

After I finished my Masters, I knew Ph.D. was the natural next step in my career but little did I know that Ph.D. is not a step but a journey. Now that the end is in sight, I would like to take a moment to express my gratitude to all the people who have guided, and supported me and served as beacons of hope throughout this journey.

First and foremost, I would like to express my deepest gratitude to my mentor, Dr. Sendurai Mani, who gave me the opportunity to work in his lab and on his projects. He was always there whenever I needed him. He has been a very understanding and supportive mentor throughout my Ph.D. and I really appreciate all that he has done for me. I would also like to thank my committee members, Dr. Joya Chandra, Dr. Rama Soundararajan, Dr. Elsa Flores, Dr. Jonathan Kurie and Dr. Zahid Siddik for their constant guidance and support.

Next, I would like to convey my vote of thanks to my lab family. Each and every lab member has been instrumental in making my time in Mani Lab a wonderful and memorable one. A special thanks to Dr. Petra Den Hollander and Dr. Rama Soundararajan for reading and editing my thesis and for being my scientific and career advisors. I would also like to extend my thanks to all the post-docs in the lab, present and past, Dr. Joseph Taube, Dr. Tapasree Roysarkar, Dr. Mike Pietila, Dr. Anurag Paranjape, Dr. Jenaro Garcia-Huidobro and Dr. Robiya Joseph for their guidance and support. I also have a very close friend in Esmeralda Ramirez-Pena who has been a wonderful companion as we navigated through Ph.D. together. Ms. Neeraja Bhangre, Dr. Rebeca Romero Aburto, Ms. Vinita Shivakumar, Ms. Yvette Gonzales, Dr. Saradhi Mallampati and Dr. Nathalie Sphyris have all been an integral part of this journey. Also a special thanks to Ms. Barbara Sadeghi who has been a very gracious and helpful person, always greeting me with

a smile and helping me whatever was needed. I really appreciate ITERT for being so student oriented and going out of the way to help trainees forge a career. I would also like to take this opportunity to thank Dr. Jeffrey Chang, who is an excellent teacher and very patient with me while I tried my hand at Bioinformatics.

It has been an honor and pride, being a part of GSBS and the cancer biology program. I am grateful to Ms. Bunny Perez, Ms. Joy Lademora and Ms. Lily Agustino for their constant support and guidance. I would like to thank the school for admitting me and making my dream come true.

Finally, my wonderful family has stood by me, supported me and tolerated me through all these years and their love for me has been by driving force. A heartfelt thank you to all my friends at UT housing, who were with me when I need anything and are our family away from home. Without them and my precious labmates, I could not have survived living alone with a kid.

So just like you need a village to bring up a baby, you need a whole world to nurture a doctoral candidate. Indeed I am blessed to have a whole loving community looking out for me and helping me realize my dreams and all I can say in return is THANK YOU from the bottom of my heart!!! God bless you all for all that you have done for me!

# Abstract

## **GSK3 $\beta$ regulates Epithelial-Mesenchymal-Transition and Cancer Stem Cell properties and is a novel drug target for Triple-Negative Breast Cancer.**

Geraldine Vidhya Raja, MS.

Advisory Professor: Sendurai Mani, Ph.D.

Triple-Negative breast cancers (TNBCs) are highly aggressive and lack the expression of Estrogen Receptor (ER), Progesterone Receptor (PR) as well as Human Epidermal Growth Factor Receptor (HER2). Consequently, patients diagnosed with TNBCs have poor overall- and disease-free survival rates compared to other subtypes of breast cancer due to lack of targeted therapies as well as *de novo* or acquired chemoresistance, disease recurrence, and lack of targeted therapy. Hence it is critical to identify novel targets to treat TNBCs. TNBCs are characterized by the presence of mesenchymal-like cells, which is indicative that EMT (epithelial-mesenchymal-transition) plays an important role in the progression of this disease. EMT has also been implicated in chemoresistance, tumor recurrence and generation of cancer stem cells (CSCs). The Wnt signaling pathway has been determined to be one of the major players in EMT and CSCs. Therefore, we analyzed patient survival data to determine a correlation between the expression of Wnt components and overall survival. Of the several possible players, higher expression of GSK3 $\beta$  correlated with poorer overall patient survival. In support of this observation, we identified a GSK3 $\beta$  inhibitor, BIO, in a drug screen as one of the most potent inhibitors of EMT. Since TNBCs are enriched with mesenchymal-like cells, we treated mesenchymal cell lines with the GSK3 $\beta$  inhibitors and found that GSK3 $\beta$  inhibitors were among the few drugs that could selectively kill mesenchymal-like TNBC cells compared to epithelial-like breast cancer cells. To determine if GSK3 $\beta$  inhibitors specifically target mesenchymal-like cells by affecting the CSC population, we employed the mammosphere assay and analyzed the CD44<sup>hi</sup>/24<sup>lo</sup> population of

these cell lines. We found that GSK3 $\beta$  inhibitors indeed decreased the CSC properties of the mesenchymal-like cell lines, and also decreased the expression of mesenchymal markers. Inhibition of GSK3 $\beta$  decreased the migratory properties suggesting that the inhibition of EMT by GSK3 $\beta$  inhibitor could contribute to the inhibitory effect of GSK3 $\beta$  on the migratory potential of the mesenchymal-like cells. Taken together, our studies demonstrate that GSK3 $\beta$  is a novel target for TNBCs and suggest that the GSK3 $\beta$  inhibitors could serve as selective inhibitors of EMT and CSC properties of the aggressive TNBCs, and may hence be ideal for combination treatment with standard-of-care drugs for women with this deadly disease.



# GSK3 $\beta$ REGULATES EPITHELIAL-MESENCHYMAL TRANSITION AND CANCER STEM CELL PROPERTIES AND IS A NOVEL DRUG TARGET FOR TRIPLE-NEGATIVE BREAST CANCER.

## Contents

<b>Acknowledgement .....</b>	<b>iv</b>
<b>Abstract .....</b>	<b>vi</b>
<b>List of tables.....</b>	<b>xi</b>
<b>List of figures .....</b>	<b>xii</b>
<b>Chapter 1 – TNBC and the potential role of EMT, CSCs and GSK3<math>\beta</math>.....</b>	<b>1</b>
1A. Introduction to Triple-Negative Breast Cancer (TNBC).....	1
1A.a. Absence of targeted therapy for TNBC .....	3
1A.b. Contribution of tumor relapse and chemoresistance to TNBC-related fatality.....	4
1B. TNBCs are highly metastatic.....	6
1C. Epithelial-Mesenchymal-Transition is a vital player in the chemoresistance, tumor relapse and metastasis of TNBCs.....	11
1C.a. Regulation of EMT.....	13
1C.b. Wnt signaling has been implicated in EMT and CSC enriched TNBCs.....	19
1D. Role of Glycogen Synthase Kinase 3 $\beta$ in tumor progression.....	21
1E. Role of GSK3 $\beta$ in cellular processes vital to metastasis .....	26
1E.a. Cell Cycle .....	26
1E.b. Apoptosis.....	27
1E.c. Migration.....	28
1E.d. Contribution of GSK3 $\beta$ to breast cancer. ....	31
1F. GSK3 $\beta$ , EMT and cancer stem cells. ....	33
<b>Chapter 2 – Statement of objective.....</b>	<b>35</b>
2A. Knowledge gap .....	35

2B. Hypothesis .....	35
2C. Study questions – Aims .....	36
<b>Chapter 3 – Experimental Approaches .....</b>	<b>41</b>
<b>Chapter 4 – Aim 1 – Determine if GSK3<math>\beta</math> is upregulated in breast cancer and if this upregulation has clinical significance. ....</b>	<b>50</b>
4A. GSK3 $\beta$ is upregulated in breast cancer .....	50
4B. Elevated expression of GSK3 $\beta$ correlates with worse overall survival among TNBC patients.....	51
<b>Chapter 5 – Aim 2 – Investigate the relationship between GSK3<math>\beta</math> and Epithelial-Mesenchymal Transition (EMT) and cancer stem cells (CSCs) in TNBCs .....</b>	<b>58</b>
5A. Small molecule screen indicates that BIO is a potential candidate capable of decreasing mesenchymal phenotype.....	58
5B. GSK3 $\beta$ inhibitors decrease the mesenchymal properties of the stem cell-enriched mesenchymal-like cell lines. ....	76
5C. Inhibition of GSK3 $\beta$ decreases the migratory properties of the cells with mesenchymal phenotype by inhibiting the induction of EMT.....	80
5D. GSK3 $\beta$ inhibitors decrease the stem cell properties of mesenchymal-like cells.....	84
5E. shRNA to GSK3 $\beta$ decreases the CSC properties of cells with mesenchymal attributes. ....	90
5F. GSK3 $\beta$ knock-out MEFs show decreased ability to form spheres. ....	92
5G. GSK3 $\beta$ inhibitors alter the CD24/44 profile of the mesenchymal-like cells.....	93
5H. Cells with mesenchymal phenotype are more sensitive to GSK3 $\beta$ as compared to their epithelial counterparts.....	95
<b>Chapter 6 – Aim 3 – Test if GSK3<math>\beta</math> inhibitor can be effectively used <i>in vivo</i> to target CSC-enriched breast cancers. ....</b>	<b>101</b>

GSK3 $\beta$ inhibitors did not inhibit tumor size and metastatic potential of mesenchymal cells <i>in vivo</i> .....	101
<b>Chapter 7 - Conclusions</b> .....	106
<b>Chapter 8 – Discussion and future directions</b> .....	109
<b>References</b> .....	116
<b>Vita</b> .....	128

## List of tables

Table 1: Wnt signaling molecules and their Hazard Ratios	54
Table 2: List of the drugs from the Sellekchem small molecule library that were tested in with their commonly used acronyms in parenthesis.	61
Table 3: Drug Screen Results	74

## List of figures

Figure 1 – Classification of Triple-Negative breast cancers (TNBCs).	3
Figure 2 – Epithelial-mesenchymal-transition (EMT).	12
Figure 3 – Schematic depiction of the study.	37
Figure 4 – GSK3 $\beta$ is significantly upregulated in breast cancer.	51
Figure 5 - Higher GSK3 $\beta$ expression correlates with worse overall breast cancer survival.	53
Figure 6 – Circos plot of the hazard ratios of components of Wnt signaling pathway.	55
Figure 7 – The upregulation of GSK3 $\beta$ significantly correlated with worse survival of TNBCs.	57
Figure 8 – GSK3 $\beta$ is the only signaling molecule in the Wnt signaling pathway that has a high hazard ratio and a significant p-value.	58
Figure 9 – MDA MB 231 reporter cell line.	60
Figure 10 – CUDC1 and BIO are capable of inhibiting EMT.	76
Figure 11- GSK3 $\beta$ inhibitors decrease the expression of mesenchymal markers.	80
Figure 12 – GSK3 $\beta$ inhibitors decrease the expression of mesenchymal markers.	81
Figure 13 – GSK3 $\beta$ inhibitors significantly inhibit the ability of the highly migratory cells to close the wound.	83
Figure 14 – Treatment with TWS119, inhibited the expression of FOXC2 at the wound site of HMLE cells and thereby inhibits wound healing and migration.	85
Figure 15 – The GSK3 $\beta$ inhibitor BIO decreases mammosphere forming potential of mesenchymal cells.	87

Figure 16 – GSK3 $\beta$ inhibitors decrease the mammosphere forming ability of the mesenchymal cells in a dose dependent manner.	89
Figure 17 – Pretreatment with GSK3 $\beta$ inhibitors decreases the mammosphere forming ability, but not proliferation of the mesenchymal cells.	91
Figure 18 – Knockdown of GSK3 $\beta$ by shRNA.	92
Figure 19 – Knockdown of GSK3 $\beta$ decreases the mammosphere forming capability of the mesenchymal cells.	93
Figure 20 – GSK3 $\beta$ knockout MEFs have decreased sphere forming potential, but not proliferation, as compared to the wildtype MEFs.	94
Figure 21 – GSK3 $\beta$ inhibitors increase the CD24 positive population in mesenchymal cells.	95
Figure 22 – Mesenchymal cells are more sensitive to GSK3 $\beta$ inhibitors as compared to epithelial cells.	97
Figure 23 – BIO and CP-673451 selectively kill mesenchymal cells whereas PD selectively kills epithelial cells.	98
Figure 24 – GSK3 $\beta$ inhibitors selectively kills mesenchymal cells.	100
Figure 25 – GSK3 $\beta$ inhibitor TWS119 with HMLER-Snail cells <i>in vivo</i> .	103
Figure 26 – GSK3 $\beta$ inhibitor TWS119 with 4T1 cells <i>in vivo</i> .	105
Figure 27 – Immunohistochemistry of xenograft tumors treated with TWS119	106

## **List of abbreviations**

APC – Adenomatous Polyposis Coli

APS – Ammonium Persulfate

Arf6 – ADP Ribosylation Factor 6

ATF3 – Activating Transcription Factor

ATP – Adenosine triphosphate

BCL9/LGS – B-cell Lymphoma/Legless

bHLH – beta Helix Loop Helix

BIO – 6-Bromoindirubin-3'-oxime

BL – Basal-like

BMP – Bone Morphogenetic Protein

B-TRCP – Beta-Transducin Repeats-Containing Protein

C/EBP – CCAAT-Enhancer-Binding Proteins

CD – Cell Differentiation marker

CDH – Cadherin

CDK – Cyclin Dependant Kinase

CDK – Cyclin Dependent Kinase

CHIP – Carboxy Terminus of Hsc70 Interacting Protein

CK – Casein Kinase

CMGC – Cyclin Dependent Kinase (CDK), Mitogen Activated Protein Kinase (MAPK), Glycogen Synthase Kinase (GSK) and CDC-like Kinase (CLK)

COX – Cyclooxygenase

CREB – cAMP response element binding protein

CSC – Cancer stem cell

CSF – Colony Stimulating Factor

CTBP – c-terminal Binding Protein

CTC – Circulating Tumor Cell

CXCR – C-X-C motif Chemokine Receptor

DAB2 – Disabled 2

DKK – DICKKOPF

DNA – Deoxyribonucleic Acid

Dvl – Disheveled

E2F – E2 Factor

ECM – Extracellular Matrix

EGF – Epidermal growth factor

EGFR – Epidermal growth factor receptor

EMT – Epithelial-Mesenchymal-Transition

EndMT – Endothelial-Mesenchymal-Transition

ER - Estrogen Receptor



EREG – Epiregulin

EZH2 – Enhancer of Zeste Homolog 2

FACS – Fluorescence assisted cell sorting

FAK – Focal Adhesion Kinase

FAK – Focal Adhesion Kinase

FGF – Fibroblast Growth Factor

Fzd – Frizzled

G1 – Phase – Gap 1 Phase

G2 – Phase – Gap 2 Phase

GAP – GTPase Activating Protein

GSK3 $\alpha$  – Glycogen synthase kinase 3  $\alpha$

GSK3 $\beta$  – Glycogen synthase kinase 3  $\beta$

GSKIP – Glycogen Synthase Kinase Interacting Protein

HDACs – Histone Deacetylases

HER2 – Human Epidermal Growth Factor Receptor

HGF – Hepatocyte growth factor

HGFR – Hepatocyte Growth Factor Receptor

HIF1A – Hypoxia Induced Factor 1 A

HMGA2 – High Mobility Group AT-Hook 2

HMLE – Human Mammary Epithelial cells

hnRNPE1 – Heterogeneous Nuclear Ribonucleoprotein E1

HR – Hazard Ratio

ID – Inhibitor of Differentiation

IGF – Insulin-like Growth Factor

IGFR – Insulin-like Growth Factor Receptor

IL – Interleukin

ILEI – Interleukin –like EMT Inducer

IM - Immunomodulatory

JNK – c-Jun N-Terminal Kinase

KRT - Keratin

LAR – Luminal Androgen Receptor

LATS2 – Large Tumor Suppressor 2

LOX – Lysyl Oxidase

LRP – Low Density Lipoprotein Receptor related Protein

LSD1 – Lys-Specific Demethylase 1

M Phase – Mitotic Phase

MAPK – Mitogen Activated Protein Kinase

MET – Mesenchymal-Epithelial-Transition

miR – Micro RNA

MMP – Matrix Metalloprotease

MRTF – Myocardin Related Transcription Factor

MSL – Mesenchymal stem-like

MTOC – Microtubule Organizing Center

NFAT – Nuclear Factor Activated T-Cells

NFkB – Nuclear Factor kappa-light-chain-enhancer of activated B cells

PAGE – Polyacrylamide Gel Electrophoresis

PAK – p21 Activated Kinase

PAR6 – Partitioning Defective 6

pCR – Pathological Complete Response

PDGF – Platelet Derived Growth Factor

PGAP3 - Post-GPI Attachment to Proteins 3

PI3K – Phosphoinositol 3 Kinase

PKA – Protein Kinase A

PKD1 – Protein Kinase D 1

PP1 – Protein Phosphatase 1

PP2A – Protein Phosphatase 2A

PR – Progesterone Receptor

PRC2 – Polycomb Repressive Complex II

PTEN – Phosphatase and Tensin Homolog

PYK2 – Proline – rich Tyrosine Kinase 2

qRT-PCR – Quantitative Real Time Polymerase Chain Reaction

Rb – Retinoblastoma

RNA – Ribonucleic Acid

S Phase – Synthesis Phase

SCP1 – Small c-terminal domain Phosphatase

SDF – Stromal cell Derived Factor

SDS – Sodium Dodecylsulfate

SMAD – Suppressor Mother Against Decapentaplegic

SOX – Sry Box

STAT3 – Signal Transducer and Activator of Transcription 3

Sufu – Suppressor of Fused

SUV39H1 – G9a and Suppressor of variegation 3-9 Homolog 1

SWI/SNF – Switch/Sucrose non-fermentable

TGF $\beta$  – Transforming Growth Factor  $\beta$

TIC – Tumor Initiating Cell

TNBC – Triple-Negative Breast Cancer

TSC – Tuberous Sclerosis Complex

TrkB - Tropomyosin receptor kinase B (TrkB)

VEGF – Vascular Endothelial Growth Factor

# **Chapter 1 – TNBC and the potential role of EMT, CSCs and GSK3 $\beta$ .**

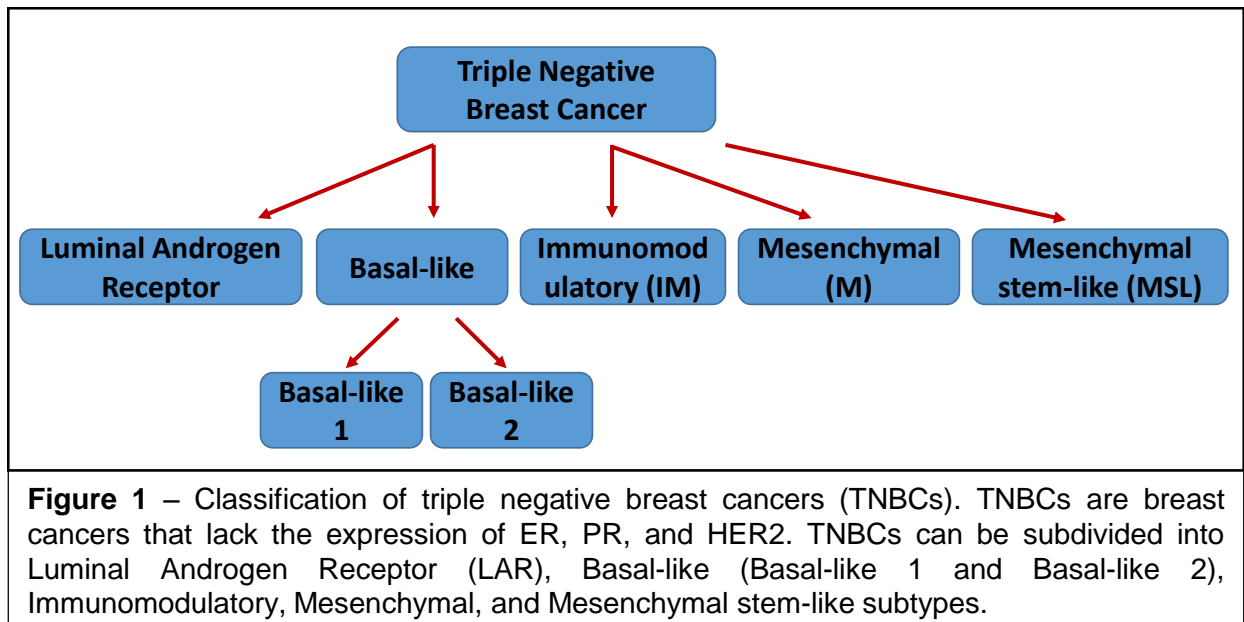
## **1A. Introduction to Triple-Negative Breast Cancer (TNBC).**

Breast cancer is one of the leading causes of death among women and is second only to lung cancer. Breast cancer affects 1 in 8 women in the United States [1]. Breast cancers are molecularly classified into various subtypes. Primarily, breast cancers are classified based on the expression of Estrogen Receptor (ER), Progesterone Receptor (PR) and ERBB2 (HER2) using immunohistochemical analysis. The Triple-Negative Breast Cancers (TNBCs) are breast cancers that do not express elevated levels of ER, PR or HER2 genes. TNBCs account for 15-20% of the newly diagnosed breast cancer cases. Most of the TNBCs are diagnosed in young patients and the disease is at an advanced stage by the time it is diagnosed [2]. TNBC tumors are usually larger in size, are of higher grade, and have lymph node involvement at the time of diagnosis [3]. Immunohistochemically, there is no specific marker to pinpoint a TNBC, rather the diagnosis of TNBC depends on the absence of the known markers, ER, PR and HER2.

An additional level of complexity that accompanies TNBCs, is the presence of intra-tumoral and inter-patient heterogeneity [4]. TNBCs carry about 1.68 mutations per mega base of coding regions which is approximately 60 mutations per tumor [4, 5]. With that being said, the mutation burden is not uniform throughout the tumor and this is often accompanied by copy number alterations in genes involved in several different pathways. Mutations are random events and therefore, no two patients have the same mutations. So while all the TNBCs have similar gene expression profile, there is high inter-patient heterogeneity. The genetic composition of the tumors and thus their response to treatment is completely different from one patient to another.

TNBCs are classified as a single subtype, but the emergence of molecular profiling and other “omics” technologies have shown a large amount of heterogeneity among these tumors. Of these different breast cancer subtypes, the basal-like cancers mostly overlap with the TNBCs, but despite the overlap are not synonymous [2]. The term basal-like indicates that these cancer cells express genes like KRT5, KRT14 and KRT17 and EGFR that are normally expressed by normal basal or myoepithelial cells [4]. More than 90% of basal-like breast cancers are TNBCs. Though basal-like tumors have a high level of heterogeneity, they have distinct molecular characteristics compared to other TNBCs [4]. In order to investigate the heterogeneity that exists in TNBC, the histopathological characteristics and gene expression profiles of 97 TNBCs were analyzed and it was found that the hierarchical cluster analysis also showed the presence of five distinct subgroups [2, 6-8]. Another group investigated the gene expression profiles of 587 TNBCs. In these analyses 6 different TNBC subtypes were identified: 2 basal-like-related subgroup (basal-like 1 (BL1) and basal-like 2 (BL2)), 2 mesenchymal-related subgroups (mesenchymal (M) and mesenchymal stem-like (MSL)), one immunomodulatory subgroup (IM) and luminal androgen receptor group (LAR) [3, 4, 9] (Figure 1).

In summary, TNBCs are highly aggressive breast cancers that have lower overall and disease free survival rates as compared to the other types of cancer. The main reasons for the lower survival rates are – absence of targeted therapy, tumor recurrence and chemoresistance, and metastasis.



#### 1A.a. Absence of targeted therapy for TNBC

Patients with TNBCs have relatively poorer prognosis as compared to other subtypes of breast cancer. Currently chemotherapy is the only treatment option that is available for patients with TNBCs irrespective of their stage [4], due to the lack of targeted treatment. [4]. As previously mentioned, TNBC tumors do not express ER, PR or HER2 genes, all of which are molecular targets of therapeutic agents used to treat breast cancer. Due to the extensive genetic and molecular profiling studies several different targetable mutations have been identified [4]. In addition to the mutations in P53 and PIK3CA gene, other actionable targets such as deletions of *PTEN* or *INPP4B* genes and amplifications such as *KRAS*, *BRAF*, *EGFR*, *FGFR1*, *FGFR2*, *IGFR1*, *KIT* and *MET* have been identified [4]. However, the actionability of these targets is yet to be established because each tumor has multiple mutations which play major roles in several vital intertwined pathways, thus making it difficult to predict the outcome of targeting these mutations. Additionally, due to the intra-tumoral heterogeneity within TNBCs, a target that may affect one

clonal population may not affect another clonal population thus giving rise to chemoresistance or lack of response to targeted therapies.

#### *1A.b. Contribution of tumor relapse and chemoresistance to TNBC-related fatality*

In addition to lack of targeted therapy, the factor that increases the lethality of the TNBCs is the risk of tumor recurrence and emergence of chemoresistance. Extensive research has rendered breast cancers curable as long as it is discovered at an early stage. However, many a times the disease-free survival is disrupted by the reappearance of the tumor at the primary or a secondary site. Recurrence is one of the major reasons for breast cancer-related fatalities [10, 11]. The rate of recurrence of breast cancer is estimated to be 15-20% [12, 13]. Of these, 60-80% of tumor recurrences occur within 3 years, but the chances of recurrence exist up to 20 years after the diagnosis of the disease [9]. Therefore several studies have been undertaken to discover a predictor or pattern that might indicate the probability of recurrence and thus aid in preventing the relapse of the disease [10].

In an effort to predict recurrence, the correlation between subtype of tumor and the disease relapse has been examined. It has been observed that the rate of recurrence is higher for the ER-negative subtype of breast cancer in the first 5 years following the diagnosis and treatment [10, 14]. As discussed earlier, the aggressive TNBCs have a higher rate of recurrence both at the primary and secondary site as compared to tumors that are ER-positive. It was also found that the ER+ and PR+ patient had lower rate of tumor recurrence as compared to TNBCs [10, 15]. These studies indicate the importance of molecular classification of tumors in the clinics both for the treatment and for taking preventive measures.



There are mainly 2 hypotheses to explain tumor recurrence. The first hypothesis is that the recurrence exists before the primary diagnosis and may have been detected as a multifocal tumor. The second hypothesis is the wound oncogene wound healing (WOWH) hypothesis [10, 16]. The WOWH hypothesis proposes that there is an intricate link between stress and oncogenesis. The stress could be either physical like radiation, chemical, like carcinogens or biological like inflammation, trauma, presence of pre-cancerous lesions, oncogenes and the progression of cancer [16]. When a tumor is diagnosed and treated, the region of treatment is damaged and faces a harsh environment followed by inflammation [10, 16]. This could in turn aggravate an existing injured cell to undergo transformation or injure new cells and create a new wound. Thus, depending on the presence of a pre-existing wound or creation of a new wound and the different insults weathered by the body in question, the tumor recurs [10, 16].

The causes of breast cancer recurrence are still unknown but following are the molecular factors which have been found to contribute to the tumor recurrence including epithelial-mesenchymal-transition (EMT), cancer stem cells (CSCs), Wnt signaling, circulating tumor cells (CTCs) and few other factors such as  $\beta$ 1 Integrin, notch signaling, hedgehog signaling, and miRNAs [12]. Until a clear insight is gained into the mechanism of breast cancer recurrence, it would be impossible to develop targeted therapies to prevent breast cancer recurrence. However, few drugs such as bisphosphonates and aromatase inhibitors and natural compounds such as curcumin, sulforaphane, isoflavones, EGCG and resveratrol are being investigated for their potency in preventing breast cancer recurrences [10, 17].

## 1B. TNBCs are highly metastatic

As mentioned above, metastasis and not the primary tumor is the principle cause of cancer-related fatalities. More than 90% of cancer-related deaths are due to the metastasis and therefore it is imperative that we find a means of disrupting or reverting this lethal process [18, 19]. Metastasis is a cascade of steps in which cancer cells from the primary tumor dissociate, invade the surrounding connective tissue and intravasate into the vasculature to enter circulation. These tumor cells, now called the circulating tumor cells (CTCs), find anchor on the endothelium and extravasate to enter the secondary site where they form micrometastases. These subsequently establish a favorable niche where they proliferate to form macrometastases which is what is detected as the metastatic lesion [20]. Usually, these metastatic lesions are formed in vital organs or regions that are difficult to surgically resect thus further endangering the life of the patient. TNBCs have 4 times more the tendency to metastasize to the visceral organs as compared to the other subtypes of breast cancers [21, 22]. Each step of the metastatic cascade is essential for the cells to successfully metastasize and the ability of the cell to complete each of these steps determines its metastatic potential. Therefore each step serves as an opportunity to impede and halt the process. Understanding these processes in depth is vital for reducing the metastatic potential of the cancer cells. The steps of the metastatic cascade are as follows;

**Invasion** - Normally, the tumor is comprised of epithelial cells that have polarity and a basement membrane along with providing the architectural support also provides signaling molecules that help the cells determine and retain their polarity [18, 23]. When the cells try to break free from the bonds and polarity, the signaling and the basement membrane serve as a barrier [18]. In the mammary gland, the myoepithelial cells and the alterations in the stiffness of the connective tissue and several other factors serve as a deterrent for the invasion of the basement membrane [18, 24, 25]. The invading cancer cells might utilize either the EMT-mediated mesenchymal program or the amoeboid invasion program [18, 26]. The induction of EMT results in the loosening of the

cell-cell bonds and also enhances the secretion of matrix metalloproteases (MMPs) and other enzymes that aid in the breakdown of the basement membrane and the connective tissue limiting the tumor mass. Once the cells have breached the basement membrane, they come in contact with the stroma. The tumor-associated stroma may be inflamed or trying to heal the wound and depending on the state of the stroma might contain fibroblasts, endothelial cells, mesenchymal stem cells, adipocytes and immune cells. This creates a positive feedback loop where the invading tumor cells condition the stroma to aid in metastasis and the inflamed stroma promotes invasion of the cancer cells. TNBCs are associated with the presence of invasive edges and the presence of lymphocytic infiltrates at these edges [27].

**Intravasation** – Intravasation is a process, where the cancer cells leave the primary site and enter the 2 main circulatory systems of our body, the lymphatic system and the vasculature [18]. While the cells that enter the lymphatic system mostly serve for diagnostic purposes, the cells that enter the vascular circulation are the ones that are primed to metastasize to a secondary distant location [18, 19]. When the tumor cells intravasate, they and the assisting stromal and immune cells secrete molecules such as transforming growth factor- $\beta$  (TGF $\beta$ ), Epidermal growth factor (EGF) and colony-stimulating factor-1 (CSF-1) that alter the pericytes and weaken the trans-endothelial barrier and allow the cells to invade [18, 28]. The other mechanism is the formation of new blood vessels. As the tumors grow in size, they secrete vascular endothelial growth factor (VEGF), MMP-1 and 2, cyclooxygenase-2 (COX2), epiregulin (EREG) that stimulate the formation of new blood vessels that serve to supply oxygen and nutrition to the growing tumor [29]. However, this neoangiogenesis leads to the formation of leaky vasculature due to weak endothelial interactions and lack of pericytes which allows the entrance of the tumor cells into circulation [18, 30].

**Circulation** – Once the cancer cells intravasate and enter into circulation, they are known as circulating tumor cells or CTCs. These tumor cells have to survive in the circulation. The first major challenge is that capillaries are smaller in diameter than the tumor cells and this results in CTCs getting trapped in capillaries [18]. The next challenge faced by them is the onset of anoikis. Normal cells are anchorage dependent and when disconnected from the extracellular matrix, anoikis sets in and leads to cell death. However, CTCs avoid anoikis by metabolic reprogramming and upregulating suppressors of anoikis like Tropomyosin receptor kinase B (TrkB) [31-33]. Another theory proposed is that several of the CTCs get trapped in capillaries or exit circulation and extravasate before anoikis could be triggered in cells [18]. The other challenges that the CTCs face are the circulating immune cells and the hemodynamic shear that can lead to the disruption of the cell. In order to overcome these, the CTCs have been found to attach to platelets in circulation and form large emboli that cannot be detected by the immune cells and to tolerate the shear force [34].

**Extravasation** – The CTCs that survive the circulation and get trapped in the capillary beds at different locations have to enter back into the tissues in order to form metastatic lesions. There are mainly 2 ways in which this is achieved. The trapped cells can proliferate and form colonies and these colonies then secrete factors that can help break down the endothelial barrier and provide access to the secondary site of metastasis. The primary tumor cells and the CTCs themselves secrete factors such as angiopoietin-like-4 (Angptl4), EREG, MMPs, VEGF etc. that increase the permeability of the vasculature [35]. Additionally, certain immune cells such as inflammatory monocytes have been known to enhance extravasation of breast cancer cells into the lungs [36].

**Micrometastasis** – The cells that have extravasated have to then adapt to the new microenvironment which is usually different from that of the primary site. However, it has been observed that the micrometastatic niche is primed before the arrival of the cancer cells to the metastatic site [37]. The primary tumor has been found to secrete factors which include Lysyl Oxidase (LOX) [37]. LOX stimulates the production of fibronectin which in turn attracts VEGF receptor-positive hematopoietic progenitor cells [37, 38]. These cells secrete MMPs which breaks down the ECM at the site of future metastasis. The breakdown of the ECM is accompanied by the release of chemoattractants such as stromal cell derived factor 1 (SDF-1) [37]. While these priming processes take place at the site of metastasis, the homing tumor cells also make alterations in their signaling to adapt to the new environment. Breast cancer cells that form micrometastasis in the bone have been observed to activate Src signaling and this promotes cell viability in the bone microenvironment without affecting the homing capacity of these cells. While suppressing Src signaling decreased metastatic lesions in the bone, it did not prevent the same breast carcinoma cells from colonizing the lungs [18, 39].

**Macrometastasis** – Macrometastasis is a process in which the micrometastatic colonies proliferate to form diagnosable colonies. Not all the micrometastatic colonies form macrometastasis. The unfavorable microenvironment can serve as a deterrent for the growth of these colonies. Many of these colonies either die slowly over a long period of time due to lack of favorable stimuli or remain dormant and just stay viable such that there is no alteration in the cell number. In the case of breast cancer, it has been observed that cells that are unable to stimulate Focal Adhesion Kinase (FAK), integrin  $\beta 1$  and Src pathways are unsuccessful in forming metastatic colonies [40-42]. Additionally, absence of stimulating factors in the microenvironment could also contribute to this quiescence. However, some of the factors secreted by the primary tumors may serve as stimulants for the dormant metastatic colonies [43, 44].

Another reason for the inability of the micrometastatic colonies to grow into macrometastases is the low proliferative rate of these cells as compared to the high apoptotic potential of these cells. This has been attributed to the lack of neoangiogenesis in these lesions as a result of which they are deprived of both oxygen and nutrition [45]. One of the means of overcoming these barriers, is by the induction of EMT. As mentioned previously, the cells that have undergone EMT gain stem-like properties which enable them to have immense proliferative and self-renewing potential which aids these cells in the micrometastatic colonies to proliferate and form macrometastatic colonies.

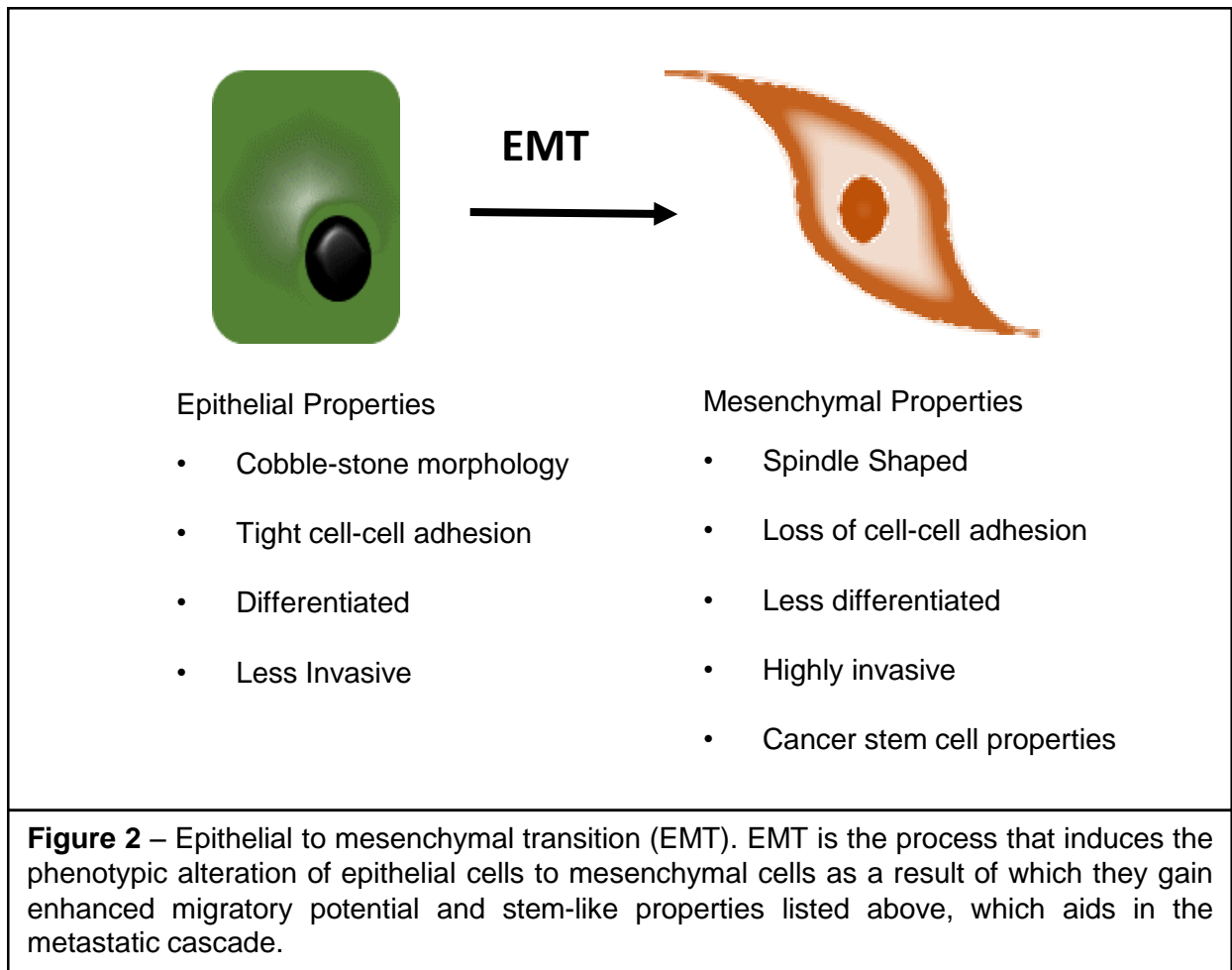
Another factor that determines the ability of the cells to colonize and form metastatic lesions is their ability to turn on the genes required to make them compatible with the microenvironment at the metastatic site. This fact was discovered by Paget when he put forward the seed and soil hypothesis [46]. Not all the cancer cells can survive in all the microenvironments that they home to. Only the ones that are capable of adapting to the new microenvironment survive and colonize the secondary metastatic site. As a proof of this concept, it has been observed that the genetic and epigenetic profile of the breast cancer cells that metastasize to the bone is dramatically different from that of the cells metastasizing to the brain, lung or liver [47-50]. However, the genetic and epigenetic profile is not determined by the destined organ alone. For example, the genetic and epigenetic makeup of the breast cancer cells colonizing the bone is very different from the profile of prostate cancer cells which metastasize to the bone [18].

Due to the high complexity of this cascade, only very few of the cells that are disseminated from the primary tumor actually reach their target and establish macrometastasis. It is these few cells that need to be targeted and inhibited from successfully completing this cascade. One of the crucial events that enhances the metastatic potential of the cancer cells is the process of EMT. Hence, understanding and targeting EMT is essential to inhibit metastasis. In summary, TNBCs

are highly aggressive subtype of breast cancers. This tumor subtype has high similarity to basal-like breast cancers. Due to the absence of targeted therapy, TNBCs are difficult to retreat. These tumors predominantly develop resistance to chemotherapy also develop metastasis at high rate. As these tumors are highly enriched for cells with EMT/CSC properties, targeting EMT may be a potential means of inhibiting TNBCs.

#### 1C. Epithelial-Mesenchymal-Transition is a vital player in the chemoresistance, tumor relapse and metastasis of TNBCs.

Epithelial-mesenchymal-transition is a dynamic process that was initially discovered by Dr.Elizabeth Hay in 1980 [51, 52]. She observed a phenomenon in which the epithelial cells acquire mesenchymal properties in the primitive streak of a chick embryo and named it mesenchymal transformation [51, 52]. This process was later renamed as the epithelial-mesenchymal-transition to reflect its transient nature [52]. During the process of EMT, an epithelial cell which is normally attached to the basement membrane in an apical-basal orientation, gains mesenchymal characteristics such as a spindle-shaped morphology, increased migratory and invasive potential, resistance to apoptosis and senescence and expresses significantly greater amount extra-cellular matrix genes [52, 53] (Figure 2). EMT is a well-established central player in embryonic development, wound healing and tumor progression and as a result a lot of effort has been devoted to unraveling the mechanism and regulation of EMT. In breast cancer, circulating tumor cells (CTCs) isolated from peripheral blood of patients, share several properties with mesenchymal cells indicating that these cells have undergone EMT [53-55]. Furthermore, basal-like and claudin-low breast cancers are transcriptionally similar to mesenchymal cells [56-58].



EMT is also closely linked to cancer stem cells (CSCs) [59]. Cancer stem cells are cells that have unlimited self-renewal potential and are capable of giving rise to both undifferentiated and differentiated daughter cells. FOXC2, a transcription factor was demonstrated to be an important EMT marker as well as an indicator of CSC properties, thus suggesting the EMT and CSCs are intricately linked [59, 60].

All these changes effected by EMT involve a complex cascade of signaling that orchestrates this smooth transition. Several transcription factors, cell surface markers, cytoskeletal organization proteins, and micro-RNAs (miRs) play a pivotal role in choreographing this intricate process.



However, this signaling can be inhibited or reversed which in turn induces the process known as the mesenchymal-epithelial-transition or MET [52]. This ability of the cells to switch back and forth between the epithelial and the mesenchymal phenotype is known as plasticity [52]. The presence of this plasticity in TNBCs enhances their metastatic potential. Understanding the regulation of EMT will facilitate the identification of regulatory nodes that can be targeted to inhibit metastasis of TNBCs.

### *1C.a. Regulation of EMT*

Induction of EMT is accompanied by an alteration in gene expression in order to help the cells gain mesenchymal properties. However, these changes in the gene expression are not uniform and differ depending on the factor inducing EMT and the tissue in which the transition is taking place. While the post-translational modifications disrupt epithelial cell adhesions and polarity, the presence of the epithelial cell adhesion molecules will promote re-assembly of these adhesions. Therefore, in order to prevent *de novo* formation of epithelial cell adhesions and acquisition of polarity, the transcription of these molecules have to be inhibited and replaced with molecules that form mesenchymal adhesions. E-cadherin is repressed in all cells undergoing EMT regardless of the cell type or the EMT-inducing factor [51]. During the cadherin switch, which is considered to be one of the hallmarks of EMT, the expression of N-cadherin is upregulated [53, 61]. N-cadherin connects to the actin cytoskeleton via  $\beta$ -catenin and  $\alpha$ -catenin, forms homotypic interactions with other mesenchymal cells which facilitates migration, and interacts with receptor tyrosine kinases such as PDGF and FGF receptors [62-64].

The composition of the extracellular matrix also undergoes a dramatic change. There is increased expression of mesenchymal ECM molecules such as vimentin and fibronectin and decrease in the expression of epithelial ECM molecules such as keratins [65]. Additionally, the expression of

cellular molecules that interact with the ECM is also altered. To choreograph this transition, several different transcription factors, non-coding RNAs, alternative splicing, composition of the microenvironment, ligands and growth factors contribute to ensure the effective switch from the epithelial to the mesenchymal phenotype.

There are several transcription factors that are potent inducers of EMT. The mechanism by which they induce EMT has been well-studied and established. Some of the most well-studied transcription factors that regulate EMT include Snail, Slug, Zeb1, Twist and FOXC2 [51, 60, 66, 67]. The Snail family of transcription factors is made up of 2 sub-families, the Snail family that includes Snail and Slug and the other sub-family is Scratch [51, 68, 69]. Of these different Snail family members, only Snail and Slug have been implicated in EMT and therefore in development, fibrosis and cancer [51].

Numerous EMT inducers such as TGF $\beta$ , Wnt, Notch and receptor tyrosine kinases activate the expression of Snail [51, 66]. Snail induces the mesenchymal phenotype by the repression of E-cadherin. Snail binds to the E-cadherin promoter and recruits epigenetic modifier, Polycomb Repressive Complex II (PRC2) which comprises methyltransferase enhancer of Zeste homologue 2 (EZH2), G9a and suppressor of variegation 3-9 homologue 1 (SUV39H1), the co-repressor SIN3A, histone deacetylases 1, 2, and 3 and Lys-specific demethylase 1 (LSD1) [70-75]. All these components of the complex work together to ensure the epigenetic inhibition of E-cadherin [51]. Snail also induces the expression of mesenchymal markers such as fibronectin, N-cadherin, collagen, MMPs, Twist and Zeb1 [51].

One of the primary regulators of Snail is glycogen synthase kinase 3  $\beta$  (GSK3 $\beta$ ) [76]. GSK3 $\beta$  is a multifaceted serine threonine kinase that has regulatory functions in several vital cellular processes such as cell cycle, apoptosis, migration, metabolism etc. [77]. Several signaling pathways regulate Snail function via their effect on GSK3 $\beta$ . The Wnt, Notch, NF $\kappa$ B and AKT-PI3K signaling pathways inhibit GSK3 $\beta$  thereby promoting the function of Snail [51, 78-80]. Phosphorylation of Snail by (small C-terminal domain phosphatase 1) SCP1 interferes with the ability of GSK3 $\beta$  to phosphorylate Snail thereby stabilizing it [51, 81]. Phosphorylation by p21 Activated Kinase 1 (PAK1) and Large Tumor Suppressor 2 (LATS2) promotes nuclear localization of Snail [82, 83]. The players that negatively regulate Snail include (Protein Kinase D1) PKD1 and p53, which promote the nuclear export, and the ubiquitination and degradation of Snail respectively [51, 84].

Along with Snail, Zeb1 is also a potent inducer of EMT [66]. Zeb1 recognizes the E-Box for binding. It can act both as an activator and as a repressor depending on the co-factor present [51, 66]. Zeb1 represses the expression of E-cadherin in the presence of the co-repressor Switch/sucrose nonfermentable (SWI/SNF) chromatin remodeling protein BRG1 rather than in the presence of its usual co-repressor, the C-terminal binding protein (CTBP) [85]. Zeb1 expression is upregulated during EMT by Snail or by the activity of ligands such as TGF $\beta$  and Wnt [86]. The expression of Zeb1 is also regulated by miR200 which is associated with the epithelial phenotype [87].

The other transcription factors influencing the process of EMT include the bHLH transcription factors, the FOX family and the GATA family of transcription factors. FOXC2 is one of the transcription factors that has been reported to be upregulated following EMT regardless of the pathway via which EMT is induced [60]. Additionally, inhibition of FOXC2 is sufficient to inhibit EMT induced by potent EMT inducers such as Snail, Twist, Goosecoid and TGF $\beta$  [60].

Overexpression of FOXC2 has been shown to induce EMT in human mammary epithelial (HMLE) cells and FOXC2 has been shown to be responsible for the CSC properties of the cells that have undergone EMT [60, 88, 89]. Of the several members of the bHLH transcription factor family, E12, E47, Twist 1, Twist 2 and inhibitor of differentiation (ID) have been shown to play a role in EMT [66]. As tumors progress and grow, certain regions undergo hypoxia, which turns on the expression of HIF1 $\alpha$  which transcriptionally upregulates the expression of Twist and induces EMT in the tumor. The next layer of regulation of Twist depends on the interacting proteins. Twist functions as a dimer and can form homo- or heterodimers with E12, E47 or ID. Dimerization with ID inhibits Twist function and therefore ID needs to be repressed for the effective functioning of Twist [90]. TGF $\beta$  can cause repression of ID thus promoting the transcriptional activity of Twist [91]. Twist is also capable of recruiting epigenetic modifiers to the promoter regions of its target genes and modifying their expression. Twist is capable of repressing the expression of E-cadherin in multiple ways independent of Snail [86, 92, 93]. The other transcription factors involved in the induction of EMT includes members of the forkhead box (FOX), GATA and Sry box (SOX) transcription factors [94, 95].

Next to transcription factors, the growth factors are most frequently studied in association with EMT. Several growth factors including, EGF, FGF, HGF, IGF, PDGF, TGF $\beta$ , and Wnt have been examined for their effect on EMT. Fibroblast growth factor (FGF) induces EMT in epithelial cells by upregulating the expression of Slug,  $\alpha$ 2 $\beta$ 1 integrin, and MMP13 and by destabilizing the desmosomes [96, 97]. Hepatocyte growth factor (HGF) binds and activates the c-Met receptor which is also known as the HGF receptor (HGFR). HGF was identified as a “scatter factor” due to its ability to transform kidney epithelial cells to fibroblast-like motile cells. HGF induces EMT by stimulating the expression of Snail or Slug depending on the type of cell and requires the activity of ERK-MAPK pathway [98]. HGF also represses the expression of desmoplakin which in turn destabilizes the desmosomes [99]. In certain breast cancer cells, Insulin-like growth factor 1

(IGF1) has been observed to induce EMT, which is characterized by an increase in the expression of N-Cadherin, vimentin and fibronectin and decrease in the expression of E-cadherin [100]. The Snail-NF $\kappa$ B signaling pathway is activated in these breast cancer cells [100]. The IGF receptor (IGFR) interacts with E-cadherin to form a complex which is disrupted upon activation of the receptor by the ligand IGF1 [101]. This disruption of the E-cadherin IGFR complex enhances the motility of the cells. However, the response elicited by IGF1 is not the same in all the cell types. In other cell lines, IGF1 was seen to upregulate the expression of Zeb1 in a PI3K and MAPK dependent manner [102]. Epidermal growth factor (EGF) is another growth factor that has been known to induce EMT in breast cancer cells. Exposure to EGF leads to the endocytosis of E-cadherin and upregulation of Snail and Twist [103]. MMPs are upregulated and the ERK-MAPK pathway is activated in breast cancer cells that have been exposed to EGF [104]. Platelet-derived growth factor (PDGF) induces EMT by stimulating the nuclear localization of  $\beta$ -catenin and repression of E-cadherin [105].

TGF $\beta$  family of ligands consists of 3 TGF $\beta$  ligands, 2 activins, bone morphogenetic proteins (BMPs) and several other ligands [106]. TGF $\beta$ 3 has been implicated in the induction of EMT during development whereas TGF $\beta$ 1 has been attributed with the role of inducing EMT during wound healing, in cancer and fibrosis and also in endothelial-mesenchymal-transition (EndMT) [107-111].

TGF $\beta$  ligands bind to tetrameric transmembrane receptors to activate TGF $\beta$  signaling [112]. When the ligand binds to the receptor containing TGF $\beta$ RII, it phosphorylates and activates TGF $\beta$ RI which turns on SMAD signaling by phosphorylation of the C-termini [113]. Activated SMAD2 and/or 3 interact with activated SMAD4 to form a trimer which translocates to the nucleus to alter the transcription of mesenchymal genes such as fibronectin and collagen  $\alpha$ 1 [112]. Depending on the other SMADs that are activated, SMAD4 can bind to SMAD1 or SMAD5. If the inhibitory

SMAD6 or 7 bind to the receptors, the TGF $\beta$  signaling is interrupted [114]. Thus the activation of the TGF $\beta$  signaling involves a delicate interplay of ligands binding to the receptors and the presence of the appropriate SMADs to relay the signal. In addition to spurring EMT by promoting the transcription of the target genes, the components of the TGF $\beta$  pathway also indirectly aid the function of other EMT inducers. For example, Snail in the presence of SMAD3 upregulates the transcription of its target genes whereas the expression of Slug is indirectly upregulated by the SMAD3 mediated increase in the expression of myocardin-related transcription factor (MRTF) which transcribes Slug [115]. SMAD3/4 complex can bind and regulate the transcriptional activity of the Zeb1 transcription factor [116]. They also interact with activating transcription factor 3 (ATF3), which enables the repression of ID, facilitating the activity of Twist. Additionally, they can also upregulate the expression of HMGA2 [116].

TGF $\beta$  also functions independently of SMADS to promote EMT. The TGF $\beta$  receptor interacts with and phosphorylates partition defective (PAR6), which is an integral part of the tight junction responsible for maintaining the cell polarity [117]. This aids in dissolving the junction which is one of the very first steps in early EMT. It also plays a role in activating the RHO pathway which enhances cell mobility by facilitating the formation of lamellipodia and filopodia [118]. The activation of the PI3K-AKT pathway is essential for the TGF $\beta$  induced EMT to such an extent that inhibiting PI3K prevents the induction of TGF $\beta$  mediated EMT [119]. TGF $\beta$  induces Akt-mediated phosphorylation of heterogeneous nuclear ribonucleoprotein E1 (hnRNPE1), which releases it from the 3' untranslated region of disabled 2 (DAB2) and interleukin (IL) like EMT inducer (ILEI) mRNA, which allows their translation and promotes EMT [120]. The BMPs play a role in both EMT and MET and of the many BMPs, BMP 2, 4 and 7 promote EMT [121, 122]. Like the TGF $\beta$  signaling pathway, the Wnt signaling pathway is one of the well-studied pathways that plays an important role in development and EMT [123, 124].

*1C.b. Wnt signaling has been implicated in EMT and CSC enriched TNBCs.*

The Wnt signaling pathway is one of the well-studied pathways that play an important role in development and disease [123, 124]. The Wnt signaling pathway is named after the *Wnt1* gene, homolog of Wingless gene in flies, which was shown to regulate polarity during development. There are 19 Wnt genes in humans and most mammals, which are classified into 12 subfamilies [125]. All the Wnt genes encode for secreted cysteine-rich, 40kDa glycoproteins which share about 35-85% homology. Of these 19 Wnts, 7 ligands have been found to be expressed in mouse mammary tissue and Wnt 2, 3, 4, 5A, 7B, 10B, 13 and 14 are expressed in human mammary gland [125-127]. Due to their structural similarity, Wnt ligands are redundant in function. The Wnt ligands bind to a heterodimeric receptor. The cell surface receptor that binds the Wnt ligands is comprised of a seven transmembrane domain protein belonging to the Frizzled (Fzd) family and a LDL receptor-related protein (LRP 5/6) [124, 125]. There are at least 10 known Frizzled proteins in humans and any of these can bind to any of the Wnt ligands to activate the downstream signaling [124]. When Wnt binds to the cysteine-rich part of the Fzd's extracellular domain, it forms a trimeric complex with Fzd and LRP which induces a conformational change in the cytoplasmic domain of LRP 5/6 [125]. Based on the downstream signaling, the Wnt pathway has been classified as the canonical or the non-canonical pathway [124, 125]. Of the 2 signaling pathways the canonical signaling pathway is relevant to our studies and hence is described in detail.

The canonical Wnt signaling, also known as the Wnt/ $\beta$ -Catenin signaling is the most studied of the Wnt signaling pathways.  $\beta$ -Catenin has roles both in the cytoplasm and the nucleus of the cell. In the cytoplasm, it forms complexes with E-cadherin and other proteins involved in

maintaining cell-cell adhesion, thus aiding in the maintenance of tissue integrity [125]. In the nucleus, it acts as a regulator of transcription [125]. When the Wnt signaling is off or the Wnt ligand is absent, newly synthesized  $\beta$ -catenin is marked for destruction by the destruction complex. The destruction complex is made up of scaffolding proteins, adenomatous polyposis coli (APC) and Axin 1 or 2, and kinases casein kinase 1 (CK1) and glycogen synthase kinase 3 $\beta$  (GSK3 $\beta$ ).  $\beta$ -catenin is sequentially phosphorylated by CK1 followed by GSK3 $\beta$ , which marks it for ubiquitination and ultimately for destruction by the proteasome. When Wnt signaling is activated, cytoplasmic changes in LRP5/6 promotes its binding to Axin in the destruction complex. Fzd on the other hand, binds to Disheveled (Dvl) which is an Axin-binding protein [124]. Both these actions together prevents the destruction of  $\beta$ -Catenin, which starts accumulating in the cytoplasm and enters the nucleus. When the Wnt signaling is inactive, TCF (T-cell factor) /Lef are bound by a co-repressor called Groucho, which prevents transcription of their target genes [124]. When Wnt is activated and  $\beta$ -catenin enters the nucleus, it displaces Groucho and facilitates the interaction of TCF/Lef with co-activators such as B-cell lymphoma 9/legless (BCL9/LGS) and Pygopus (pygo) and promotes the transcription of its target genes [124]. The target gene list for the Wnt/ $\beta$ -catenin pathway has been growing since the day it was discovered and some of the target genes such as cyclin D1 and c-myc have been identified as being tumor promoters [125].

In TNBCs and basal-like breast cancer Wnt signaling, both canonical and non-canonical pathways, is commonly dysregulated and contributes to enhanced tumorigenesis and metastasis [128-130]. Dyregulation of Wnt in TNBC patients was found to be associated with poor prognosis and higher risk of developing lung and brain metastasis [128, 131, 132]. The aberrations in the Wnt signaling pathway is evident from the fact that  $\beta$ -catenin nuclear localization, enhanced levels of cyclin D1 in invasive TNBCs, and increased levels of DKK1, another Wnt/B-catenin target gene, are observed [124]. In the nucleus, BCL9, a co-factor that binds and promotes  $\beta$ -catenin has



been found to be upregulated in basal-like breast cancers, and LBH and SOX9 both of which are  $\beta$ -catenin targets have been reported to be upregulated as well [124]. Immunohistological studies have shown high levels of  $\beta$ -catenin to be present in either the cytoplasm and/or nucleus of breast cancer tissue. In some of these cases, the increase in the expression of  $\beta$ -catenin was also accompanied by elevated levels of cyclin D1, a  $\beta$ -catenin target, and this correlated with poor survival [133-135]. These findings are also supported by the fact that elevated levels of  $\beta$ -catenin protein were detected in tumor lysates using western blotting technique, and this served as a molecular confirmation of the immunohistological observations [134]. Non-canonical Wnt signaling has also been demonstrated to promote TNBC metastasis via the JNK pathway [128, 136]. TNBCs are highly enriched for CSCs which contribute to their higher rate of relapse and chemoresistance and studies have shown that this effect can be attributed to the dysregulation of Wnt signaling pathways in these CSCs [137]. These finding emphasize the need to target the Wnt signaling pathway to inhibit EMT and CSC-mediated progression of TNBCs. Therefore, we assessed the clinical significance of several key players of the Wnt signaling pathway using the KMPlotter and our preliminary studies drew our attention to GSK3 $\beta$  which is a critical player not only in the Wnt signaling pathway but also several other vital pathways that play a pivotal role in governing and regulating the cells. Therefore we decided to take a deeper look into this ubiquitous and multifaceted kinase, GSK3 $\beta$ .

#### 1D. Role of Glycogen Synthase Kinase 3 $\beta$ in tumor progression

Glycogen Synthase Kinase 3 (GSK3), ATP:Phosphotransferase E.C.2.7.1.37 is a serine threonine kinase belonging to the CMGC (Cyclin-Dependent Kinases (CDKs), Mitogen Activated Protein Kinases (MAPKs), Glycogen Synthase Kinases (GSKs), CDK-like Kinases (CLKs)) family of kinases [138]. Kinases are a family of enzymes that catalyze the transfer of phosphate group from adenosine triphosphate (ATP) to their target substrates [139]. Serine-threonine kinases

specifically transfer the phosphate group to either serine or threonine residue on the substrate [139]. This phosphorylation can in turn regulate the stability, localization and function of the substrate.

GSK3 was first isolated from the rabbit skeletal muscle [139, 140]. GSK3 is a highly conserved kinase and orthologs of this kinase are expressed in plants, fungi, worms, flies, sea squirts, and all the vertebrates [138]. Even species as far apart as humans and flies have 90% similarity within the protein kinase domain [141]. GSK3 was first discovered for its ability to phosphorylate glycogen synthase, the rate-limiting enzyme in the glycogen synthesis pathway and hence the name glycogen synthase kinase [140]. At about the same time GSK3 was found to activate ATP-Mg-dependent form of type-1 protein phosphatase (Factor A) [140]. GSK3 was first isolated as a complex with Factor A and was cloned based on partial peptide sequencing [142, 143]. Two different cDNAs were isolated from rat brain and these corresponded to GSK3 alpha (GSK3 $\alpha$ ) and GSK3 beta (GSK3 $\beta$ ) [138, 143]. The 2 isozymes are coded on 2 different genes. GSK3 $\alpha$  is coded on chromosome 7 in mouse and on chromosome 19 in human and has molecular weight of 51 kDa [143]. GSK3 $\beta$ , on the other hand, is coded on mouse chromosome 16 and human chromosome 3 and has a molecular weight 47 kDa [143]. Although they are coded on different genes, they have 98% similarity in the kinase domain but only 85% overall sequence homology [143]. GSK3 $\alpha$  has an extended glycine rich, 63 residues N-terminal region that might act as a pseudosubstrate [138, 139]. Both the isoforms are conserved in most of the species except birds which seem to have evolutionarily lost the expression of GSK3 $\alpha$  [138]. A third isoform of GSK3, GSK3 $\beta$ 2 has been recently discovered to be expressed in the brain tissue [144, 145]. This splice isoform is generated due to splicing between the exon 8 and 9 of GSK3 $\beta$  and results in the introduction of 13 amino acids into the kinase domain of GSK3 $\beta$  [144, 145]. Though GSK3 $\alpha$  and GSK3 $\beta$  are highly conserved and have high level of homology, they are not functionally

redundant. This was evident when the transgenic mouse, in which the exon 2 of GSK3 $\beta$  was selectively deleted, was embryonic lethal due to extensive hepatocyte apoptosis, even after having a fully functional GSK3 $\alpha$  [139, 146]. Of the 3 isoforms, GSK3 $\beta$  is the well-studied isoform. GSK3 $\beta$  is made up of 2 major domains. The  $\beta$ -strand domain is present in the N-terminus spanning the amino acid residues 25-138 and the  $\alpha$  helical domain occurs at the C-terminus from amino acid residue 139 to 343 [146, 147]. The ATP binding domain is present at the interface of the 2 major domains. Arg96, Arg180 and Lys205 form a small pocket that recognizes the priming phosphorylation present on the primed substrates of GSK3 $\beta$  [146, 147].

GSK3 $\beta$  is a ubiquitously expressed gene and both isoforms are expressed in all mammalian tissues. GSK3 $\beta$  is highly expressed in the brain, both in the neurons and the glia. The name is very misleading as GSK3 $\beta$  was soon discovered to be associated with innumerable cellular functions including metabolism, cell signaling, cellular transport, apoptosis, proliferation, gene transcription, protein synthesis, stem cell renewal and differentiation, circadian rhythm, axial orientation, patterning, response to DNA damage and migration [139].

GSK3 $\beta$  is involved in innumerable pathways that regulate myriads of cellular functions and is therefore highly regulated. In fact GSK3 $\beta$  is regulated at multiple levels. GSK3 $\beta$  recognizes substrates that have been previously primed by other kinases. This adds to the selectivity of kinase activity of GSK3 $\beta$  toward a substrate. Usually, GSK3 $\beta$  recognizes the motif "S/T-X-X-X-S/TP" where the S/TP stands for the primed phosphorylated residue on the substrate [148]. However, GSK3 $\beta$  is capable of binding and phosphorylating both primed and unprimed substrates in a context-dependent manner. The ability of GSK3 $\beta$  to bind unprimed substrates also make the

phosphorylation status of the S9 residue irrelevant to its function in relation to that particular substrate [148].

Another major regulatory mechanism is the post translational modifications of the enzyme itself. GSK3 $\beta$  activity is regulated through phosphorylation by other kinases such as Akt, ERK, FYN, p38MAPK, PKA, PYK2, and Src and by phosphatases such as PP1 and PP2A [77, 148]. Phosphorylation of GSK3 $\beta$  on Ser9 residue (Ser21 for GSK3 $\alpha$ ) inactivates the kinase whereas the phosphorylation of Tyr216 within the activation loop, increases its kinase activity [149, 150]. However, this regulation by phosphorylation is not as simple or straight forward as it appears. The phosphorylation status of GSK3 $\beta$  on the Ser9 residue is in a constant state of oscillation between phosphorylated and unphosphorylated [148, 151]. The phosphorylated residue inhibits GSK3 $\beta$  function by binding to the pocket to which primed substrates bind. Therefore, this inhibitory effect also depends on the concentration of the primed substrate present [148]. When the concentration of the primed substrate increases, it displaces the phosphorylated S9 residue and the enzyme is rendered active again. Additionally, in order for the catalytic activity to take place both the major domains, the  $\beta$ -strand domain and the  $\alpha$ -helical domains, must align into a catalytically active conformation to effectively bind appropriate substrates [148].

The substrate specificity and availability of GSK3 $\beta$  is also dictated by the association of the kinase with different protein complexes. The association of GSK3 $\beta$  with the destruction complex is one of the well-studied ones [148]. About 10% of the GSK3 $\beta$  present in the cells is found to be bound to Axin. Axin, in the destruction complex, binds GSK3 $\beta$ , Casein Kinase 1 (CK1) and  $\beta$ -Catenin and this facilitates the phosphorylation of  $\beta$ -Catenin by GSK3 $\beta$  [148]. However,  $\beta$ -Catenin is not the only substrate that binds both Axin and GSK3 $\beta$ . Other substrates of GSK3 $\beta$  such as Smad3,

tuberous sclerosis complex 1 (TSC1)/ hamartin and TSC2/tuberin have also been found to bind to Axin and this binding facilitates their phosphorylation by GSK3 $\beta$  [148]. Other scaffolding proteins with which GSK3 $\beta$  forms complexes include but are not limited to 14-3-3 proteins, glycogen synthase kinase 3 $\beta$  interacting proteins (GSKIP), protein 4.1R and suppressor of fused (sufu) [148].

In addition to the above-mentioned means of regulation, GSK3 $\beta$  is also regulated by subcellular localization. GSK3 $\beta$  is present in 3 different pools, i.e. the mitochondrial pool, cytosolic pool, and nuclear pool [148]. The mitochondrial GSK3 $\beta$  could play a role in the regulation of apoptosis. It has been noted that during the induction of apoptosis, the active form of GSK3 $\beta$  is dramatically upregulated in the mitochondria [148, 152, 153]. However, much is yet to be discovered about the roles and regulation of mitochondrial pool of GSK3 $\beta$ . The nuclear pool of GSK3 $\beta$  is better studied as a major proportion of GSK3 $\beta$  substrates are transcription factors. Some of the transcription factors regulated by GSK3 $\beta$  include Fos/Jun, AP-1, CREB, heat shock factor 1, nuclear factor of activated T cells (NFAT), myc, C/EBP, NF $\kappa$ B, p53, and signal transducer and activator of transcription-3 (STAT3) [148, 154-156]. Interaction with FRAT protein facilitates nuclear export of GSK3 $\beta$  [157]. Recently, roles in epigenetic alterations have also been attributed to GSK3 $\beta$ . Evidence indicates that GSK3 $\beta$  phosphorylates histones and promotes phosphorylation of histones by other kinases [158, 159]. In addition, GSK3 $\beta$  also has been shown to phosphorylate and either activate or inactivate HDACs and in turn HDACs alter the activity of GSK3 $\beta$  [160-163].

Cytoplasmic pool of GSK3 $\beta$  is present in several compartments within the cytoplasm [148]. This pool of GSK3 $\beta$  is in a constant flux shuttling between different compartments [164]. The well-

studied portion of cytoplasmic GSK3 $\beta$  is the one that is found in the destruction complex. This pool of GSK3 $\beta$  is often found to be compartmentalized in the endosomes [165]. It is important to understand that this compartmentalization plays a very important role in contextual signaling of GSK3 $\beta$ . For example, the endosomal compartmentalization of GSK3 $\beta$  associated with the destruction complex allows GSK3 $\beta$  to signal both in Wnt-dependent and Wnt independent pathways at the same time [165]. While facilitating the versatility of GSK3 $\beta$ , compartmentalization also adds another layer of complexity while targeting GSK3 $\beta$ .

## 1E. Role of GSK3 $\beta$ in cellular processes vital to metastasis

### 1E.a. *Cell Cycle*

Cell cycle is a highly regulated process by which the cells replicate. Cell cycle mainly is divided into 4 phases – Gap1 (G1 phase), synthesis (S phase), gap 2 (G2 phase) and mitosis (M phase) [166]. This complex cycle is regulated by cyclins and cyclin dependent kinases (CDKs) which function together as complexes [166]. The CDKs are inactive kinases until they form complexes with the appropriate cyclins and this complex can then bind and phosphorylate the substrates. The CDKs are ubiquitous but the levels of cyclins change dramatically depending on the phase of the cell cycle [166]. Thus the cyclins follow a predictable pattern of expression and degradation and this serves to regulate the cell cycle. For example, cyclin D is upregulated in the G1 phase and binds to CDK4/6 whereas cyclin E is upregulated later in the G1 phase and binds to CDK2 and facilitates the transition from G1 to S phase [166]. There are several cyclins and several CDKs, and the binding partners are yet to be determined. However, of all the cyclins, cyclin D1 is highly altered in cancer [166, 167]. Cyclin D1 mRNA and protein levels are upregulated following a mitogenic signal and remains high until the mitogenic signal persists. Cyclin D1 interacts with CDK4/6 to form a complex which is phosphorylated and activated by CDK activating kinase (CAK) [168]. The activated cyclin D1/CDK4/6 complex then acts as a sequestering protein to prevent

the interaction of CDK-inhibitory proteins from the cyclin E/CDK2 complex thus resulting in the accumulation of this complex. Cyclin E/CDK2 phosphorylates and inactivates Rb protein which acts as a gatekeeper protein by inhibiting its substrate E2F from transcribing its target gene such as cyclin E which is required for progressing to the next cell cycle phase [166]. When the cell enters the S phase, cyclin D1 is exported from the nucleus and is ubiquitinated and degraded by 26S proteasome [166]. It is in regulating the degradation of cyclin D1 that GSK3 $\beta$  plays a vital role. Cyclin D1 is phosphorylated on threonine 286 by GSK3 $\beta$  [166]. This phosphorylation leads its interaction with CRM1 which facilitates the export of cyclin D1 to the cytoplasm for subsequent ubiquitination by SCF E3 ligase family and degradation [166]. Thus GSK3 $\beta$  is essential for the turnover of cyclin D1 which is necessary for the progression of the cell cycle.

#### *1E.b. Apoptosis*

Apoptosis or programmed cell death is a well-orchestrated process by which a cell undergoes self-destruction through a cascade of events. GSK3 $\beta$  has been demonstrated to play a very important role in the regulation of apoptosis [169]. GSK3 $\beta$  has been attributed with the induction of apoptosis following DNA damage, hypoxia and endoplasmic reticulum stress. It mainly brings about this effect by phosphorylating and inhibiting pro-survival proteins such as CREB, heat shock factor 1 and p53 [154, 169]. GSK3 $\beta$  phosphorylates the C-terminus of p53 at Ser-33 and facilitates its pro-apoptotic function [170, 171]. p53 is a short lived protein and phosphorylation by GSK3 $\beta$  facilitates other post-translational modifications that stabilize p53 [169]. GSK3 $\beta$  also promotes the transcription of p53 target genes and regulates its subcellular localization. Binding of GSK3 $\beta$  to p53 also alters GSK3 $\beta$ . In addition to this, GSK3 $\beta$  also phosphorylates and inhibits MDM3 which is an E3 ubiquitin ligase responsible for ubiquitination and subsequent degradation of p53 [169, 172].

GSK3 $\beta$  also regulates the intrinsic mitochondrial apoptotic pathway. The intrinsic apoptotic pathway depends on the proportion of active anti-apoptotic Bcl-2, Bcl-X<sub>L</sub>, Bcl-w, Mcl1, and A1 and pro-apoptotic proteins Bax and Bim belonging to the Bcl-2 family of protein [169, 173, 174]. Bax sequesters the anti-apoptotic proteins and binds to the mitochondrial membrane that results in the disruption of the mitochondrial membrane and the release of cytochrome c which in turn triggers caspase cascade and apoptosis [169, 174, 175]. GSK3 $\beta$  is capable of phosphorylating and activating Bax and phosphorylating Mcl1 and inhibiting its function [169]. Though, a pro-apoptotic function has been attributed to GSK3 $\beta$ , several studies have also highlighted the ability of GSK3 $\beta$  to inhibit apoptosis. Thus, the ability of GSK3 $\beta$  to induce apoptosis depends on substrate availability and its subcellular localization.

### *1E.c. Migration*

Migratory potential of the cells is a major contributor to its metastatic potential. One of the means by which EMT promotes metastasis is by enhancing the migratory properties of the cancer cells. GSK3 $\beta$  has been reported to play a pivotal role in the migration of the cancer cells. There are three major means by which GSK3 $\beta$  influences the migratory capacity of the cancer cells. These mechanisms include regulation of the actin cytoskeleton dynamics, microtubule formation and the interaction of the cells with their extracellular matrix (reviewed in [176]).

The actin cytoskeleton is mainly regulated by the Rho family of GTPases and of these Rac, which influences lamellipodia formation, and Cdc42, which induces filopodia formation, are the most studied members and control actin polymerization [176-178]. Rho is another member that is equally well-studied but contributes to the cellular contractility. The Rho family proteins are highly regulated by GTPases activating proteins (GAP) and p190 RhoGAP is one such protein that is capable of regulating the activity of Rho family members and is in turn regulated by several kinases including GSK3 $\beta$  [176, 179-181]. In p190A RhoGAP knockout fibroblasts, the actin



polymerization was highly dysregulated and this could be corrected by overexpressing wild-type p190A RhoGAP in these cells [176, 181]. However, the introduction of mutant p190A RhoGAP that lacked the phosphorylation site for GSK3 $\beta$  was not capable of restoring the actin polymerization to normalcy in the p190A RhoGAP  $-/-$  cells, indicating the importance of GSK3 $\beta$  in the actin polymerization process [176, 181]. Thus, GSK3 $\beta$  can regulate cell migration by activating Rho. It is important to note that p190A RhoGAP and not p190B RhoGAP is phosphorylated by GSK3 $\beta$  and therefore GSK3 $\beta$  only influences the Rho proteins regulated by p190A RhoGAP and not those influenced by p190B RhoGAP [176, 181]. GSK3 $\beta$  has also been reported to activate ADP-ribosylation factor 6 (Arf6) which plays crucial role in vesicle trafficking, membrane ruffling and lamellipodia formation [176, 182, 183]. GSK3 $\beta$  also activates Rac in several different cell models and enables the cells to migrate. Thus GSK3 $\beta$  positively regulated cell migration by exerting its influence on different factors controlling actin polymerization.

While actin polymerization provides the force for the cellular migration, the microtubules influence the directionality of the movement. GSK3 $\beta$  has been reported to regulate several of the proteins that are involved in the microtubule dynamics such as microtubule motor protein, proteins in the microtubule organizing center (MTOC) and protein complexes at the plus ends of the microtubules [176, 184]. The microtubules also serve to deliver different proteins from one part of the cell to the other. Kinesins are proteins that are made of 2 heavy chains that bind the microtubule provide a motor functionality to the protein and 2 light chains that can bind to the proteins such as APC and focal adhesion dissociation factors [185, 186]. GSK3 $\beta$  is known to phosphorylate the kinesin light chain and facilitate the dissociation of the protein bound to the light chain at its destination site [176, 185]. This function of GSK3 $\beta$  plays a very important role in facilitating the cellular migration and dissociation of focal adhesion complexes.

A migrating cell is in constant contact with its extracellular matrix. These interactions serve to determine the direction of the movement and also serve as temporary anchors to facilitate the forward movement. Cell movement takes place by dissolution of the existing focal adhesion and formation of the new focal adhesion. Paxillin is a component of the focal adhesion complex that is regulated by several kinases such as focal adhesion kinase (FAK), Src and GSK3 $\beta$  [187, 188]. Phosphorylation of paxillin by GSK3 $\beta$  allows for the formation and maturation of the focal adhesions [176, 189]. Thus GSK3 $\beta$  regulates both dissolution and formation of focal adhesions to facilitate cell motility and this is of note as the subcellular localization of GSK3 $\beta$  and the availability of the substrate dictates whether GSK3 $\beta$  functions to dissolve or form focal adhesions.

In summary, GSK3 $\beta$  functions in diverse manners to facilitate the progression of cell cycle, promotes apoptosis and facilitates cellular migration. Thus the effect of inhibition of GSK3 $\beta$  is dependent on the cumulative effect of GSK3 $\beta$  on all the different cellular processes. Inhibition of GSK3 $\beta$  might stall the cell cycle and thereby decrease the proliferation of the cells while inhibiting apoptosis which is essential for inhibiting tumor progression. In addition to these effects inhibition of GSK3 $\beta$  is also going to inhibit the migratory potential of the cancer cell. Thus the effect of GSK3 $\beta$  inhibitor on a cancer depends on the cell type, the pool of GSK3 $\beta$  affected, the substrates available and the cellular processes predominantly affected. This proves that the role of GSK3 $\beta$  as a tumor promoter or suppressor is entirely context dependent. The most important observation from these studies is that GSK3 $\beta$  plays context dependent role in cancer and this is mediated both in a Wnt signaling dependent and Wnt signaling independent manner and as GSK3 $\beta$  plays different roles in different cancers, it is essential to understand the role of GSK3 $\beta$  in breast cancer.

#### *1E.d. Contribution of GSK3 $\beta$ to breast cancer.*

Several studies have been conducted to delineate the role of GSK3 $\beta$  in breast cancer. GSK3 $\beta$  has multiple targets and regulates several key players in breast cancer progression. In breast cancer, hyperactivation of Wnt/ $\beta$ -catenin pathway is implicated as discussed above and GSK3 $\beta$  is a negative regulator of the Wnt signaling pathway. However, no mutations in GSK3 $\beta$  have been reported in breast cancers [190]. GSK3 $\beta$  is also associated with the induction of apoptosis in breast cancer. Exogenous overexpression of kinase dead GSK3 $\beta$ , which is presumed to function as an inhibitor of endogenous GSK3 $\beta$ , was observed to promote breast cancer [191, 192]. In MCF7 cell line, kinase dead GSK3 $\beta$  led to the emergence of chemoresistance to doxorubicin and decreased its sensitivity to tamoxifen as compared to the MCF7 cells overexpressing the wild-type GSK3 $\beta$  [191, 193]. On the other hand, the same MCF7 cells overexpressing kinase dead GSK3 $\beta$ , which displayed decreased sensitivity to doxorubicin and tamoxifen, exhibited increased sensitivity to rapamycin as compared to the MCF7 cells overexpressing the wild type GSK3 $\beta$  [191, 193]. Overexpression of constitutively active GSK3 $\beta$  increased chemosensitivity and induced cell cycle arrest both of which contributed to reduced tumorigenicity [191]. GSK3 $\beta$  inhibitor SB415286 was shown to induce EMT in MCF10A cells [194]. GSK3 $\beta$  is known to inactivate NF $\kappa$ B, which is an activator of Snail, an EMT inducing transcription factor in epithelial cells [191, 194]. This study demonstrated that GSK3 $\beta$  inhibitor SB415286 induced EMT by activating NF $\kappa$ B which in turn activated Snail [191, 194]. GSK3 $\beta$  has also been shown to phosphorylate and regulate both Snail and Slug, by marking them for degradation [195, 196].

While several studies indicate that GSK3 $\beta$  is a tumor suppressor in breast cancer, other studies contradict these findings. Studies have shown that GSK3 $\beta$  overexpression, detected by immunohistochemistry, correlates with poor prognosis [197]. Quintayo et.al, used the Edinburgh Breast Conservation series to study the correlation between GSK3 $\beta$  and disease prognosis in

these breast cancer patients [197]. The Edinburgh Breast Conservation Series consists of 1812 patient samples along with the complete history of their treatment and outcomes collected between 1981 and 1998 [197]. Of these samples, only 1681 tissue blocks were available and were included in this study [197]. These were sectioned to create a tissue microarray, which was used for immunohistochemical staining for GSK3 $\beta$ , p-GSK3 $\beta$  as well as other markers, and the stained tissues were histoscored [197]. The patient samples were classified into high or low expressing tissues based on the median histoscores and their distant relapse-free survival was plotted [197]. Of the 1681 samples, about 70% of the samples were stained successfully and the analysis showed that the samples that had high staining of GSK3 $\beta$  had shorter distant relapse-free survival, whereas no such correlation was observed in the case of p-GSK3 $\beta$  [197]. The increased expression of GSK3 $\beta$  also correlated with the presence of metastatic lesions in the lymph node [197]. Overexpression of GSK3 $\beta$  correlated with higher tumor grade and tumor size. These tumors also lacked ER $\alpha$ , PR, and were characterized by an increased proliferative potential [197].

Small molecule studies have also highlighted the fact that GSK3 $\beta$  inhibitors can serve as therapeutic agents in breast cancer to overcome chemoresistance [198]. While GSK3 $\beta$  has been attributed with tumor suppressive qualities [199], experiments have demonstrated that inhibition of GSK3 $\beta$  is correlated with positive outcome in breast cancer. Clinical trials conducted with Eli Lilly GSK3 $\beta$  inhibitor, LY2090314, have demonstrated that GSK3 $\beta$  inhibitors improved the efficacy of platinum drugs and the patients in whom stable disease was observed following treatment with LY2090314 included a breast cancer patient [200]. Therefore, GSK3 $\beta$  inhibitors could serve as novel therapeutic agents to treat breast cancers, either as a single agent or in combination with standard of care drugs to help overcome chemoresistance or prevent the relapse of the disease.

## 1F. GSK3 $\beta$ , EMT and cancer stem cells.

GSK3 $\beta$  is a ubiquitous kinase regulating multiple signaling pathways and also playing an important role in EMT. While GSK3 $\beta$  was first discovered for its role in regulating metabolism, it gained much of its prominence as a key player in the Wnt/ $\beta$ -Catenin Signaling. Wnt is a well-known promoter of stem cell properties and therefore GSK3 $\beta$ , an inhibitor of the Wnt signaling pathway is commonly recognized as an inhibitor of stem cell properties. However, GSK3 $\beta$  is a highly regulated kinase and therefore its role and function is dictated by the context in which it is studied. GSK3 $\beta$  influences EMT by regulating the key players of EMT such as Snail, Slug and  $\beta$ -Catenin.

GSK3 $\beta$  binds to and phosphorylates Snail [195]. The phosphorylation of Snail by GSK3 $\beta$  at a single site marks it for ubiquitination by  $\beta$ -Trcp and thereby for destruction [195]. Phosphorylation of a second site on Snail regulates its subcellular localization and results in the translocation of Snail from the nucleus to the cytoplasm [195]. Inhibition of GSK3 $\beta$  was observed to upregulate the expression of Snail and thereby inhibit the expression of E-cadherin, one of the most prominent marker of epithelial phenotype [195]. GSK3 $\beta$  has also been shown to inhibit the function of NF $\kappa$ B, which is an activator of Snail in MCF10A cells and this is the mechanism proposed by which GSK3 $\beta$  helps epithelial cells to retain the epithelial phenotype [194]. Like Snail, Slug is known to bind and inhibit the expression of E-cadherin. Phosphorylation of Slug by GSK3 $\beta$  marks it for ubiquitination and subsequent degradation by carboxyl terminus of Hsc70-interacting protein (CHIP) [196].

In summary, GSK3 $\beta$  functions in diverse manners to facilitate the progression of cell cycle, promotes apoptosis and facilitates cellular migration. Thus, the effect of inhibition of GSK3 $\beta$  is dependent on the cumulative effect of GSK3 $\beta$  on all the different cellular processes. Inhibition of GSK3 $\beta$  might stall the cell cycle and thereby decrease the proliferation of the cells while inhibiting apoptosis which is essential for inhibiting tumor progression. In addition to these effects inhibition of GSK3 $\beta$  is also going to inhibit the migratory potential of the cancer cell. Thus, the effect of GSK3 $\beta$  inhibitor on a cancer depends on the cell type, the pool of GSK3 $\beta$  affected, the substrates available and the cellular processes predominantly affected. This proves that the role of GSK3 $\beta$  as a tumor promoter or suppressor is entirely context dependent.

## Chapter 2 – Statement of objective

### 2A. Knowledge gap

TNBCs are highly metastatic tumors that are characterized by the presence of cells that have undergone EMT and are enriched for cancer stem cells. As a result, there is higher risk of developing chemoresistance, tumor relapse and metastasis that often prove to be fatal. The mainstay of treatment for TNBCs is chemotherapy as they lack targeted therapy. Only about 30% of the tumors respond to the chemotherapy and even these eventually tend to relapse and gain chemoresistance [201]. The chemotherapeutic agents mainly function by killing the rapidly proliferating cells in the tumors. However, TNBCs are enriched with CSCs and these cells are unaffected by the standard of care chemotherapeutic agents. Therefore it is imperative to develop novel targeted therapies to treat these aggressive cancers. The Wnt signaling pathway is one of the most aberrantly activated pathways in TNBCs. This pathway has also been shown to play pivotal role in the generation and sustenance of CSCs. GSK3 $\beta$  is a central player in the Wnt signaling cascade, capable of independently regulating stemness [202]. Our goal was therefore to examine the role of GSK3 $\beta$  in promoting EMT/CSC properties driving TNBCs & identify potential druggable targets. Based on our preliminary findings in CSC-enriched TNBC cells, as well as patient survival data analyzed from publicly available databases, we formulated the following hypothesis.

### 2B. Hypothesis

**GSK3 $\beta$  inhibition can impede epithelial-mesenchymal-transition (EMT) and cancer stem cell (CSC) properties and will serve as a novel drug target for EMT/CSC-enriched triple-negative breast cancers (TNBCs).**

## 2C. Study questions – Aims

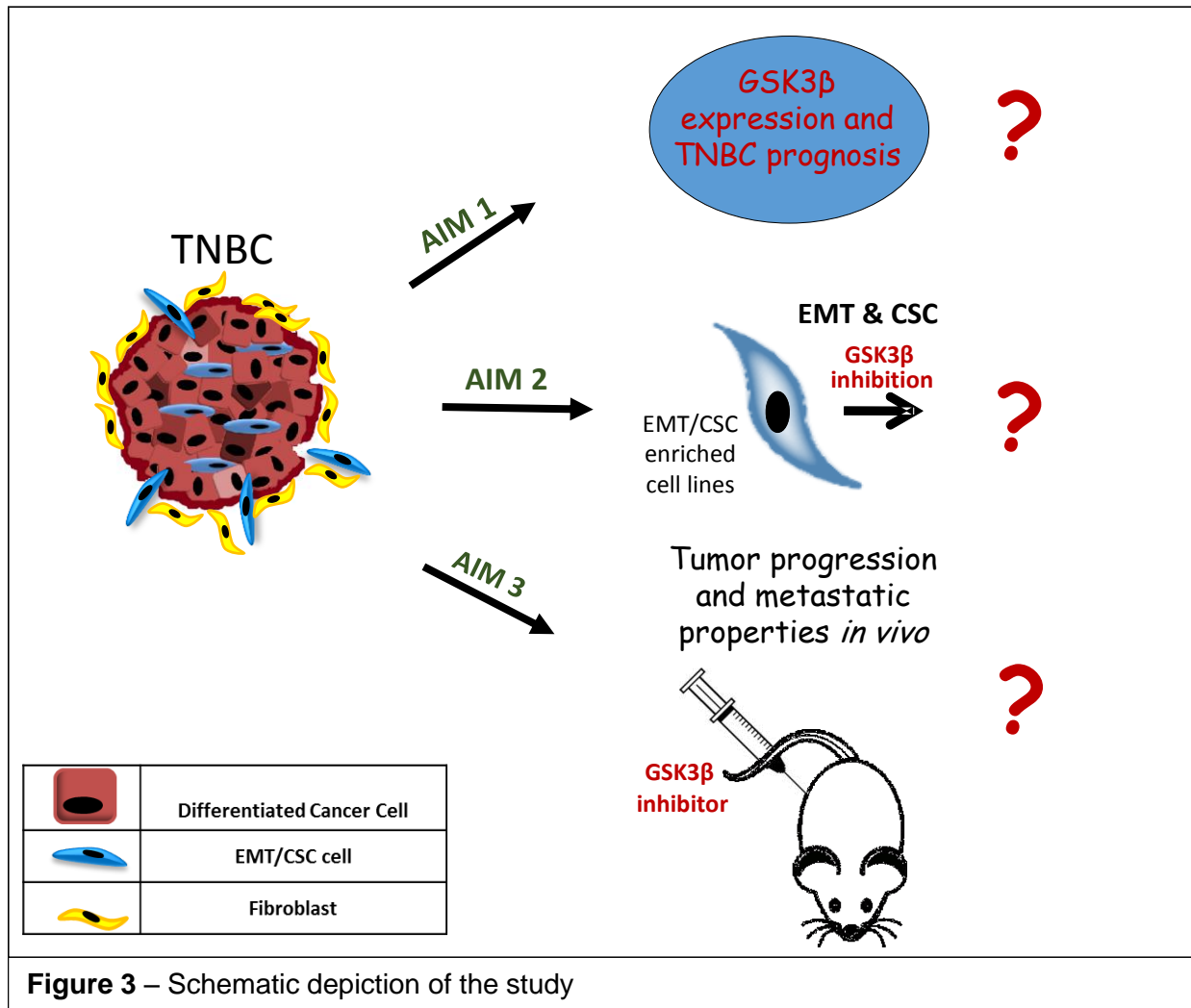
**Aim 1** - Determine if GSK3 $\beta$  is upregulated in breast cancer and if this upregulation has clinical significance.

**Aim 2** - Investigate the relationship between GSK3 $\beta$  and Epithelial-Mesenchymal-Transition (EMT) and cancer stem cell (CSCs) properties.

**Aim 3** - Test if GSK3 $\beta$  inhibitors can be effectively used *in vivo* to target CSC-enriched breast cancer.



## 2D. Planned systematic investigation



Aim 1 - Determine if GSK3β is upregulated in breast cancer and if this upregulation has clinical significance.

Q. Is GSK3β upregulated in breast cancer?

Approach

- Publicly available datasets (Ma [203], Richardson 2 [204] and TCGA [205]) were examined to determine if GSK3 $\beta$  expression is upregulated in breast cancer tissues compared to normal mammary tissues.

Q. Does the level of expression of GSK3 $\beta$  correlate with patient survival?

#### Approach

- Kaplan-Meier plots were generated using KMPlotter to identify the players of the Wnt signaling molecule that are associated with poor survival of TNBC and basal-like breast cancer patients [206].

Aim 2 - Investigate the relationship between GSK3 $\beta$  and Epithelial-Mesenchymal-Transition (EMT) and cancer stem cell (CSCs) properties in TNBC cells.

Q. Can GSK3 $\beta$  inhibitors be used to downregulate EMT in TNBC cells?

#### Approaches

- A high throughput screen was conducted to identify small molecule inhibitors capable of inhibiting EMT in EMT/CSC-enriched MDA MB 231 reporter cells (Expressing EMT-reporters).
- Western blotting and qRT-PCR assays were employed to assess the protein and mRNA expression of markers of the epithelial and mesenchymal phenotype of treated cells.
- Wound-healing assay was used to assess the effect of GSK3 $\beta$  inhibition on the migratory properties of cells with mesenchymal phenotype, which are typically characterized by the presence of enhanced migratory potential.

Q. What is the effect of GSK3 $\beta$  inhibitors on the CSC properties of mesenchymal-like cells?

#### Approaches

- The mammosphere forming assay (surrogate assay for stemness) was utilized to examine the effect of GSK3 $\beta$  inhibition (*via* small molecule inhibitor and shRNA) on the sphere-forming ability. GSK3 $\beta$  knock out MEFs were also used to assess the effect of GSK3 $\beta$  on the sphere forming potential of MEFs.
- CD44/24 surface antigen profile (an indicator of the level of stemness and differentiation) of the mesenchymal-like cells were examined by FACS to determine the effect of GSK3 $\beta$  on the stemness of the mammary cell lines with mesenchymal and CSC properties.

Q. Do GSK3 $\beta$  inhibitors selectively inhibit mesenchymal-like cells as compared to their epithelial counterparts?

#### Approaches

- Cell lines representing normal breast cells (MCF10A), epithelial transformed cancer cells (MCF7) and EMT/CSC enriched cancer cells (Sum159) were treated with the GSK3 $\beta$  inhibitors and their sensitivity to the inhibitors were evaluated using the MTT assay.
- Cell lines exhibiting epithelial phenotype and mesenchymal phenotype were treated with the drugs selected from the small molecule screen to identify those capable of selectively inhibiting cells with mesenchymal properties.
- Cells having epithelial and mesenchymal attributes and expressing green and red fluorescent markers respectively, were plated in equal proportions to be co-cultured. The co-cultures were treated with the GSK3 $\beta$  inhibitors and the proportion of red and green cells was assessed using flow cytometry.

Aim 3 - Test if GSK3 $\beta$  inhibitor can be effectively used *in vivo* to target CSC-enriched breast cancer.

Q. Does GSK3 $\beta$  inhibitor alter the tumorigenic and metastatic potential of breast cancer cells?

Approaches

- Immortalized and experimentally transformed human mammary cell line (HMLER-Snail) and a highly metastatic murine mammary (4T1) cell line were used in an orthotopic model to assess the effect of GSK3 $\beta$  inhibitor on the tumor size and metastatic potential of these cells.
- Immunohistochemical analysis was performed on the tissues harvested from the animals to determine if the drug was effective in inhibiting GSK3 $\beta$  and consequently EMT, in these cells *in vivo*.

## Chapter 3 – Experimental Approaches

### Cell lines

Immortalized human mammary epithelial cells (HMLE), HMLE cells transduced with EMT transcription factor Snail (HMLE-Snail), and Twist (HMLE-Twist) and HMLE cells transformed with Ras and overexpressing Snail transcription factor (HMLER-Snail) were grown in HMLE media, made by mixing MEGM (Lonza) and DMEM/F12 50:50 (Corning) and bovine pituitary extract (BPE) (Lonza), insulin (Sigma), hydrocortisone (Sigma), penicillin, and streptomycin (Gibco/Life Technologies), were added to the media. EMT/CSC enriched basal-like cell line, Sum159 were cultured in Ham's F12 media (Corning) containing additional fetal bovine serum (FBS) (Sigma), hydrocortisone, insulin and penicillin and streptomycin. Transformed breast cancer cell line with epithelial phenotype, MCF7 cells were cultured in DMEM/F12 media containing 10% FBS and penicillin and streptomycin. HEK293T cells were grown in DMEM (Corning) with 10% FBS and penicillin and streptomycin and were used for transfections. TNBC representative MDA MB 231 reporter cells that were used for the small molecule screen were grown in DMEM media with 10% Tet-approved FBS and penicillin and streptomycin. Highly metastatic murine breast cancer cells, 4T1 and mouse embryonic fibroblasts (MEF) derived from wild-type and GSK3 $\beta$  knockout mice were grown in DMEM media with 10%FBS and penicillin and streptomycin. All the cell lines were a generous gift from the Weinberg Lab (Whitehead Institute, MIT) and the MEFs were a gift from the Sarbosov lab (MD Anderson Cancer Center).

### Plasmids used

shRNA to GSK3 $\beta$  in pGIPZ, a lentiviral vector, was purchased from the MD Anderson shRNA core, and was used to silence GSK3 $\beta$  in the three mesenchymal cell lines, HMLE-Snail, HMLE-Twist and Sum159. pMIG, a retroviral vector, was modified to express RFP and luciferase enzyme

to generate pMIRL plasmid, which was then used to label HMLER-Snail and 4T1 cells which were used for *in vivo* experimentation.

## **Transduction**

Transduction is a process by which a foreign DNA is inserted into the genomic DNA of a cell via a viral vector. The transduction procedure is well standardized in the lab and was performed as described previously in [207-209]. HEK293T cells were used to produce the viral particles. The HEK293T cells were plated to 20% confluence. The packaging vectors required for the transduction vary depending on whether a retroviral or the lentiviral vector was used. In case of retroviral vectors, pCMV-VSV-G and pUMVC are used as packaging vectors whereas for lentiviral vectors, pCMV-VSV-G and pCMV- $\Delta$ R8.2dpvr are used as packaging vectors. pCMV-VSV-G has the gene encoding the envelope protein whereas the pUMVC produces MuLV gag and pol required for the packaging of retrovirus and pCMV- $\Delta$ R8.2dpvr encodes the gag and pol required for the packaging of the lentiviral particles [210]. The retroviral or the lentiviral vector carrying the gene of interest or the shRNA was mixed with the appropriate packaging vectors and added to DMEM (without FBS) media. The transfection reagent Eugene was added to this mixture and the tube was gently inverted couple times to thoroughly mix the plasmids and the transfection reagent. This transfection mixture was incubated at room temperature for 15 min following which the mixture was added to the HEK293T plates in a dropwise manner. The plate was swirled gently to ensure that the transfection mix was uniformly distributed and the plates were incubated at 37°C for 12-16 hrs in an incubator. After the incubation, the HEK293T media containing the transfection mix was replaced with media made by mixing the HEK293T media and the media for the target cell line in a 1:4 ratio. This media was harvested after 24hrs, filtered and added to the target cells. This media contains the viral particles produced by the transfected HEK293T. This process was repeated twice and then the target cells that were transduced were selected based on selection

markers present in the viral vector. If the viral vector had a fluorescent marker, the cells are sorted using a flowcytometer to select the successfully transfected cells. In case of antibiotic markers, the transduced cells were replated in media containing the appropriate antibiotic. These successfully transduced cells were used for further analysis.

## **Drugs**

Lithium chloride (LiCl), one of the oldest known GSK3 $\beta$  inhibitor, was dissolved in DMSO to make a stock concentration of 10M. Stock of 10mM BIO (Calbiochem) was made in DMSO and TWS119 (Cayman Chemicals) was diluted in DMSO to make a stock of 10mM and were used in varying working concentrations as detailed in Chapter 6 and 7.

## **MTT assay**

The MTT assays were performed according to the instructions provided in the assay insert to evaluate the IC<sub>50</sub> for each of the cell type for each of the drugs. The 96-plate format was used for this assay. HMLE-Snail, HMLE-Twist and Sum159 cells were trypsinized and viable cells were counted using trypan blue. 1000 viable cells in 100ul of media were plated in each of the wells. The cells were allowed to attach and the following day, the cells were treated with a range of concentrations for each of the drugs from 0.1uM to 100uM. The control wells were treated with DMSO. Following the treatment, 20ul of the MTT reagent (CellTiter 96® AQueous One Solution Cell Proliferation Assay from Promega) was added to each of the well and the treated cells were incubated at 37C. The absorbance at 490 nm was measured and was normalized to the DMSO treated cells. The viability of the cells treated with DMSO were arbitrarily treated as 100% and the viability of the cells treated with the different concentration of the drugs were calculated based on

this. The formula used for calculating the viability of the cells treated with the drugs is as follows

—

$$\% \text{Viability} = \text{Absorbance}_{490} \text{ of treated cells} / \text{Absorbance}_{490} \text{ of DMSO treated cells} * 100$$

Using this data, a dose response curve was generated. The X-axis was transformed to log values and a non-linear regression analysis was performed using Graphpad Prism to calculate the IC50 for all the drugs used in this study.

### **Western blot**

Immunoblot procedure is well established in the lab and was followed as described in [208, 211]. The cells that were to be studied were plated in 10 cm dishes and the cells were treated. Following treatment, the cells were trypsinized and collected into 1.5 ml Eppendorf tubes. The cells were pelleted and the pellets were treated with 100ul of the protein extraction buffer. The protein extraction buffer was prepared by adding kinase inhibitor ("Complete" from Roche) and phosphatase inhibitor ("PhosphoStop" from Roche) to the RIPA buffer (Sigma). The cell pellets were incubated with the protein extraction buffer for 30 min. after which the protein extracts were spun down and the supernatant were transferred to a new Eppendorf tube and were stored at -20C. The concentrations were quantified using Bradford assay from Biorad. Bovine serum albumin (BSA) was used to generate protein standards which were used to plot a standard curve from which the concentration of the proteins was estimated. 50ug of proteins were aliquoted and added to 6X gel loading buffer consisting of bromophenol blue, glycerol and SDS. The proteins were further denatured by heating the protein and gel loading buffer mixture for 10 min at 90C. The heat denatured proteins were spun down and were loaded on to a polyacrylamide gel. The polyacrylamide gel was prepared by mixing acrylamide and bis-acrylamide, resolving or stacking buffer, water. Ammonium persulfate (APS) and tetramethylethylenediamine (TEMED) were



added to catalyze the polymerization. The gels were loaded with 50ug of proteins and the electrophoresis was carried out with the running buffer. After running, the segregated proteins on SDS-PAGE gels were transferred to nitrocellulose membranes. The membranes were blocked with milk and the blocked membranes were probed with different antibodies, Actin (SC-1616-R, Santa Cruz), GSK3 $\beta$  (Cell Signaling), FOXC2 (from collaborator Dr.Naoyuki Miura), Fibronectin (610077, BD Biosciences) and  $\beta$ -catenin (610153, BD Biosciences). Following incubation with the primary antibody, the membrane was incubated with the appropriate secondary antibody conjugated with horse radish peroxidase. Chemiluminescence was used to detect the expression of the proteins.

### **qRT-PCR**

The RNA extraction, quantification, cDNA synthesis and qRT-PCR analysis was performed using the lab standardized method previously described in [212].The cells to be analyzed were harvested and lysed using Trizol (Life Technologies). Qiagen RNA extraction kit was used to extract RNA from these cells. The extracted RNA was quantified using Nanodrop (Thermoscientific). 1000ng of RNA was used for cDNA synthesis using cDNA synthesis kit (Applied Biosystems). The cDNA generated was used for qRT-PCR analysis. 96 or 384 well formats were used for this analysis and the Vii7 system from Applied Biosystems was used to perform this analysis. SyBr green (Applied Biosystems) was used as the detection agent. The CT (threshold cycle) values generated were used to calculate  $\Delta$ CT by subtracting the CT value of the housekeeping or control gene from the CT value of the gene of interest for the same sample. This serves to normalize the CT values for each sample based on the expression of the ubiquitous genes such as Actin or GAPDH.  $\Delta\Delta$ CT was computed by subtracting the  $\Delta$ CT of a gene in the control sample from the  $\Delta$ CT of the same gene in the experimental sample.  $\Delta\Delta$ CT is used to assess the fold change in the expression of genes by using the formula  $2^{\Delta\Delta CT}$  including GSK3 $\beta$ ,

Fibronectin, Vimentin, E-cadherin and Snail. The fold changes that were calculated were graphed using Graphpad Prism.

### **Mammosphere assay**

The sphere assay was performed as described in [60]. Cells were harvested by trypsinization and counted using trypan blue to ensure that the only live cells are plated for the mammosphere assay. 1000 cells were plated into each well of the low attachment 96 well plate in 100  $\mu$ l of the mammosphere media. The mammosphere media is MEGM media with 1% methylcellulose (Sigma). EGF (10ng/ml) (Sigma-Aldrich), FGF (20ng/ml) (BD Biosciences) and heparin (4 $\mu$ g/ml) (Sigma) were added to aliquots before feeding the spheres. The spheres were allowed to grow for 10 days after which the spheres with diameter greater than 100 $\mu$ m were counted. For drug treatment, the drug was added to the media every time the media was refreshed every 2 days. For the pre-treatment assay, the cells were treated with GSK3 $\beta$  inhibitors for 24 hrs. Following treatment, viable cells were counted using trypan blue and were plated for the mammosphere assays. The mammosphere media was refreshed for every 2 days. After 10 days, the mammospheres were counted.

### **FACS analysis**

The expression of CD24/44 surface antigen was performed as previously detailed in [60]. Cells to be used for this analysis were harvested and counted using trypan blue.  $5 \times 10^5$  cells were used for this analysis. The cells to be analyzed were suspended in (fluorescence activated cell sorting) FACS buffer (PBS with 2% FBS). CD24 conjugated with PE (BD Biosciences) and CD44 conjugated with APC (BD Biosciences) were incubated with the cells for 30 min. on ice. Following the incubation, the cells were thoroughly washed with the FACS buffer which is 1% FBS in

Phosphate Buffer Saline (PBS). The cells resuspended in the FACS buffer were analyzed using BD Accuri. Unstained cells were used as negative control. FACS uses differences in the light scattering ability of the cells to differentiate between different populations of the cells within a single pool of cells. The composition of each type of cell is different and therefore scatters the light projected on it in differently. Similarly, the fluorescently labeled cells scatter light depending on the fluorophore present on the cell. FACS was used to analyze the expression of CD24 and CD44 on the surface of the cells and the cell surface profile thus generated were compared between the treated and the untreated cells.

### **Wound healing assay**

The parameters for the wound healing assay was established and described in [208]. Cells were plated on 6 well plates and on coverslips (for performing immunofluorescence studies) and allowed to grow to confluence. Once the cells were confluent, a scratch was made using a pipette tip. The loosened cells were washed away using PBS. The cells were then incubated with media containing either DMSO or GSK3 $\beta$  inhibitors. The scratch was imaged for the time 0 using the fluorescent microscope (Axio). The initial wound was measured and was used to determine the percentage of wound closed. The closing of the wound was monitored. 9 hrs. after the treatment, the unclosed wound was measured. The cells were treated with either DMSO or GSK3 $\beta$  inhibitor and the scratch was imaged and quantified after 9 hrs. Following this the scratches were fixed for immunofluorescence studies.

### **Immunofluorescence**

The immunofluorescence studies were conducted as detailed in [208]. For immunofluorescence studies, the cells were plated on coverslips. The cells were fixed with 2% paraformaldehyde (USB)

and permeabilized with Tween20 (Fisher Bioreagents). These cells were blocked with albumin overnight and exposed to primary antibody of interest for 3 hrs. Following this the cells were washed with TBST thoroughly and then exposed to the appropriate secondary antibody which was labeled with a fluorophore (Alexa Fluor from Life Technologies). The nuclei of the labeled cells were stained with DAPI and this were then mounted and covered with a coverslip. The labeled cells were then imaged using Axio microscope.

### ***In vivo* experiment to test the efficacy of TWS119**

The *in vivo* studies were carried out based on the methodology described in [60]. HMLER-Snail and 4T1 cells were labeled with pMIRL. Therefore, the cells were red and the red cells were sorted using FACS to select the cells that have been successfully transduced. pMIRL also expressed the luciferase gene and were used for *in vivo* experiments. 10 NOD/SCID mice were used for the HMLER-Snail experiments.  $1 \times 10^6$  labelled cells were injected orthotopically and the cells were allowed to grow until palpable tumors formed (1 week). The mice were randomized into 2 groups; one group was control and were treated with DMSO whereas the other group was treated with TWS119 (30 mg/kg) intraperitoneally. Similarly,  $1 \times 10^4$  labeled 4T1 cells were orthotopically injected into 20 wild-type mice. These mice were randomized into 2 groups once the mice developed palpable tumors (4 days). One group was treated with DMSO and the other group was treated with TWS119. All the mice were imaged weekly to monitor the tumor progression. At the end of the experiment, the mice were sacrificed and the tumors and the lungs were isolated, fixed and embedded. The luminescence data were analyzed and plotted.

### **Immunohistochemistry**

Immunohistochemical (IHC) staining was performed on the tumor samples isolated from mice following the procedure described in [213]. The tumor tissues were fixed with 10% formaldehyde (formalin) for about 12-16 hrs after which they were stored in phosphate buffered saline (PBS) and subsequently paraffin embedded. The paraffin embedded sections were cut to give 5µm thin sections which were used for the staining procedure. Following deparaffinization and rehydration, antigen retrieval was performed by heating the slide containing the tissue section with citrate buffer (pH-6) in a microwave for 20 min. Endogenous peroxidase activity was quenched using 3% hydrogen peroxide and the sections were blocked at room temperature with 5% BSA and 0.3% Triton-X in PBS for one hour. Sections thus processed, were incubated with 1:100 dilution of primary antibodies, overnight at 4°C. Following the removal of the primary antibodies, the slides were treated with Biotinylated secondary antibodies (Vector labs) for one hour and incubated with Vectastain ABC reagent for 30 min. Slides were treated with DAB substrate (Vector labs) for 10 min, dehydrated, counterstained with Hematoxylin and were mounted and imaged. All slides were stained simultaneously with the controls in an automated stainer (Dako AutoStainer Plus). The Envision Dual Link-HRP (Dako) was used for detection and diaminobenzidine was used as chromogen (Dako Envision Kit). Hematoxylin (Dako) was employed as counterstaining. Finally, the slides were dehydrated and mounted with a cover slip and imaged.

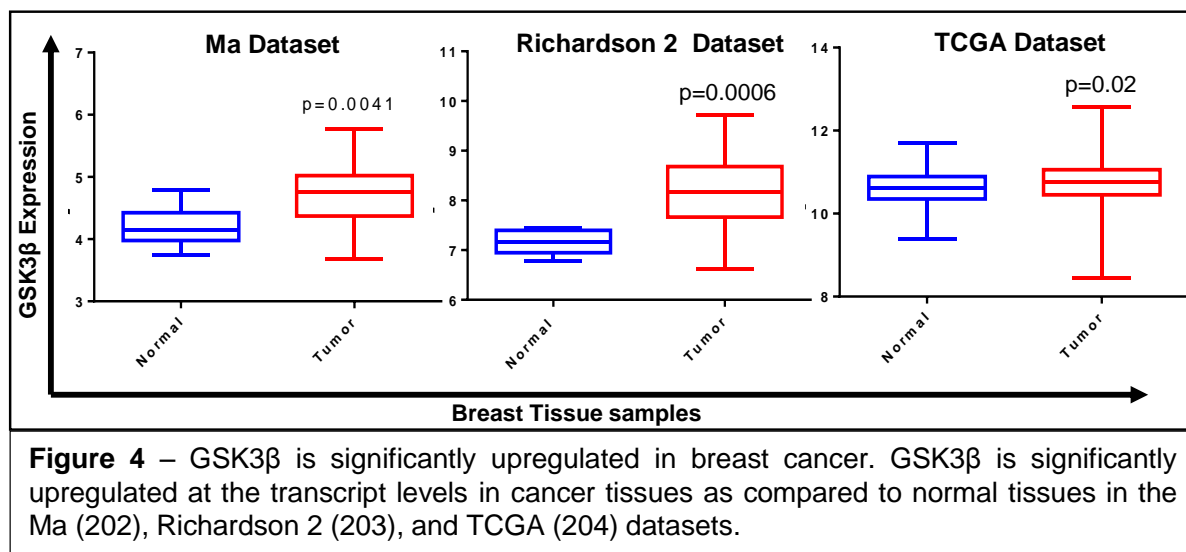
## **Statistical Method**

All the samples were assayed in triplicate. The *in vitro* experiments were repeated at least three independent times except for the validation studies and the experiments using the 11 drugs isolated from the small molecule screen which were repeated 2 times. The *in vivo* experiments included at least 5 mice per group as mention in the “experimental approaches”. All the graphs are represented as mean±s.e.m., and the p values (significance) were calculated using Student’s unpaired two-tailed *t*-test.

## Chapter 4 – Aim 1 – Determine if GSK3 $\beta$ is upregulated in breast cancer and if this upregulation has clinical significance.

### 4A. GSK3 $\beta$ is upregulated in breast cancer.

It is very difficult to classify a kinase as a tumor suppressor or promoter as its role depends on the context such as availability of substrates, localization and presence of other regulatory factors. We analyzed several publicly available datasets and found that in the Ma dataset [203], the Richardson 2 dataset [204] and the TCGA data set [205] in which there is a significant overexpression of GSK3 $\beta$  in breast cancer tissues compared to normal breast tissue [214, 215] (Figure 4). We observed a significant upregulation of GSK3 $\beta$  in the Richardson data set and this is of note because the Richardson data set mainly comprises of basal-like breast cancer samples. Therefore, the upregulation of GSK3 $\beta$  is more marked in this dataset as compared to the other datasets that consist of samples of all the different types of breast cancer.



#### 4B. Elevated expression of GSK3 $\beta$ correlates with worse overall survival among TNBC patients.

Using KM plotter, we studied the significance of the high of GSK3 $\beta$  in breast cancer. KMplotter is an online tool that allows us to query the effect of a gene of interest on the overall survival of patients [216]. This tool pools all the available patient survival data from multiple databases and probes all the data available for the gene queried and generates a KM plot where the patients are classified as high or low-expressing based on the median gene expression in the dataset. KM plots are survival curves generated to indicate the time to an event [217]. We found that the higher expression of GSK3 $\beta$  corresponds to worse overall survival in breast cancer patients. The breast cancer patients were classified on the basis of the intrinsic subtype and a similar correlation between elevated expression of GSK3 $\beta$  and worse survival was observed in patients with Luminal A breast cancer, luminal B breast cancer and basal breast cancer (Figure 5). The hazard ratio for several major players in different sub-types of breast cancer were extracted and tabulated in Table 1 and plotted using Circos plot (Figure 6). Of all the Wnt signaling molecules examined, GSK3B and FZD2 had HR greater than 1 in all the 4 categories of breast cancers investigated indicating that higher level of expression of these genes correlate with worse overall survival in these patients. However, the correlation between the expression of FZD2 and the overall survival in the breast cancer patients examined in this section was not significant ( $p>0.01$ ) (Table 1).

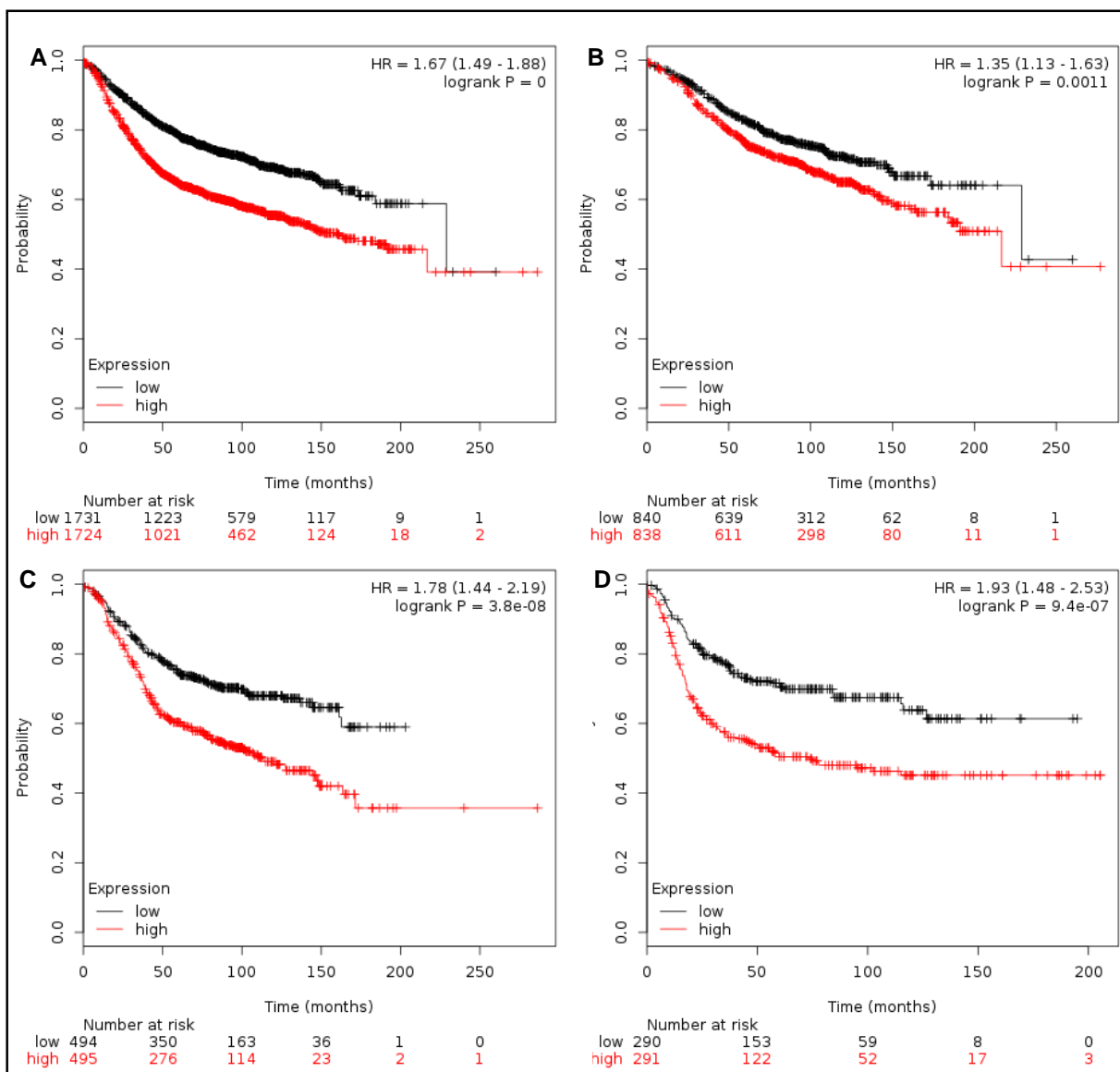


**Figure 5** – Higher GSK3 $\beta$  expression correlates with worse overall breast cancer survival. Kaplan Meier (Km) Plots for GSK3 $\beta$  in all breast cancer (A), luminal A (B), luminal B (C), and basal-like breast cancers (D).



		All		Luminal A		Luminal B		Basal	
		HR	P	HR	P	HR	P	HR	P
1	GSK3B	1.67 (1.49-1.88)		0.135 (1.13-1.63)	0.0011	1.78 (1.44-2.19)	0.000000038	1.93 (1.48-2.53)	0.00000094
2	FZD5	1.1 (0.98-1.23)	0.11	1.1 (0.92-1.32)	0.3038	1.03 (0.84-1.26)	0.77	0.74 (0.57-0.97)	0.027
3	FZD2	1.09 (0.97-1.22)	0.16	1.13 (0.94-1.35)	0.2	1.3 (1.06-1.6)	0.011	1.09 (0.84-1.41)	0.5363
4	FZD1	0.96 (0.86-1.08)	0.51	0.86 (0.72-1.03)	0.107	1.09 (0.89-1.34)	0.39	1.08 (0.84-1.4)	0.5487
5	LRP6	0.94 (0.84-1.06)	0.32	0.84 (0.7-1.01)	0.0632	1.12 (0.91-1.37)	0.27	0.88 (0.68-1.14)	0.3277
6	WIF1	0.92 (0.82-1.03)	0.16	0.84 (0.7-1.01)	0.0663	0.95 (0.78-1.17)	0.6399	0.72 (0.55-0.94)	0.0139
7	APC	0.89 (0.79-1)	0.046	0.8 (0.67-0.96)	0.018	0.97 (0.79-1.18)	0.75	1.22 (0.94-1.59)	0.127
8	DKK1	0.87 (0.78-0.98)	0.0182	0.73 (0.61-0.88)	0.0007	0.88 (0.72-1.08)	0.24	0.7 (0.54-0.9)	0.0062
9	CTNNB1	0.87 (0.77-0.97)	0.014	0.79 (0.66-0.94)	0.0099	0.85 (0.69-1.04)	0.1104	1.21 (0.93-1.57)	0.1564
10	FZD3	0.83 (0.74-0.93)	0.0015	0.83 (0.69-0.99)	0.041	0.84 (0.68-1.03)	0.087	0.8 (0.61-1.03)	0.0856
11	DVL1	0.81 (0.72-0.91)	0.00042	0.76 (0.64-0.92)	0.0036	0.91 (0.74-1.11)	0.3621	0.88 (0.68-1.14)	0.3406
12	FZD8	0.81 (0.72-0.91)	0.00034	0.86 (0.72-1.03)	0.11	0.75 (0.61-0.91)	0.0047	0.86 (0.66-1.11)	0.2494
13	LRP5	0.81 (0.72-0.91)	0.00038	0.71 (0.59-0.86)	0.00027	0.85 (0.69-1.04)	0.12	0.8 (0.62-1.04)	0.096
14	FZD4	0.8 (0.71-0.89)	0.00011	0.69 (0.57-0.83)	0.000061	0.91 (0.75-1.12)	0.38	0.88 (0.68-1.14)	0.34
15	AXIN1	0.76 (0.67-0.85)	2.10E-06	0.79 (0.65-0.94)	0.0089	0.71 (0.58-0.87)	0.00081	0.74 (0.57-0.96)	0.0216
16	GSK3A	0.75 (0.67-0.84)	8.10E-07	0.68 (0.57-0.82)	0.000038	0.78 (0.63-0.95)	0.015	0.74 (0.57-0.96)	0.0222
17	WNT3	0.73 (0.65-0.82)	8.80E-08	0.78 (0.65-0.94)	0.0074	0.94 (0.77-1.1)	0.58	1.12 (0.87-1.46)	0.3756
18	LEF1	0.71 (0.64-0.8)	9.10E-09	0.8 (0.67-0.96)	0.018	0.76 (0.62-0.93)	0.0073	0.73 (0.56-0.95)	0.017
19	DVL2	0.68 (0.6-0.76)	4.80E-11	0.62 (0.52-0.75)	0.0000003	0.75 (0.61-0.92)	0.0053	0.66 (0.51-0.86)	0.0018
20	TCF7	0.67 (0.59-0.75)	5.80E-12	0.75 (0.62-0.9)	0.0016	0.56 (0.46-0.69)	0.000000028	0.72 (0.55-0.93)	0.0119

**Table 1** – List of the hazard ratios and p-value of the players of the Wnt signaling in breast cancers.

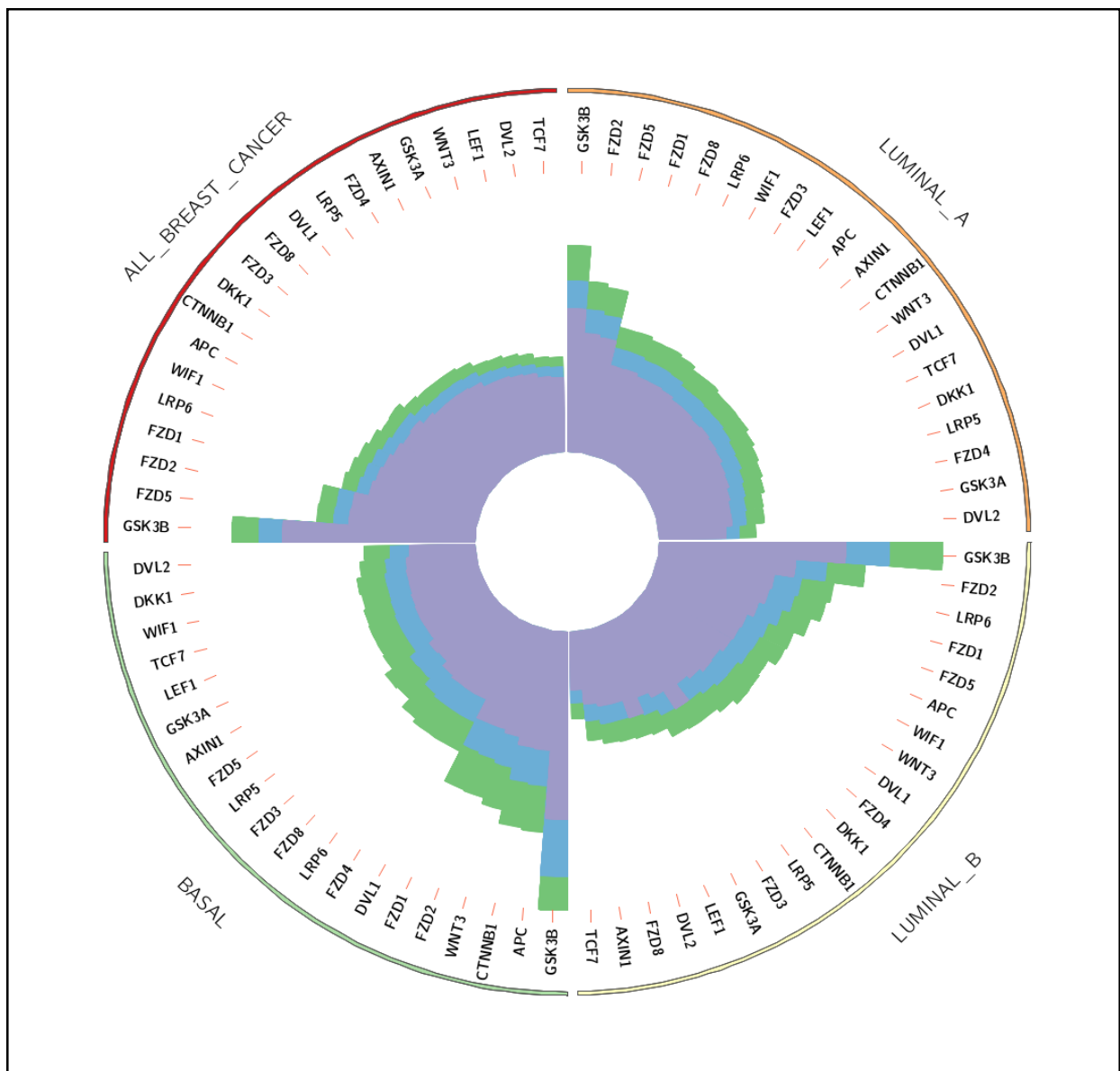


**Figure 6** – Circos plot of the hazard ratios of components of Wnt signaling pathway. The hazard ratio (HR) from the Km Plots for all the components of the Wnt signaling pathways were plotted using Circos. The green bar marks the upper limit of the HR, the purple bar plots the lower limit of HR and the blue bars plot the average HR. The HRs indicate that GSK3 $\beta$  has the highest HR among all the Wnt signaling pathway players in all the subtypes of breast cancer.

Additionally, KM plots were also generated for breast cancers based on the clinical classifications i.e. ER/PR+, HER2+ and TNBCs. The KM plots indicated that there was no significant correlation between the level of GSK3 $\beta$  expression and the overall survival of the patients with ER/PR+ or HER2+ breast cancers (Figure 7). In the case of ER/PR+ breast cancers the hazard ratio was 1.6

and the p-value was 0.08. In the case of HER2 + breast cancer patients, the hazard ratio was 0.81 and the p-value was 0.6. However, in the case of TNBCs, the hazard ratio for GSK3 $\beta$  was 2.22 and this value was higher than that for most of the other major players in the Wnt signaling pathway and with a significant p-value of 0.0051 (Figure 7). Thus the correlation between the overexpression of GSK3 $\beta$  and the worse overall survival was found to be significant only in the patients with TNBC (Figure 7). Among the Wnt signaling pathway players tested, GSK3 $\beta$  was the only molecule for which the correlation between the expression and survival was significant in TNBCs (Figure 8).

Summary – Aim 1: Thus far, we examined multiple datasets to assess the level of expression of GSK3 $\beta$  in tumor tissues in comparison with that in the normal breast tissues. We found that GSK3 $\beta$  was highly upregulated in breast cancer tissues as compared to the normal breast tissues in Ma dataset, Richardson 2 dataset and the TCGA. This indicated that the expression of GSK3 $\beta$  is dysregulated in breast cancers. We then analyzed publicly available patient survival data using KMPlotter to determine if there is a significant correlation between the expression of GSK3 $\beta$  and other Wnt signaling molecules in TNBC and indeed observed a significant correlation between elevated levels of GSK3 $\beta$  and worse overall survival among TNBC patients. Our results taken together serve to establish the basis for testing GSK3 $\beta$  as a potential target for TNBCs.

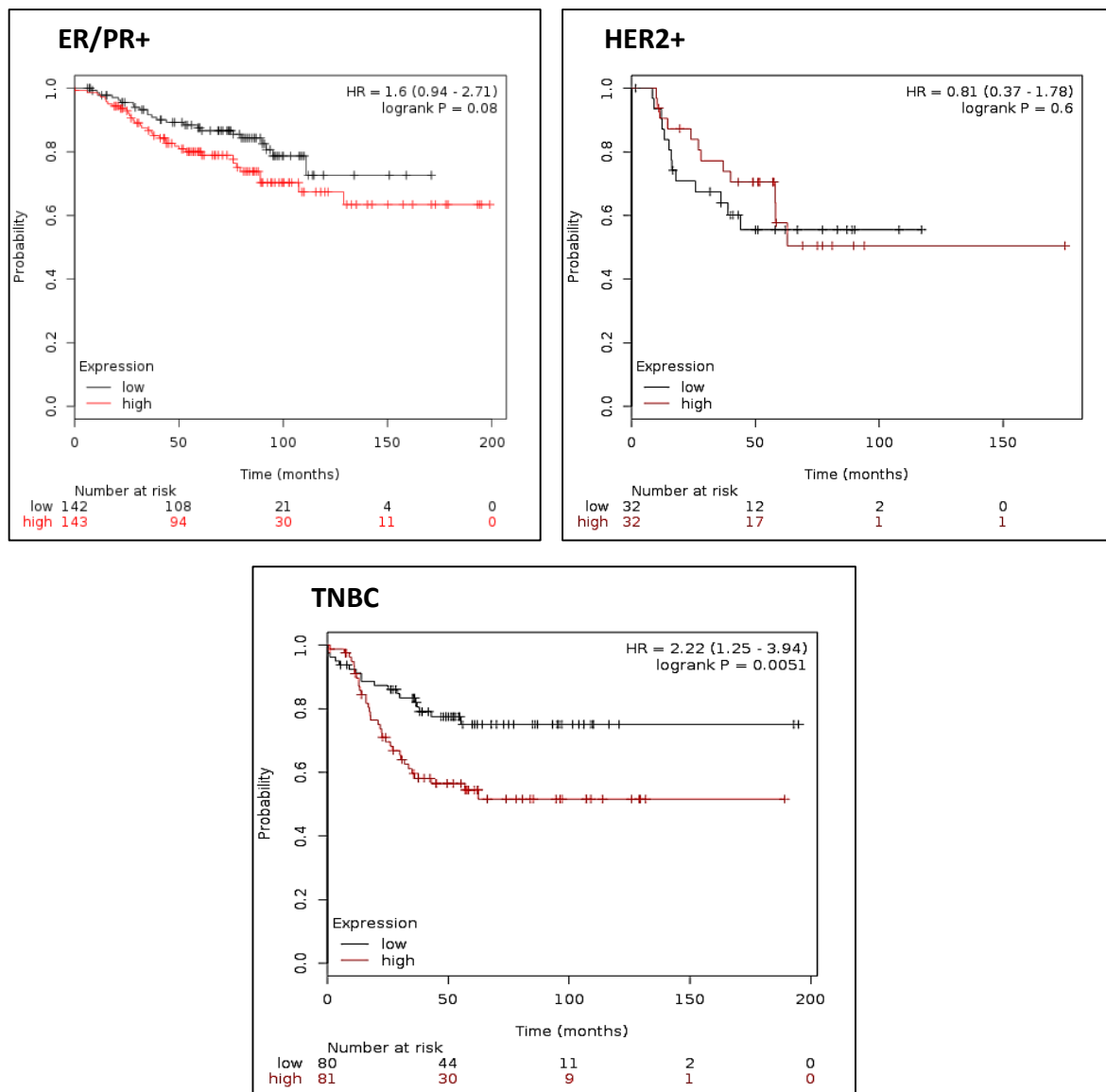
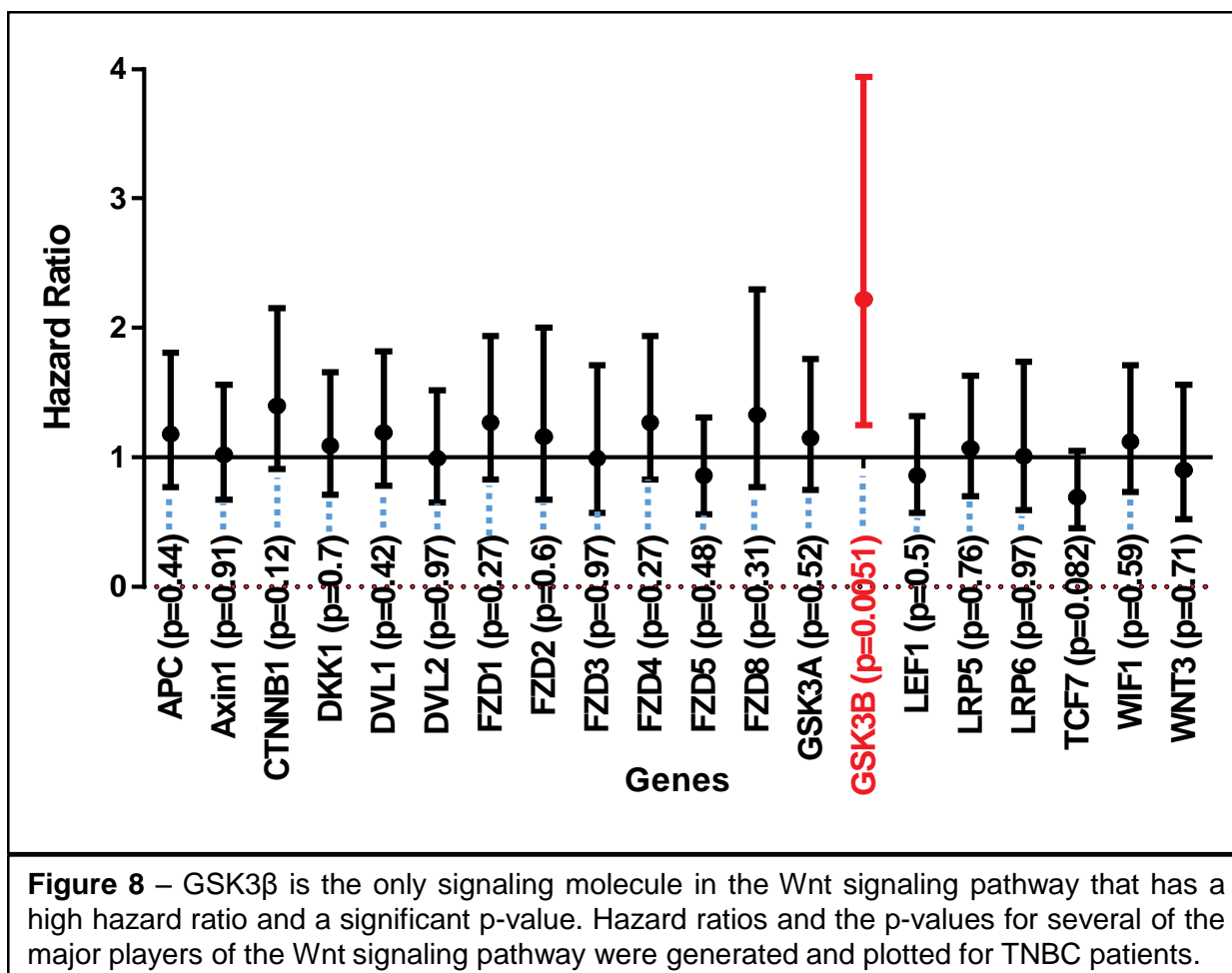


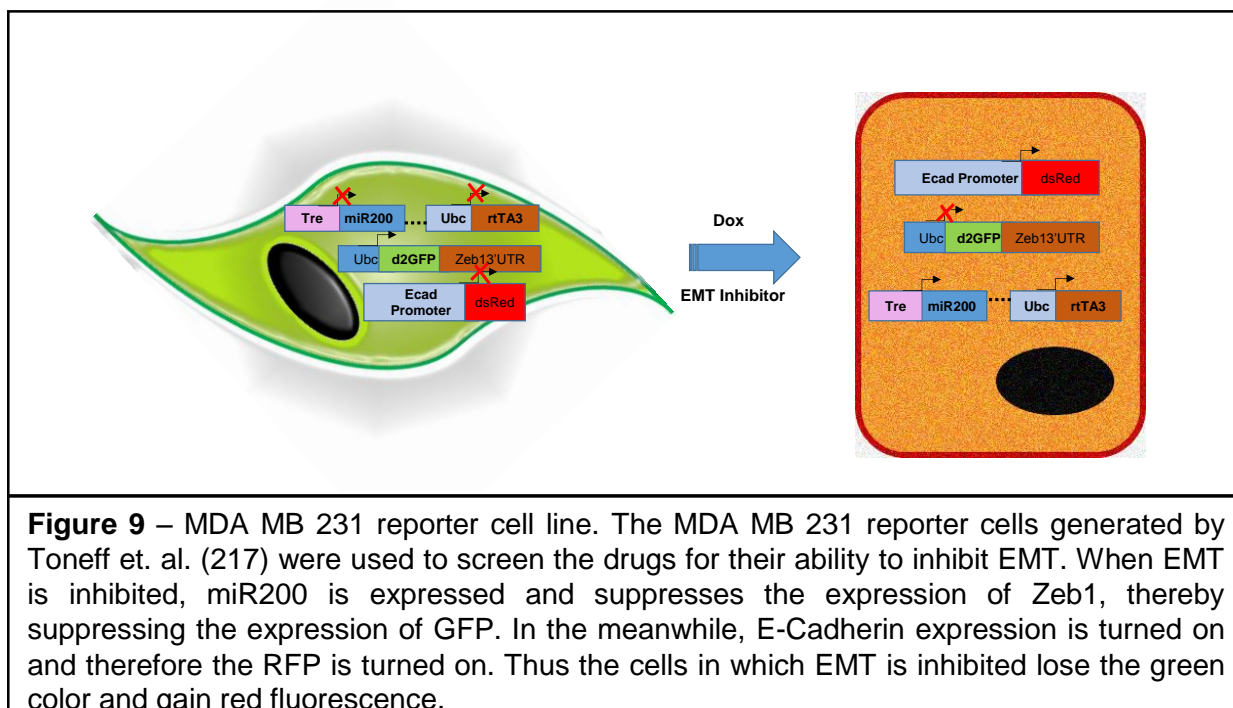
**Figure 7** – The upregulation of GSK3 $\beta$  significantly correlated with worse survival of TNBCs. Kaplan Meier Plots were generated for ER/PR+, HER2+ and TNBC patients to determine how GSK3 $\beta$  correlates with the survival of these patients. The upregulation of GSK3 $\beta$  significantly correlated with worse survival only in TNBCs and no significant correlation was observed in other types of breast cancer.



## **Chapter 5 – Aim 2 – Investigate the relationship between GSK3 $\beta$ and Epithelial-Mesenchymal Transition (EMT) and cancer stem cells (CSCs) in TNBCs**

### **5A. Small molecule screen indicates that BIO is a potential candidate capable of decreasing mesenchymal phenotype.**

A small molecule screen was conducted using MDA MB 231 reporter cells [218] (Figure 9). The reporter cells have a Zeb1 reporter and E-cadherin promoter reporter. The Zeb1 reporter consists of the 3' UTR of Zeb1 that is cloned downstream the gene coding for GFP. When the cells have a mesenchymal phenotype, miR200 expression is low and it cannot bind to the 3' UTR of Zeb1 and therefore the expression of GFP, which is cloned upstream the 3'UTR of Zeb1 gene, is not inhibited and the cells are green in color. When EMT is inhibited, the cells upregulate the expression of miR200 which can now bind to the 3'UTR of Zeb1 and inhibit the expression of Zeb1 gene and the expression of GFP in the Zeb1 reporter. Hence the green coloration associated with mesenchymal properties is lost. The reporter cells also have an E-cadherin promoter reporter in which dsRed is cloned behind the E-cadherin promoter. Therefore, with the acquisition of epithelial phenotype the cells express E-cadherin and as a result dsRed cloned downstream the E-cadherin promoter is turned on and the cells become red. The reporter cells also express doxycycline (dox)-inducible miR200 which was used as a positive control.



The MDA MB 231 reporter cells were plated in 384 wells and were treated with a library of small molecule inhibitors listed in Table 2-14. The cells were treated with three different concentrations (0.1 $\mu$ M, 1 $\mu$ M and 10 $\mu$ M) of each of drug in the library for 5 days, following which the plates were scanned for the presence of red and green fluorescence. The ratio of red to green was calculated for all the wells and 11 drugs that produced a ratio greater than 1.5 were selected (Table 15). The short listed drugs consisted of kinase inhibitors and histone deacetylase (HDAC) inhibitors. It was interesting to note that among all the compounds tested, BIO, a GSK3 $\beta$  inhibitor was one of the candidates that were able to decrease Zeb1 promoter activity (green) and increase E-cadherin promoter activity (red) in the reporter cells.

Drugs used in the small molecule screen			
1	FG-4592	45	Dovitinib (TKI-258, CHIR-258)
2	Panobinostat (LBH589)	46	Sunitinib Malate
3	Obatoclox Mesylate (GX15-070)	47	HA14-1
4	LAQ824 (Dacinostat)	48	U0126-EtOH
5	Varespladib (LY315920)	49	JNJ-38877605
6	Cabozantinib (XL184, BMS-907351)	50	SRT1720
7	Malotilate	51	17-AAG (Tanespimycin)
8	Barasertib (AZD1152-HQPA)	52	Capecitabine
9	PA-824	53	Cisplatin
10	JNJ-26854165 (Serdemetan)	54	Plinabulin (NPI-2358)
11	ENMD-2076	55	Raltitrexed
12	Nintedanib (BIBF 1120)	56	Ridaforolimus (Deforolimus, MK-8669)
13	Motesanib Diphosphate (AMG-706)	57	Temsirolimus (CCI-779, NSC 683864)
14	Nutlin-3	58	Belinostat (PXD101)
15	BTZ043 Racemate	59	GDC-0879
16	Foretinib (GSK1363089)	60	Odanacatib (MK-0822)
17	Everolimus (RAD001)	61	YM155 (Sepantronium Bromide)
18	Brivanib Alaninate (BMS-582664)	62	17-DMAG (Alvespimycin) HCl
19	Docetaxel	63	CEP-18770 (Delanzomib)
20	AT13387	64	CP-724714
21	WZ4002	65	Regorafenib (BAY 73-4506)
22	Danoprevir (ITMN-191)	66	CUDC-101
23	Afatinib (BIBW2992)	67	Erlotinib HCl (OSI-744)
24	NVP-AEW541	68	Trichostatin A (TSA)
25	AUY922 (NVP-AUY922)	69	NVP-ADW742
26	MLN8054	70	OSU-03012 (AR-12)
27	SGX-523	71	Palbociclib (PD-0332991) HCl
28	TW-37	72	Alisertib (MLN8237)
29	ADL5859 HCl	73	Ivacaftor (VX-770)
30	SNS-314 Mesylate	74	MK-8245
31	Lenvatinib (E7080)	75	WZ3146
32	MK-2866 (GTx-024)	76	WZ8040
33	BIBR 1532	77	TAK-700 (Orteronel)
34	BMS-536924	78	Lapatinib (GW-572016) Ditosylate
35	Sorafenib Tosylate	79	Y-27632 2HCl
36	PHA-665752	80	OSI-906 (Linsitinib)
37	Vatalanib (PTK787) 2HCl	81	Danuserib (PHA-739358)
38	GSK690693	82	XL147
39	BMS-754807	83	AT9283
40	Andarine	84	SNS-032 (BMS-387032)
41	S3I-201	85	Ganetespib (STA-9090)
42	ABT-751 (E7010)	86	CYC116
43	BIIB021	87	XAV-939
44	Aprepitant	88	Irinotecan

**Table 2** – List of the drugs from the Sellekchem small molecule library that were tested in with their commonly used acronyms in parenthesis.



Table 2 continued...			
89	Decitabine	133	Tivozanib (AV-951)
90	PFI-1 (PF-6405761)	134	Oxaliplatin
91	Amuvatinib (MP-470)	135	Enzalutamide (MDV3100)
92	Rufinamide	136	Avagacestat (BMS-708163)
93	Asenapine	137	Ki16425
94	Flupirtine maleate	138	Losartan Potassium (DuP 753)
95	Ki8751	139	Cefoselis Sulfate
96	Drospirenone	140	Meropenem
97	Pirarubicin	141	Tenofovir
98	Bafilomycin A1(Baf-A1)	142	Sildenafil Citrate
99	Nanchangmycin	143	PHA-680632
100	Dimesna	144	Nelarabine
101	Clofarabine	145	KU-0063794
102	Latrepirdine	146	Dienogest
103	Posaconazole	147	PD173074
104	Biperiden HCl	148	Costunolide
105	Ginkgolide B	149	GSK1059615
106	Epothilone B (EPO906, Patupilone)	150	Daptomycin
107	Ruxolitinib (INCB018424)	151	Mizoribine
108	Rocuronium Bromide	152	Tigecycline
109	Droxinostat	153	Tianeptine sodium
110	Aurora A Inhibitor I	154	Cilomilast
111	Dutasteride	155	Bleomycin Sulfate
112	OSI-930	156	2-Methoxyestradiol (2-MeOE2)
113	Vinblastine	157	Entecavir Hydrate
114	Prasugrel	158	WYE-354
115	Budesonide	159	Dexamethasone (DHAP)
116	Granisetron HCl	160	MGCD-265
117	BMS-707035	161	Doripenem Hydrate
118	Isotretinoin	162	Nafamostat Mesylate
119	Stavudine (d4T)	163	Trilostane
120	Ranolazine 2HCl	164	Varenicline Tartrate
121	Ispinesib (SB-715992)	165	Zibotentan (ZD4054)
122	PIK-75	166	Carboplatin
123	Dexrazoxane HCl (ICRF-187, ADR-529)	167	Agomelatine
124	JNJ-7706621	168	Nepafenac
125	Cinacalcet HCl	169	Adapalene
126	Epothilone A	170	Etodolac
127	TG100-115	171	Rigosertib (ON-01910)
128	Bafetinib (INNO-406)	172	Gestodene
129	Lopinavir	173	Pelitinib (EKB-569)
130	Tenofovir Disoproxil Fumarate	174	Bimatoprost
131	Rilmenidine	175	Elaiophylin
132	Tipifarnib	176	Atazanavir Sulfate

Table 2 continued...			
177	VX-745	221	Doxercalciferol
178	GW501516	222	Oligomycin A
179	Iloperidone	223	PHA-793887
180	LY2228820	224	Pracinostat (SB939)
181	SAR245409 (XL765)	225	Vinorelbine
182	BIX 02189	226	DMXAA (Vadimezan)
183	MK-3207 HCl	227	Dapagliflozin
184	PHT-427	228	Pomalidomide
185	BS-181 HCl	229	Tie2 kinase inhibitor
186	Erteberel (LY500307)	230	Darunavir Ethanolate
187	Erythromycin	231	Enalaprilat Dihydrate
188	Thiazovivin	232	Calcifediol
189	GSK429286A	233	VX-222 (VCH-222, Lomibuvir)
190	MC1568	234	Naratriptan
191	Mycophenolate Mofetil	235	Natamycin
192	AT7519	236	LY2811376
193	R406 (free base)	237	Telaprevir (VX-950)
194	AM1241	238	Nebivolol
195	AT7867	239	PD318088
196	Fasudil (HA-1077) HCl	240	Candesartan
197	Cefoperazone	241	Triamcinolone Acetonide
198	Amphotericin B	242	Lubiprostone
199	AZD6482	243	TSU-68 (SU6668, Orantinib)
200	Pimasertib (AS-703026)	244	Zosuquidar (LY335979) 3HCl
201	HMN-214	245	PIK-93
202	Lactulose	246	CCT129202
203	MK-1775	247	Hesperadin
204	Org 27569	248	Saxagliptin
205	SB408124	249	Pimobendan
206	BMS-777607	250	Tazarotene
207	BIRB 796 (Doramapimod)	251	Apixaban
208	Sildenafil	252	Allopurinol
209	Amprenavir	253	Amorolfine HCl
210	Marbofloxacin	254	Safinamide Mesylate
211	SB525334	255	Daclatasvir (BMS-790052)
212	AEE788 (NVP-AEE788)	256	Ponatinib (AP24534)
213	Cyclosporine	257	Tosedostat (CHR2797)
214	Quizartinib (AC220)	258	BIX 02188
215	CP-673451	259	EX 527 (Selisistat)
216	Febuxostat	260	AZD8055
217	VX-809 (Lumacaftor)	261	KU-60019
218	RO4929097	262	Semagacestat (LY450139)
219	Prilocaine	263	Allopurinol Sodium
220	Telbivudine	264	Flurbiprofen

Table 2 continued...			
265	Ipratropium Bromide	309	Desonide
266	Adefovir Dipivoxil	310	Esomeprazole Magnesium
267	Quetiapine Fumarate	311	Verteporfin
268	Fenoprofen Calcium	312	Azithromycin
269	Potassium Iodide	313	Alibendol
270	Nefiracetam	314	Elvitegravir (GS-9137, JTK-303)
271	PCI-34051	315	Benidipine HCl
272	Epalrestat	316	Lornoxicam
273	Tiopronin	317	Mecarbinat
274	Cilazapril Monohydrate	318	Fenoldopam
275	Isepamicin	319	Temocapril
276	Betamethasone Dipropionate	320	Divalproex Sodium
277	Azathioprine	321	Gadodiamide
278	Cefditoren Pivoxil	322	Teniposide
279	Erdosteine	323	Albendazole Oxide
280	Talc	324	Irsogladine
281	Cyclocytidine HCl	325	Maraviroc
282	PF-573228	326	Ginkgolide A
283	Phentolamine Mesylate	327	Cytidine
284	Pamidronate	328	Atorvastatin Calcium
285	Trimebutine	329	Dexmedetomidine HCl
286	Almotriptan Malate	330	Rasagiline Mesylate
287	Meprednisone	331	Emtricitabine
288	Terbinafine	332	Oxybutynin
289	Chlorprothixene	333	Ranitidine
290	Pranlukast	334	Flubendazole
291	Vitamin B12	335	Nystatin (Fungicidin)
292	Methscopolamine	336	Raltegravir (MK-0518)
293	BMS-265246	337	Uridine
294	Cyproterone Acetate	338	Gimeracil
295	Balofloxacin	339	Moexipril HCl
296	Ivabradine HCl	340	Betaxolol
297	Ambrisentan	341	Naltrexone HCl
298	Betamethasone Valerate	342	Deferasirox
299	Rifabutin	343	Pitavastatin Calcium
300	Oxytetracycline (Terramycin)	344	Acadesine
301	Atracurium Besylate	345	Dapoxetine HCl
302	Fluvastatin Sodium	346	Rimantadine
303	Adenine HCl	347	Pramipexole 2HCl Monohydrate
304	Suplatast Tosylate	348	Fenticonazole Nitrate
305	Doxifluridine	349	Terazosin HCl
306	Lafutidine	350	Clevidipine Butyrate
307	Rivastigmine Tartrate	351	Detomidine HCl
308	Temocapril HCl	352	Imidapril HCl

Table 2 continued...			
353	Cisatracurium Besylate	397	Licofelone
354	Atropine	398	Neratinib (HKI-272)
355	Dabigatran Etexilate	399	Tebipenem Pivoxil
356	Bazedoxifene Acetate	400	AG-14361
357	SB743921	401	Avasimibe
358	CYT997 (Lexibulin)	402	Raf265 derivative
359	PIK-293	403	Mubritinib (TAK 165)
360	Apatinib	404	CAL-101 (Idelalisib, GS-1101)
361	LY2157299	405	Palomid 529 (P529)
362	AR-42	406	(+)-Usniacin
363	Andrographolide	407	Bergenin
364	Dronedarone HCl	408	Dextrose
365	Roflumilast	409	LDE225 (NVP-LDE225,Erismodegib)
366	LY2608204	410	RAF265 (CHIR-265)
367	PD128907 HCl	411	LY2784544
368	BGJ398 (NVP-BGJ398)	412	AZD8931 (Sapitinib)
369	A-966492	413	BMS-794833
370	Vinflunine Tartrate	414	PP242
371	PF-3716556	415	PIK-294
372	Telatinib	416	Fesoterodine Fumarate
373	Abiraterone Acetate	417	3-Indolebutyric acid (IBA)
374	Asiatic Acid	418	Bilobalide
375	Conivaptan HCl	419	S- (+)-Rolipram
376	AZD8330	420	Sitafloxacin Hydrate
377	LY2886721	421	AZD1480
378	Rosuvastatin Calcium	422	MLN2238
379	AST-1306	423	GSK461364
380	SGI-1776 free base	424	NVP-BHG712
381	AZ 960	425	CYT387
382	UK 383367	426	VX-765
383	Esomeprazole Sodium	427	GW791343 HCl
384	BKM120 (NVP-BKM120, Buparlisib)	428	Aloe-emodin
385	Azomycin	429	Cinchonidine
386	Arbidol HCl	430	Bazedoxifene HCl
387	GSK1292263	431	CGS 21680 HCl
388	KW-2449	432	PF-4708671
389	Givinostat (ITF2357)	433	MLN9708
390	SB505124	434	R406
391	Aliskiren Hemifumarate	435	OSI-420
392	DAPT (GSI-IX)	436	SB590885
393	TAME	437	Eltrombopag
394	Volasertib (BI 6727)	438	Degrasyn (WP1130)
395	CX-4945 (Silmitasertib)	439	Laetrile
396	Baicalin	440	Cyclosporin A

Table 2 continued...			
441	Dihydroartemisinin (DHA)	485	Gramine
442	Kaempferol	486	Methyl-Hesperidin
443	Naringin	487	Oridonin
444	Puerarin	488	Sclareol
445	Stigmasterol	489	Ursolic Acid
446	Ammonium Glycyrrhizinate	490	Evodiamine
447	Indirubin	491	Rheochrysidin
448	Sophocarpine	492	Paeoniflorin
449	Astragaloside A	493	Rotundine
450	Levosimendan	494	Hexestrol
451	Manidipine 2HCl	495	Quinine HCl Dihydrate
452	Enoxolone	496	Gynostemma Extract
453	L-(+)-Rhamnose Monohydrate	497	Morin Hydrate
454	Neohesperidin Dihydrochalcone (Nhdc)	498	Orotic acid (6-Carboxyuracil)
455	Quercetin Dihydrate	499	Sclareolide
456	Tanshinone I	500	Vanillylacetone
457	Biochanin A	501	Gastrodin
458	Lappaconite HBr	502	Salidroside
459	Curcumol	503	Geniposide
460	20-Hydroxyecdysone	504	Syneprine HCl
461	Forskolin	505	Itraconazole
462	Ozagrel	506	Roxithromycin
463	Ergosterol	507	Hyodeoxycholic acid (HDCA)
464	Magnolol	508	Myricetin
465	Neohesperidin	509	Oxymatrine
466	Rutaecarpine	510	Shikimic Acid
467	Tetrahydropapaverine HCl	511	5-hydroxytryptophan (5-HTP)
468	Dioscin	512	Hematoxylin
469	Naringin Dihydrochalcone	513	Dihydromyricetin
470	Cephalomannine	514	Genipin
471	Aloperine	515	Guanosine
472	Equol	516	Lincomycin HCl
473	D-Pantothenic acid	517	Scopolamine HBr
474	Glycyrrhizic Acid	518	Icariin
475	(+)-Matrine	519	Myricitrin
476	Oleanolic Acid	520	(-)-Parthenolide
477	Salinomycin	521	Silymarin
478	Troloxerutin	522	Aloin
479	D-Mannitol	523	Hordenine
480	Sesamin	524	Sodium Danshensu
481	10-Deacetylbaicatin-III	525	Geniposidic acid
482	Apocynin	526	Inosine
483	Clindamycin HCl	527	Manidipine
484	Propafenone HCl	528	Vardenafil HCl Trihydrate

Table 2 continued...			
529	Xylazine HCl	573	Ciclopirox
530	Ceftiofur HCl	574	Trospium chloride
531	Hydralazine HCl	575	Prednisolone Acetate
532	Pramiracetam	576	Lonidamine
533	MG-132	577	OSI-027
534	PF-05212384 (PKI-587)	578	BMS-378806
535	A66	579	PF-04929113 (SNX-5422)
536	WYE-125132 (WYE-132)	580	PF-3845
537	Trametinib (GSK1120212)	581	Ibrutinib (PCI-32765)
538	PF-2545920	582	BMV 7378
539	Nepicastat (SYN-117) HCl	583	KX2-391
540	Epinephrine Bitartrate	584	L-Ascorbyl 6-palmitate
541	Scopine	585	Tolterodine tartrate
542	Cloxacillin Sodium	586	Streptomycin sulfate
543	Clindamycin palmitate HCl	587	Ribitol
544	GSK256066	588	Fostamatinib (R788)
545	PNU-120596	589	NPS-2143
546	TAK-875	590	GSK2126458 (GSK458)
547	ICG-001	591	Dolutegravir (GSK1349572)
548	A922500	592	CHIR-124
549	R547	593	TG101209
550	GDC-0980 (RG7422)	594	GSK1838705A
551	L-Adrenaline	595	Ritodrine HCl
552	Tiotropium Bromide hydrate	596	Sulbactam sodium
553	Amoxicillin Sodium	597	Dimethyl Fumarate
554	Oseltamivir phosphate	598	Noradrenaline bitartrate monohydrate
555	AZD5438	599	LY2603618
556	GW3965 HCl	600	DCC-2036 (Rebastinib)
557	NU7441 (KU-57788)	601	5-hydroxymethyl Tolterodine (PNU 200577, 5-HMT, 5-HM)
558	WAY-100635 Maleate	602	A-674563
559	BRL-15572	603	KW-2478
560	WAY-600	604	Resminostat
561	RS-127445	605	LY2109761
562	Phenytoin sodium	606	Isoconazole nitrate
563	Scopine HCl	607	Cortisone acetate
564	Medroxyprogesterone acetate	608	Tolvaptan
565	Tioxolone	609	TAK-733
566	Omecamtiv mecarbil (CK-1827452)	610	Tubastatin A HCl
567	URB597	611	CCT128930
568	SNX-2112 (PF-04928473)	612	MK-0752
569	Clinofibrate	613	PF-00562271
570	Flavopiridol HCl	614	NVP-BSK805 2HCl
571	ADX-47273	615	XL335
572	CH5132799	616	YO-01027

Table 2 continued...			
617	Geldanamycin	661	AMG-900
618	Dacomitinib (PF299804, PF299)	662	MK-8776 (SCH 900776)
619	MK-4827 (Niraparib)	663	AMG-458
620	Milciclib (PHA-848125)	664	TH-302
621	Alectinib (CH5424802)	665	Dovitinib (TKI-258) Dilactic Acid
622	MK-2461	666	GW842166X
623	AZD2014	667	INCB28060
624	Torcetrapib	668	HCV-796 (Nesbuvir)
625	CEP-33779	669	INK 128 (MLN0128)
626	Torin 2	670	OC000459
627	Torin 1	671	SAR131675
628	LY411575	672	ZM 336372
629	SB415286	673	TG101348 (SAR302503)
630	PF-04691502	674	Anacetrapib (MK-0859)
631	HER2-Inhibitor-1	675	CUDC-907
632	MK-2048	676	MK-5108 (VX-689)
633	Nocodazole	677	M344
634	TAK-285	678	Tofacitinib (CP-690550, Tasocitinib)
635	VU 0357121	679	AZD4547
636	Dabrafenib (GSK2118436)	680	Ciproxifan
637	CI994 (Tacedinaline)	681	Tideglusib
638	Clindamycin	682	BI-D1870
639	CP-91149	683	JTC-801
640	Crenolanib (CP-868596)	684	PAC-1
641	CCT137690	685	BGT226 (NVP-BGT226)
642	Tivantinib (ARQ 197)	686	Canagliflozin
643	3-Methyladenine	687	Dalcetrapib (JTT-705, RO4607381)
644	CPI-613	688	I-BET151 (GSK1210151A)
645	A-803467	689	Istradefylline
646	WP1066	690	Galeterone
647	GDC-0068	691	BYL719
648	TAE226 (NVP-TAE226)	692	ML133 HCl
649	ARN-509	693	Cathepsin Inhibitor 1
650	TAK-901	694	PH-797804
651	AZ 3146	695	GSK1070916
652	AZ 628	696	GW788388
653	Varlitinib	697	NVP-BVU972
654	Dinaciclib (SCH727965)	698	SB705498
655	PF-5274857	699	GW4064
656	Laquinimod	700	Sotrastaurin
657	Lonafarnib	701	Sirtinol
658	MPEP	702	Tyrphostin AG 879
659	RG108	703	Desmethyl Erlotinib (CP-473420, OSI-774)
660	R428 (BGB324)	704	SB269970 HCl

Table 2 continued...			
705	BRL-54443	749	MK-801 (Dizocilpine)
706	CTEP (RO4956371)	750	U-104
707	GW5074	751	A-205804
708	VU 0361737	752	MLN0905
709	Lumiracoxib	753	Pirfenidone
710	GW9662	754	Mozavaptan
711	CHIR-99021 (CT99021) HCl	755	Pifithrin- $\alpha$ (PFT $\alpha$ )
712	Rivaroxaban	756	Deuterated Atazanivir-D3-2
713	Piceatannol	757	Vildagliptin (LAF-237)
714	Purmorphamine	758	Solifenacin succinate
715	Azilsartan Medoxomil	759	Diclofenac Diethylamine
716	BML-190	760	StemRegenin 1 (SR1)
717	VU 0364770	761	Alogliptin
718	Camostat Mesilate	762	PJ34
719	SB742457	763	Cobicistat (GS-9350)
720	PF-477736	764	Tempol
721	ML161	765	PF-4981517
722	Evacetrapib (LY2484595)	766	Pifithrin- $\mu$
723	Telithromycin	767	Deuterated Atazanivir-D3-3
724	Fenoprofen calcium hydrate	768	Sitaxentan sodium
725	Cinepazide maleate	769	Bosentan Hydrate
726	Medetomidine HCl	770	Guanosine Hydrate
727	MRS 2578	771	Golvatinib (E7050)
728	ML130 (Nodinitib-1)	772	TG100713
729	Prucalopride	773	PF-562271
730	ZM 323881 HCl	774	CCG 50014
731	JNJ-7777120	775	WZ811
732	HC-030031	776	Icotinib
733	Apoptosis Activator 2	777	Carbazochrome sodium sulfonate (AC-17)
734	Zanamivir	778	Rimonabant
735	Linagliptin	779	Bepotastine Besilate
736	Azilsartan	780	Rupatadine Fumarate
737	Epinephrine HCl	781	Vanillin
738	SB271046	782	IEM 1754 dihydrobroMide
739	VUF 10166	783	T0070907
740	Acesulfame Potassium	784	GW441756
741	ZM 306416	785	S-Ruxolitinib (INCB018424)
742	Ki16198	786	Dapivirine (TMC120)
743	IOX2	787	Salubrial
744	TAK-715	788	Clevudine
745	Zaltoprofen	789	PMSF
746	Bindarit	790	Fosaprepitant dimeglumine salt
747	Otilonium Bromide	791	Azelinidipine
748	Diclofenac Potassium	792	Caspofungin Acetate



Table 2 continued...			
793	Dexmedetomidine	837	2-Thiouracil
794	Tylosin tartrate	838	Adrenalone HCl
795	Reboxetine mesylate	839	Sitagliptin phosphate monohydrate
796	Cyclamic acid	840	Avanafil
797	Acridinium Bromide	841	Methazolamide
798	Valganciclovir HCl	842	Vitamin D3
799	Zinc Pyrithione	843	Vitamin A Acetate
800	Halobetasol Propionate	844	Voglibose
801	Lorcaserin HCl	845	Desvenlafaxine
802	Succinylcholine Chloride Dihydrate	846	Levodropropizine
803	Cyclizine 2HCl	847	Penfluridol
804	Etravirine (TMC125)	848	Moguisteine
805	Altrenogest	849	Azatadine dimaleate
806	Schisandrin B (Sch B)	850	Pentamidine
807	Ouabain	851	Sodium Picosulfate
808	Sennoside A	852	Olsalazine Sodium
809	Retapamulin	853	Escitalopram Oxalate
810	Ticagrelor	854	Lomerizine HCl
811	Ifenprodil Tartrate	855	Eprosartan Mesylate
812	Estradiol Benzoate	856	Triclabendazole
813	Tilmicosin	857	Deoxyarbutin
814	Bacitracin	858	Doxycycline Hyclate
815	Ulipristal	859	Sodium salicylate
816	Anagrelide HCl	860	Ticarcillin sodium
817	Betulinic acid	861	Mirabegron
818	Allylthiourea	862	Tolcapone
819	Vitamin D2	863	Nafcillin Sodium
820	Methyclothiazide	864	Guanidine HCl
821	Sulfacetamide Sodium	865	Levobetaxolol HCl
822	Difluprednate	866	Diminazene Aceturate
823	Dicloxacillin Sodium	867	Isovaleramide
824	Sodium Phenylbutyrate	868	Clorprenaline HCL
825	Azithromycin Dihydrate	869	Cyromazine
826	Indacaterol Maleate	870	Sertaconazole nitrate
827	Eletriptan HBr	871	Azlocillin sodium salt
828	Cabozantinib malate (XL184)	872	Hyoscyamine
829	Sennoside B	873	Homatropine Methylbromide
830	Doxapram HCl	874	Estradiol Cypionate
831	Sodium Nitroprusside	875	Sodium Nitrite
832	Spiramycin	876	Oxymetholone
833	Dexlansoprazole	877	Closantel Sodium
834	Desvenlafaxine Succinate	878	Pefloxacin Mesylate Dihydrate
835	Retinyl (Vitamin A) Palmitate	879	Eprazinone 2HCl
836	Amfenac Sodium Monohydrate	880	Teriflunomide

Table 2 continued...			
881	1-Hexadecanol	925	Penciclovir
882	Ethacridine lactate monohydrate	926	Dirithromycin
883	Erythritol	927	Sodium ascorbate
884	Luliconazole	928	Ebastine
885	Brimonidine Tartrate	929	Bromocriptine Mesylate
886	Colistimethate Sodium	930	R-(-)-Apomorphine HCl Hemihydrate
887	Noscapine HCl	931	Mepenzolate Bromide
888	Fosfomycin Tromethamine	932	Lithium Citrate
889	Picrotoxinin	933	Misoprostol
890	SC-514	934	Delphinidin Chloride
891	Tofacitinib (CP-690550) Citrate	935	Ataluren (PTC124)
892	Trometamol	936	Domiphen Bromide
893	Aminothiazole	937	Ribostamycin Sulfate
894	Fidaxomicin	938	Prucalopride Succinat
895	Vilazodone HCl	939	Efaproxiral Sodium
896	Benfotiamine	940	Calcium Gluceptate
897	Emetine	941	Ractopamine HCl
898	Pinacidil	942	Nomifensine Maleate
899	Bentiromide	943	Oxeladin Citrate
900	Procodazole	944	TTNPB (Arotinoid Acid)
901	SN-38	945	Cyanidin Chloride
902	Pimecrolimus	946	AP26113
903	Climbazole	947	Cyclandelate
904	Isosorbide	948	Valnemulin HCl
905	Bucladesine Sodium Salt	949	Bromfenac Sodium
906	Tamibarotene	950	Etofibrate
907	Anisotropine Methylbromide	951	Ceftazidime Pentahydrate
908	Mepiroxol	952	Thiostrepton
909	Carbenoxolone Sodium	953	Pyrilamine Maleate
910	Brucine	954	Oxiglutatione Disodium Salt
911	Nitarson	955	JNK-IN-8
912	Quercetin 4'-glucoside	956	Petunidin Chloride
913	LY404039	957	PF-04880594
914	Mezlocillin Sodium	958	Cinchophen
915	Tenatoprazole	959	Liothyronine Sodium
916	Deoxycorticosterone acetate	960	Epinastine HCl
917	EUK 134	961	Nicaraven
918	Apomorphine HCl	962	Clinafoxacin HCl
919	Moxalactam Disodium	963	Tolmetin Sodium
920	Nicotine Ditartrate	964	Bekanamycin
921	Dichlorisone Acetate	965	Pasiniazid
922	Sodium 4-aminohippurate Hydrate	966	JZL184
923	Quercetin 3,4'-di-O-β-glucopyranoside	967	Peonidin Chloride
924	NXY-059	968	EPZ005687

Table 2 continued...			
969	MEK162 (ARRY-162, ARRY-438162)	1013	Birinapant
970	Stattic	1014	XL388
971	PD168393	1015	Oprozomib (ONX 0912)
972	LY2090314	1016	T0901317
973	IWP-2	1017	SANT-1
974	SCH772984	1018	(+)-JQ1
975	AMG-517	1019	XL888
976	PYR-41	1020	BMS-833923
977	AZD1080	1021	Ilomastat (GM6001, Galardin)
978	UNC1999	1022	ONX-0914 (PR-957)
979	AGI-5198	1023	GZD824
980	PP2	1024	CZC24832
981	IPI-145 (INK1197)	1025	XL019
982	AZD3514	1026	VX-661
983	FMK	1027	Cilengitide
984	IWR-1-endo	1028	KY02111
985	GDC-0032	1029	NLG919
986	AZD3839	1030	SC144
987	P22077	1031	CFTRinh-172
988	VER 155008	1032	LY2835219
989	SSR128129E	1033	AVL-292
990	I-BET-762	1034	RKI-1447
991	GDC-0152	1035	GDC-0834
992	AZD2461	1036	Wnt-C59 (C59)
993	BAY 1000394	1037	PP1
994	EMD 1214063	1038	SGC 0946
995	GSK2334470	1039	PD123319
996	BAM7	1040	Zebularine
997	3-Deazaneplanocin A (DZNeP)	1041	KPT-185
998	IU1	1042	TCID
999	Batimastat (BB-94)	1043	OTSSP167
1000	LY900009	1044	PF-543
1001	GSK2190915 (AM803)	1045	(Z)-Pugnac
1002	SGI-110	1046	Z-VAD-FMK
1003	EPZ004777 HCl	1047	Epoxomicin
1004	BMN 673	1048	EPZ5676
1005	GSK J4 HCl	1049	LDK378
1006	GSK923295	1050	(-)-Blebbistatin
1007	AZD3463	1051	NU6027
1008	MLN2480	1052	EPZ-6438
1009	LDN-57444	1053	BMS-911543
1010	Marimastat	1054	Mdivi-1
1011	LY3039478	1055	BAF312 (Siponimod)
1012	PF-04620110	1056	GlcNAcstatin

Table 2 continued...			
1057	BIO	1101	AZD2858
1058	Bromosporine	1102	CO-1686 (AVL-301)
1059	SGI-1027	1103	AZ191
1060	Rilpivirine	1104	RGD (Arg-Gly-Asp) Peptides
1061	Rocilinostat (ACY-1215)	1105	Vortioxetine (Lu AA21004) HBr
1062	CEP-32496	1106	UPF 1069
1063	PRT062607 (P505-15, BIIB057) HCl	1107	Macitentan
1064	Dynasore	1108	Gefitinib (ZD1839)
1065	NSC 405020	1109	RG2833 (RGFP109)
1066	UNC1215	1110	OAC1
1067	Nexturastat A	1111	AZD1981
1068	DBeQ	1112	TAK-632
1069	Erastin	1113	JSH-23
1070	Suvorexant (MK-4305)	1114	AG-18
1071	EHop-016	1115	Empagliflozin (BI 10773)
1072	GSK2636771	1116	GDC-0349
1073	TAK-438	1117	Lomeguatrib
1074	Apremilast (CC-10004)	1118	Vorinostat (SAHA, MK0683)
1075	ABT-199 (GDC-0199)	1119	OTX015
1076	PluriSIn #1 (NSC 14613)	1120	RepSox
1077	C646	1121	MM-102
1078	ZM 39923 HCl	1122	ZCL278
1079	CNX-2006	1123	EPZ004777
1080	Ferostatin-1 (Fer-1)	1124	PRX-08066 Maleic acid
1081	Edoxaban	1125	Tarividar
1082	Tasisulam	1126	Scriptaid
1083	BIX 01294	1127	Pacritinib (SB1518)
1084	AZD5363	1128	AG-490 (Tyrphostin B42)
1085	VU 0364439	1129	UNC669
1086	Tubastatin A	1130	RGFP966
1087	Bardoxolone Methyl	1131	Golgicide A
1088	OG-L002	1132	RVX-208
1089	SMI-4a	1133	Tenovin-1
1090	Thiamet G	1134	GW9508
1091	KPT-276	1135	NSC 23766
1092	JIB-04	1136	BMS-345541
1093	IOWH032	1137	P276-00
1094	VE-821	1138	WHI-P154
1095	GW0742	1139	ME0328
1096	Butein		
1097	ETP-46464		
1098	Dasatinib		
1099	SGC-CBP30		
1100	Skepinone-L		

**Table 2** – List of the drugs from the Sellekchem small molecule library that were tested in with their commonly used acronyms in parenthesis.

	Drug	Target
1	TSU-68 (Orantinib)	VEGFR, PDGFR, FGFR
2	Rocilinostat (ACY-1215)	HDAC
3	Trichostatin A (TSA)	HDAC
4	CUDC-101	HDAC, HER2, EGFR
5	PD168393	EGFR
6	SCH79797	Par1 antagonist
7	CP-673451	PDGFR
8	Panobinostat (LBH589)	HDAC
9	BIO	GSK3
10	Cabozantinib malate	VEGFR, Axl
11	GW9662	PPAR

**Table 3** – List of the drugs that were most effective in inhibiting EMT in the mesenchymal MDA MB 231 reporter cells and their reported targets.

All the 11 drugs that were shortlisted in the screen were validated using flow cytometry (Table 15). The reporter cells were plated in 24-well plates. The reporter cells were treated with 3 different concentrations of the drugs (0.1 $\mu$ M, 1 $\mu$ M and 10 $\mu$ M) for 5 days and following treatment the cells were analyzed using flow cytometry. MDA MB 231 cells that did not express the reporters were used to set the quartiles to define the red positivity and green positivity. All the treated cells were sorted and the percentage of cells in each quartile was plotted (Figure 10). The cells that fall in the first quartile denote the reporter cells that have gained red color but lost the green color indicating that the expression of Zeb1 is turned off and the expression of E-cadherin is turned on. These cells are denoted in blue in Figure 10. The cells that fall in the second quartile are the cells that have both red and green fluorescence indicating that both Zeb1 and E-cadherin are turned on. Red is used to represent these cells in Figure 10. The cells that fall in the third quartile are cells that express green but not red fluorescence indicating that these cells have retained mesenchymal properties following the treatment and therefore the expression of Zeb1 is not

inhibited and the E-cadherin is not expressed. These cells are marked in green in the graphs in Figure 10. The cells that fall in the fourth quartile lack the expression of both red and green fluorescence and are cells that neither express Zeb1 nor E-cadherin. These cells are represented in purple in Figure 10. The drugs that were able to increase the expression of E-cadherin and consequently increase the proportion of the cells in the second quartile were selected. Among all the drugs tested, GSK3 $\beta$  inhibitor, BIO and CUDC-101 were the only drugs that effectively enabled the transition of the mesenchymal-like cells to red expressing reporter cells (Figure 10). CUDC-101 is a multi-therapeutic drug that is capable of inhibiting HER2, EGFR and HDAC [219]. However, we were seeking to identify novel targets for treating TNBCs that lack the amplification and overexpression of HER2. There are several studies examining the effect of HDAC inhibitors on TNBCs [220-224]. Therefore, CUDC-101 did not appear to be a good candidate for this study. As patient studies indicated that GSK3 $\beta$  could be a viable target to treat TNBCs that have been observed to upregulate this kinase, BIO was selected for further studies.

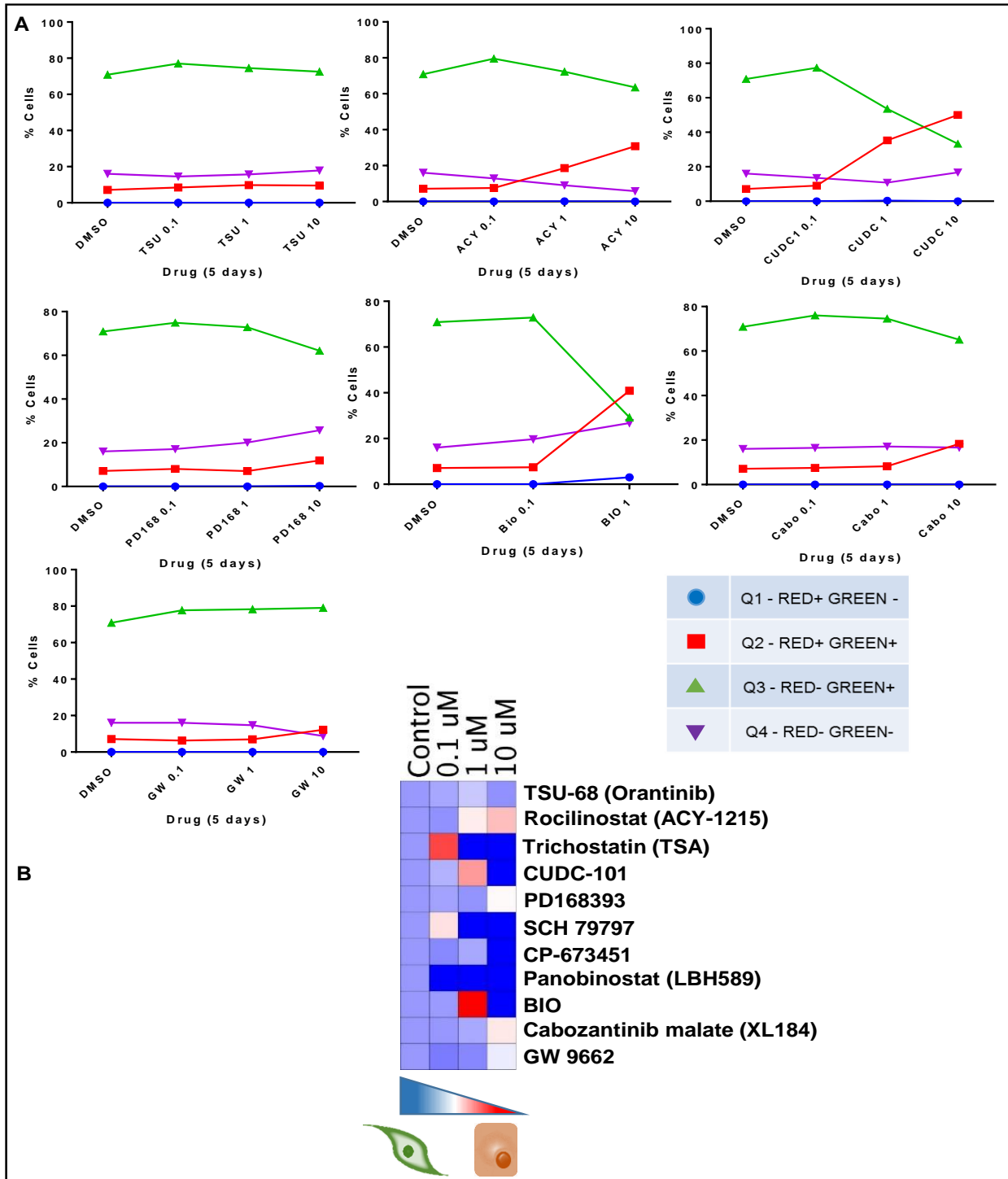


**Figure 10** – CUDC1 and BIO are capable of inhibiting EMT. **A.** MDA MB 231 reporter cells were treated with different doses of the drugs shortlisted from the screen for 5 days. These cells were then analyzed using flowcytometry. Few of the drugs killed the cells and therefore could not be analyzed. Among these drugs, only CUDC1 and BIO were capable of decreasing the number of green positive cells while also upregulating the expression of RFP. **B.** Heatmap of the ratio between red and green cells. Red indicated more epithelial cells.

BIO refers to 6-Bromoindirubin-3'-oxime which is a bromo derivative of indirubin [225]. Bis-indole alkaloid indirubin and its analogs, collectively known as indirubins, were first discovered as inhibitors of cyclin dependent kinases (CDKs) [225, 226]. Indigo and indirubin are isomers that are derived from isatin and indoxyl via non-enzymatic dimerization [225]. The 2 components of the indirubins are usually found free or conjugated with carbohydrates [225]. Indirubins can be extracted from dye- producing plants, Muricidae mollusks and wild-type and recombinant bacteria [226]. Interestingly, indirubin is an active ingredient in Danggui Longhui, a traditional Chinese medicine recipe used to treat chronic myelocytic leukemia [225]. While it was discovered as a CDK inhibitor, it was later determined that it could also inhibit GSK3 $\beta$  [225]. Recent studies have indicated that chemical modifications to indirubins alter their affinity for kinases and thus 6-Bromoindirubin-3'-oxime was found to have higher affinity for GSK3 $\beta$  as compared to other kinases and methyl-derivative of BIO was found to be ineffective in binding to GSK3 $\beta$  [225].

Thus, this screen served to further attest that GSK3 $\beta$  may be an important player in TNBC and that GSK3 $\beta$  inhibitors could serve as a potent therapeutic agent to revert EMT/CSC properties of TNBC cells.

#### 5B. GSK3 $\beta$ inhibitors decrease the mesenchymal properties of the stem cell-enriched mesenchymal-like cell lines.

The small molecule screen and the subsequent validation clearly demonstrated that the GSK3 $\beta$  inhibitor, BIO is a potent inhibitor of EMT in TNBC cells. However, it was essential to test if this phenomenon was limited to BIO or whether this is true for other GSK3 $\beta$  inhibitors too. To ensure that our observations are robust we test 3 different GSK3 $\beta$  inhibitors that function *via* different mechanisms on 3 different cell lines with mesenchymal properties. The 3 GSK3 $\beta$  inhibitors used in this study include BIO, which was one of the lead candidates of the screen, LiCl, which has

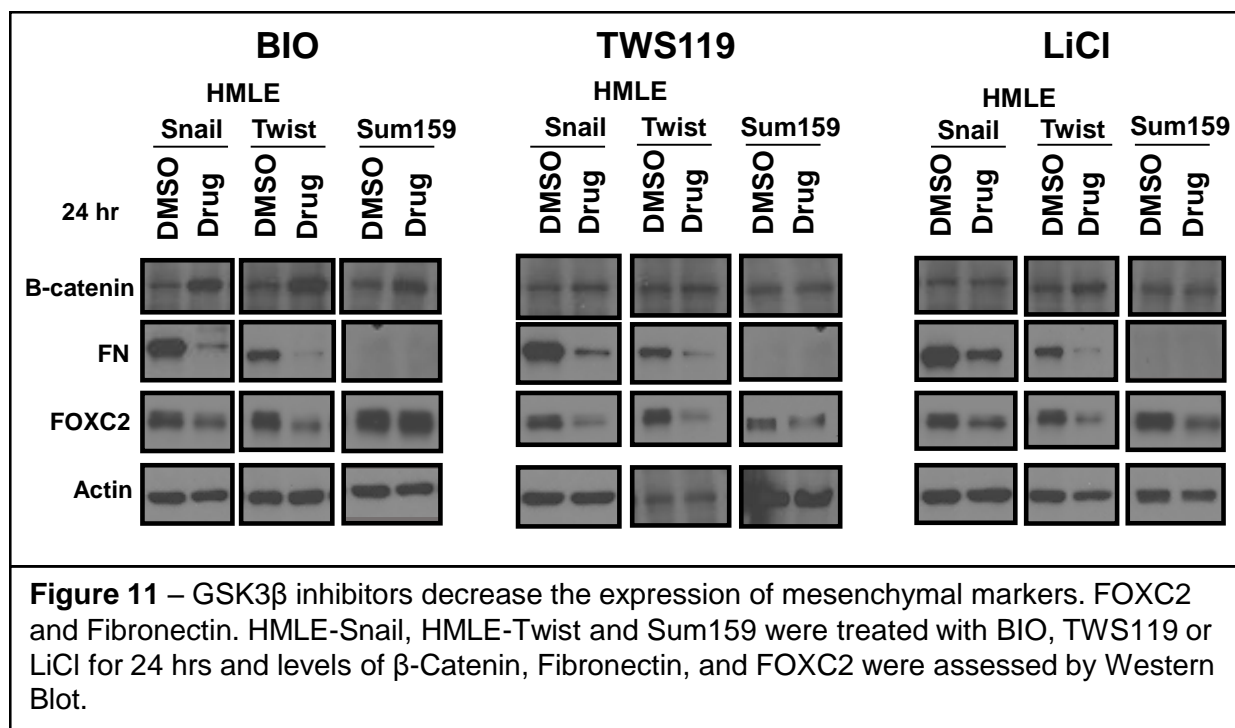


been in the clinic for treatment of neurological disorders for more than half a decade and TWS119, a GSK3 $\beta$  inhibitor for which GSK3 $\beta$  is the only established target [202, 227].

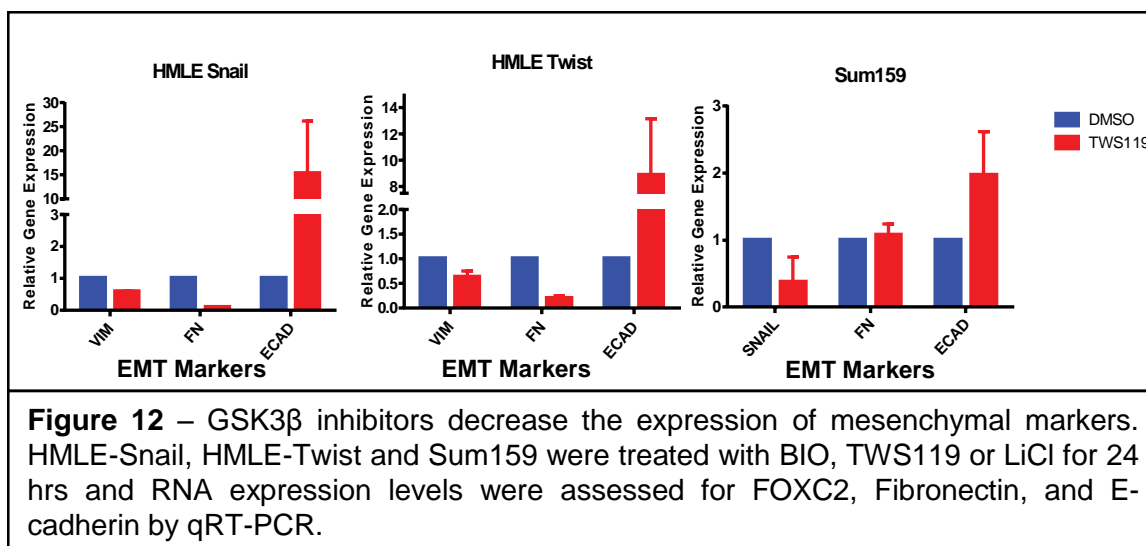
After 50 years of using lithium for treating manic-depression (Bipolar disorder), GSK3 $\beta$  was identified as one of its targets [227]. Lithium inhibits GSK3 $\beta$  *via* 2 different mechanisms [227]. It competes with the magnesium ions for binding to the kinase [227]. Magnesium ions are essential for the catalytic activity of kinases. The other mechanism of action of lithium is to increase the inhibitory serine-9 (inactivating) phosphorylation of GSK3 $\beta$  [227-229]. This indirect effect has been attributed to the effect of lithium on protein-phosphatase-1 or on the activated Akt [227, 230, 231]. Unlike most of the other GSK3 $\beta$  inhibitors, lithium does not inhibit CDKs [232]. Inhibition of GSK3 $\beta$  using lithium chloride decreases the active form of GSK3 $\beta$  in all the 3 sub-cellular compartments (cytoplasm, nucleus and mitochondria) in which GSK3 $\beta$  has been detected and reported. As lithium has been in the clinic for a very long time, it has a known safety profile. Notably, studies have shown that prolonged use of lithium doesn't increase tumor incidence [233, 234].

TWS119 is a 4,6-disubstituted pyrrolopyrimidine. It was originally discovered in a screen used to identify small molecules that were capable of inducing differentiation in P19 embryonic stem cells (ESC) [202]. TWS119, which was identified in this screen was shown to bind to GSK3 $\beta$  via affinity chromatography and this interaction was confirmed by western blotting and surface plasmon resonance (SPR) [202]. Additionally, some of the studies mentioned TWS119 to be specific for GSK3 $\beta$  inhibition [215].

The 3 cell lines consistently used in these studies include HMLE-Snail cells, HMLE-Twist cells and Sum159 cells. HMLE cells are human mammary epithelial cells that have been immortalized and have an epithelial phenotype. The overexpression of EMT inducing transcription factors Snail and Twist in the HMLE cells gives rise to the HMLE-Snail and HMLE-Twist cells respectively. Therefore, HMLE-Snail and HMLE-Twist cells are epithelial cells that have been forced to undergo EMT by the overexpression of EMT inducing transcription factors and thereby exhibit mesenchymal properties and are enriched for stem-like cells. Sum159 cells are mesenchymal-like cells that are enriched for CSCs. All the three cell lines were treated with BIO (1 $\mu$ M), LiCl (20mM) and TWS119 (2 $\mu$ M) for 24hrs. These concentrations are close to IC25 calculated for 24hrs for these drugs for the cell lines used in this experiment. The lowest IC25 among the IC25s of the 3 cell lines (HMLE-Snail, HMLE-Twist and Sum159) was finalized as the concentration for treating all the cells). 0.5x10<sup>6</sup> cells were plated in a 10 cm dish and the cells were allowed to attach overnight. The attached cells were treated with the appropriate concentration of the drugs and the control cells were treated with DMSO (0.05%) for 24 hrs following which the cells were harvested for protein and RNA extraction. The protein extraction was performed as described in the “Experimental approaches” section and the proteins were quantified using the BioRad Bradford Assay. 50ug of each protein sample was loaded onto the gel and the western blot analysis was performed as described in Experimental approaches. The membrane was probed for  $\beta$ -Catenin, FOXC2, Fibronectin and  $\beta$ -Actin. The  $\beta$ -Catenin levels were seen to increase following treatment with GSK3 $\beta$  inhibitors, indicating that GSK3 $\beta$  is indeed inhibited leading to the accumulation of  $\beta$ -Catenin in the treated cells. The expression of FOXC2 and fibronectin which serve as indicators of mesenchymal phenotype was decreased (Figure 11).



The RNA was extracted using the Qiagen RNA extraction kit and the RNA was quantified using the Nanodrop from Thermoscientific. The cDNA generated using this RNA was used for qRT-PCR and the levels of expression of mesenchymal and epithelial markers fibronectin, vimentin and E-cadherin were tested for HMLE-Snail and HMLE-Twist cells and fibronectin, Snail and E-cadherin were tested for Sum159 cells. The expression of the housekeeping gene, GAPDH gene was used for normalization. In line with the western blot analysis, we found a decrease in expression of mesenchymal markers, fibronectin, vimentin and Snail and a significant increase in the expression of epithelial marker, E-cadherin at the transcript level (figure 12).



In summary, the KM Plots demonstrated a correlation between the expressions of GSK3 $\beta$  and overall patient survival in TNBCs and the small molecule screen confirmed that GSK3 $\beta$  indeed could be a regulator of EMT, which is a major player in TNBC. The western blot analysis and qRT-PCR analysis, demonstrated a decrease in the expression of mesenchymal markers and an increase in the expression of epithelial markers following exposure to GSK3 $\beta$  inhibitors suggesting that GSK3 $\beta$  could serve as a druggable target to inhibit EMT/CSC enriched TNBCs.

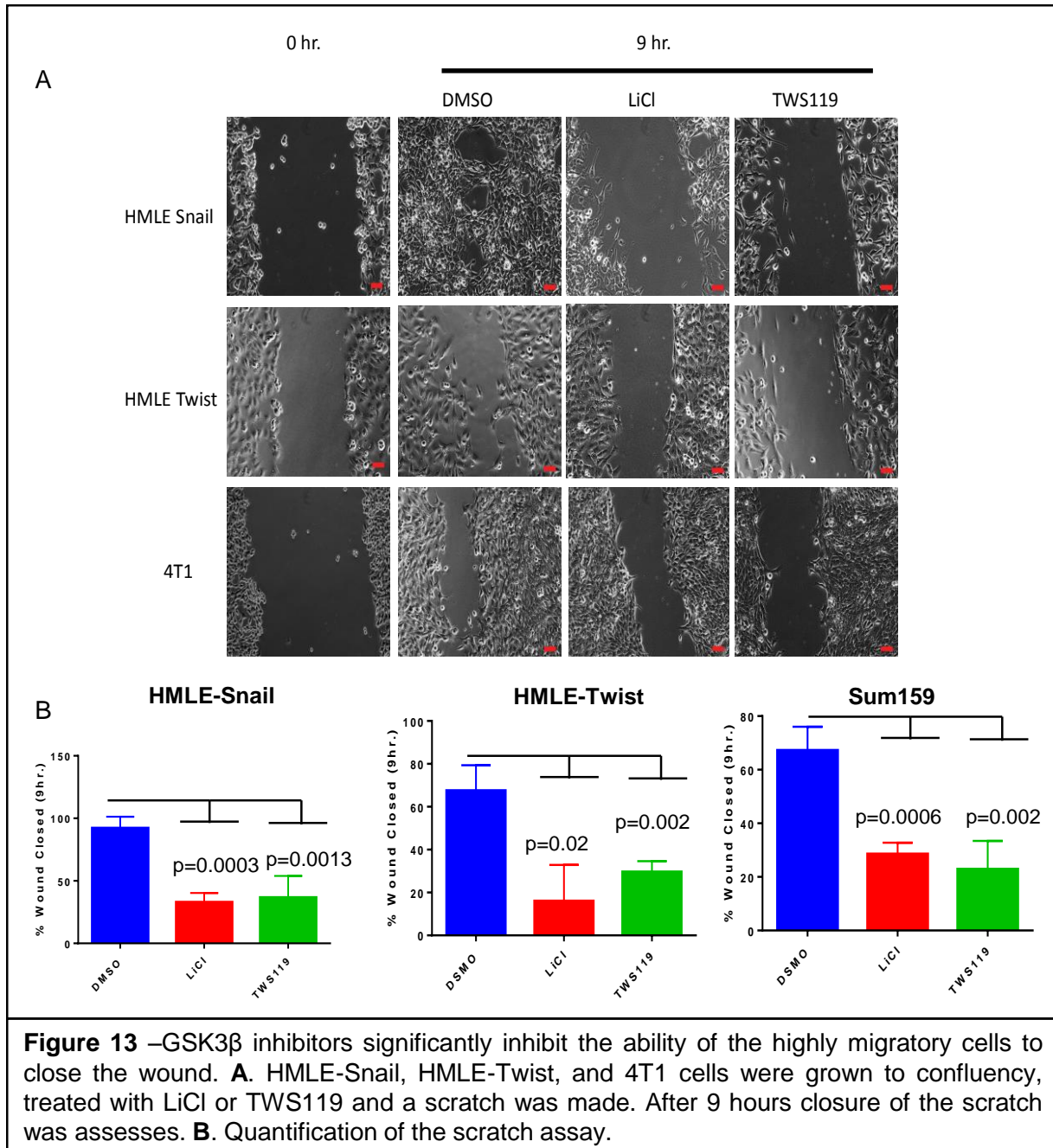
### 5C. Inhibition of GSK3 $\beta$ decreases the migratory properties of the cells with mesenchymal phenotype by inhibiting the induction of EMT.

EMT along with bestowing mesenchymal properties to the cells also enhances the migratory potential of the cells. GSK3 $\beta$  inhibitors have been known to inhibit migration of cells [227, 235, 236]. Since our experiments demonstrated that GSK3 $\beta$  inhibitors inhibit the mesenchymal properties of the cells, this led us to investigate if GSK3 $\beta$  inhibitors could inhibit the migratory properties of the cells with mesenchymal properties. The wound healing assay was employed to test the efficacy of the GSK3 $\beta$  inhibitors in inhibiting the migratory potential of the cells with mesenchymal properties. HMLE-Snail cells, HMLE-Twist cells and 4T1 cells were plated for the

scratch assay. 4T1 cells are highly metastatic murine mammary tumor cells [237, 238]. These have been previously shown to have high migratory potential [237, 238]. All the cells were allowed to grow to confluency and a scratch was made to mimic a wound as described in experimental approaches. The control was treated with DMSO (0.05%) (vehicle) whereas the experimental cells were treated with two GSK3 $\beta$  inhibitors, LiCl (20mM) and TWS119 (1 $\mu$ M). The scratch was imaged at 0 hr and at regular intervals following treatment (Figure 13). Within 9hr following the scratch, a significant difference was observed in the ability of the treated and the untreated cells to close the wound. 3 images were acquired of each scratch at 0hr and at 9hr and the scratch was measured in 3 different spots along the wound in each image. The measurements were averaged to determine the distance between the wound edges. The percentage of the wound closed was calculated as follows

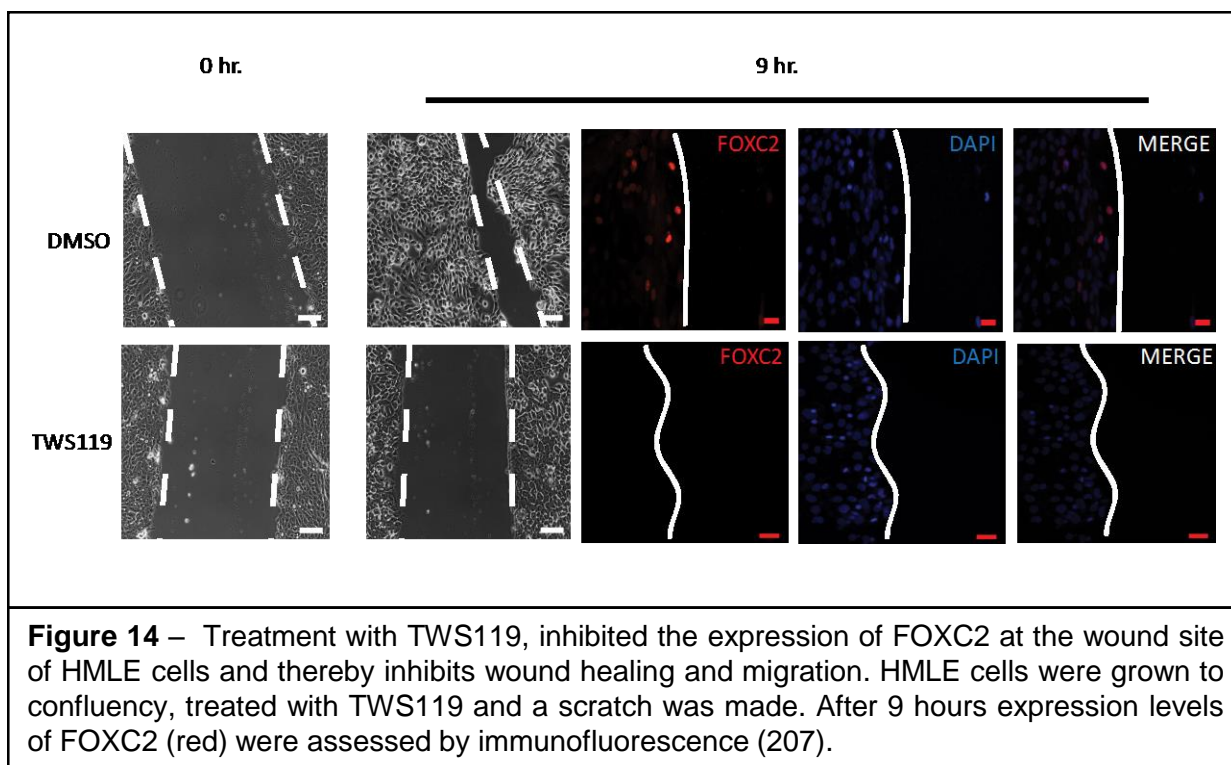
$$\% \text{ wound closed} = \frac{(\text{wound at 0hr} - \text{wound at 9hr})}{\text{wound at 0hr}} \times 100$$

The % wound closed was plotted using GraphPad Prism. The images and the graphs clearly demonstrate a significant decrease in the ability of the cells treated with GSK3 $\beta$  inhibitors to close the wound as compared to that of the DMSO treated cells. This observation indicates that exposure to GSK3 $\beta$  inhibitor significantly decreases the migratory potential of the cells with mesenchymal properties (Figure 13).



This observation prompted the question of whether the EMT inhibition is one of the means by which GSK3 $\beta$  inhibitors reduce the migratory potential of the cells with mesenchymal attributes. In order to answer this question, a modification of the scratch assay was employed as previously described in [208]. The cells used for the scratch assay were grown on coverslips and the scratch

was made on the confluent layer of cells on the coverslip. A scratch assay was performed using HMLE cells, which are epithelial cells and therefore do not express genes such as FOXC2 which are exclusively expressed in cells that display mesenchymal phenotype [60, 89]. However, it has been established that EMT is induced at the wound edge to facilitate the wound healing process [111]. Therefore, when a scratch is made in HMLE cells grown to confluence, EMT is induced at the wound edge to promote the closing of the wound. This has been tested in our lab previously and when a scratch made in HMLE cells is stained for FOXC2 after 9hrs of having made the scratch, FOXC2 expression was observed in the cells present at the wound edge indicating the induction of EMT in these cells [208]. Using this as the basis for our experimental design, we plated HMLE cells and allowed them to grow to confluence. A scratch was made in these cells and the controls were treated with DMSO (0.02%) (vehicle) and the experimental cells were treated with TWS119 (1uM). As expected, treatment with TWS119 decreased the ability of the HMLE cells to close the wound as compared to the DMSO treated cells. These coverslips were stained for the expression of FOXC2 and the nuclei were stained with DAPI. The DMSO-treated scratch showed the upregulation of FOXC2 at wound edge but there was no upregulation of FOXC2 at the wound edge in the scratch treated with TWS119 (Figure 14). This observation indicates that GSK3 $\beta$  inhibitors decrease the migratory properties of the cells by inhibiting the induction of EMT in the migrating cells.



#### 5D. GSK3 $\beta$ inhibitors decrease the stem cell properties of mesenchymal-like cells.

Cells that have undergone EMT along with exhibiting mesenchymal properties also possess more stem-like properties [67]. It is well established in literature that EMT and CSC properties are intricately linked. As GSK3 $\beta$  inhibitors were capable of inhibiting EMT, it was logical to investigate if GSK3 $\beta$  inhibitors were capable of inhibiting the CSC properties of these mesenchymal-like cells. The drugs that were shortlisted from the small molecule screen were tested for their ability to inhibit the CSC properties of the MDA MB 231 reporter cells.

The MDA MB 231 reporter cells were counted and 1000 cells per well were plated in ultra-low attachment plates in the viscous mammosphere media. The control wells were treated with DMSO (0.05%) and the rest of the wells were appropriately treated with the 3 different



concentrations of all the small molecule inhibitors that were indicated to be EMT inhibitors from the screen. The media was replenished with the drugs every 2 days. At the end of 10 days the number of mammospheres formed in each well were counted and plotted using GraphPad Prism (Figure 15). BIO was found to be one of the drugs that were capable of inhibiting the sphere forming capacity of these mesenchymal-like cells (Figure 15).

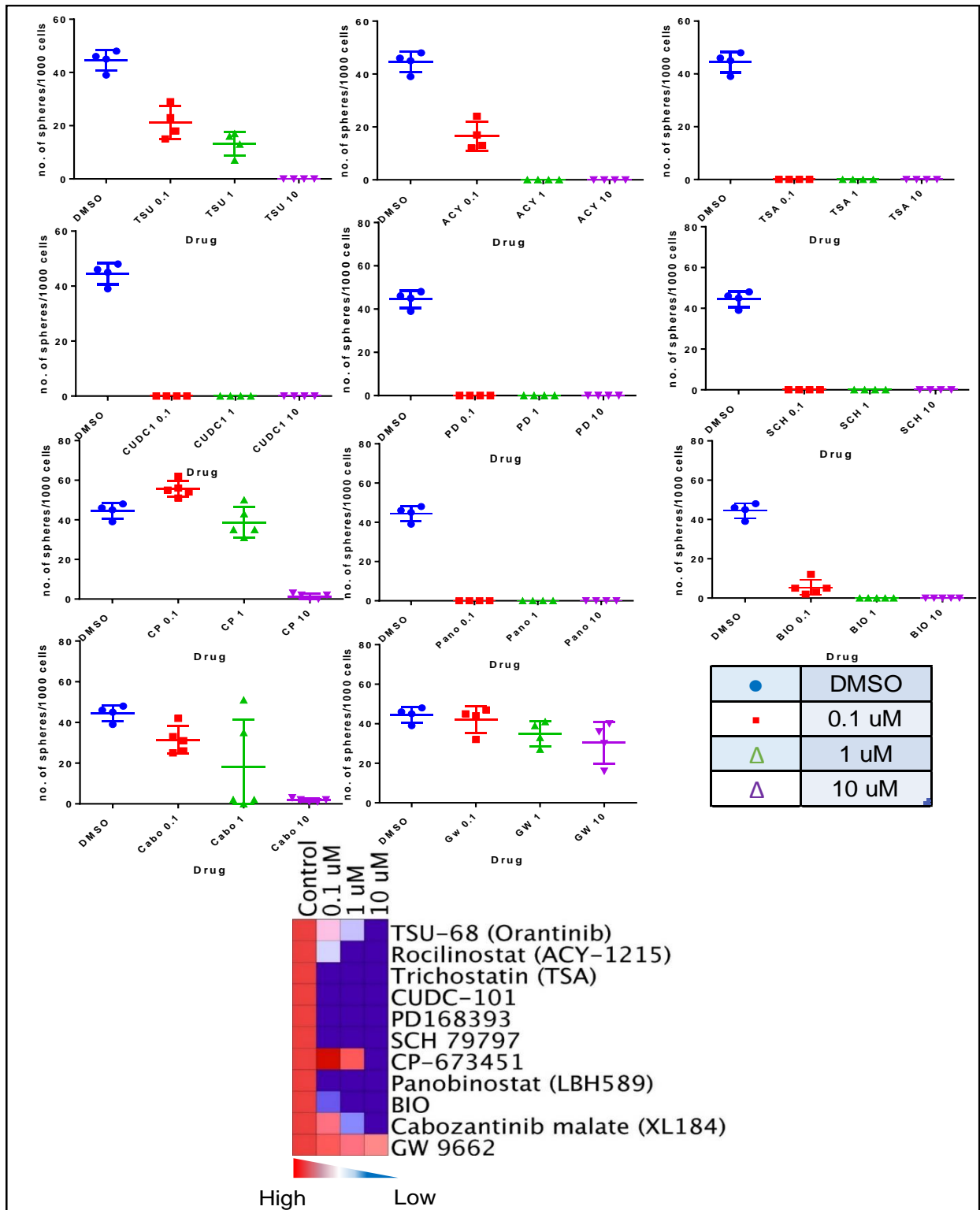
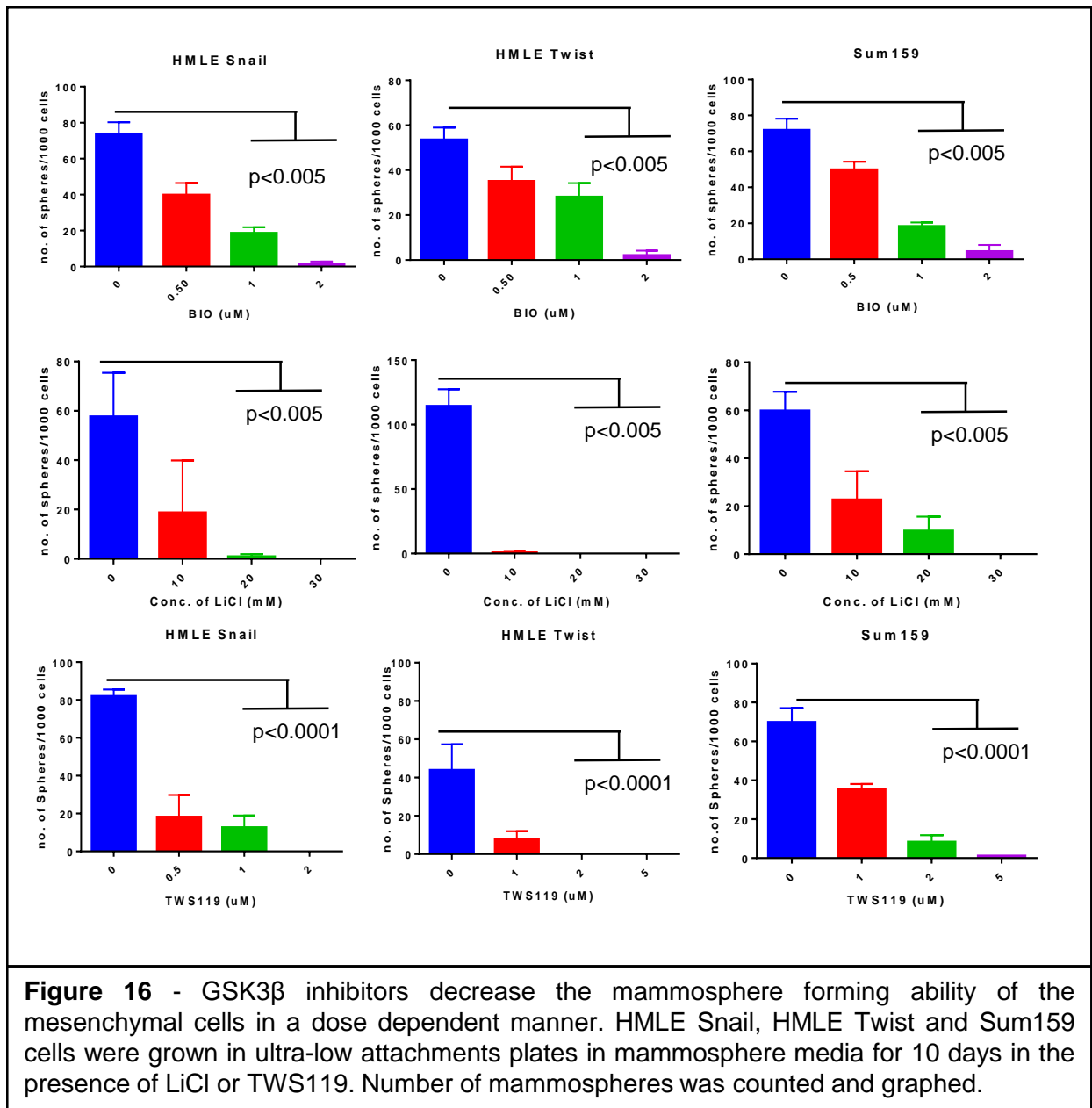


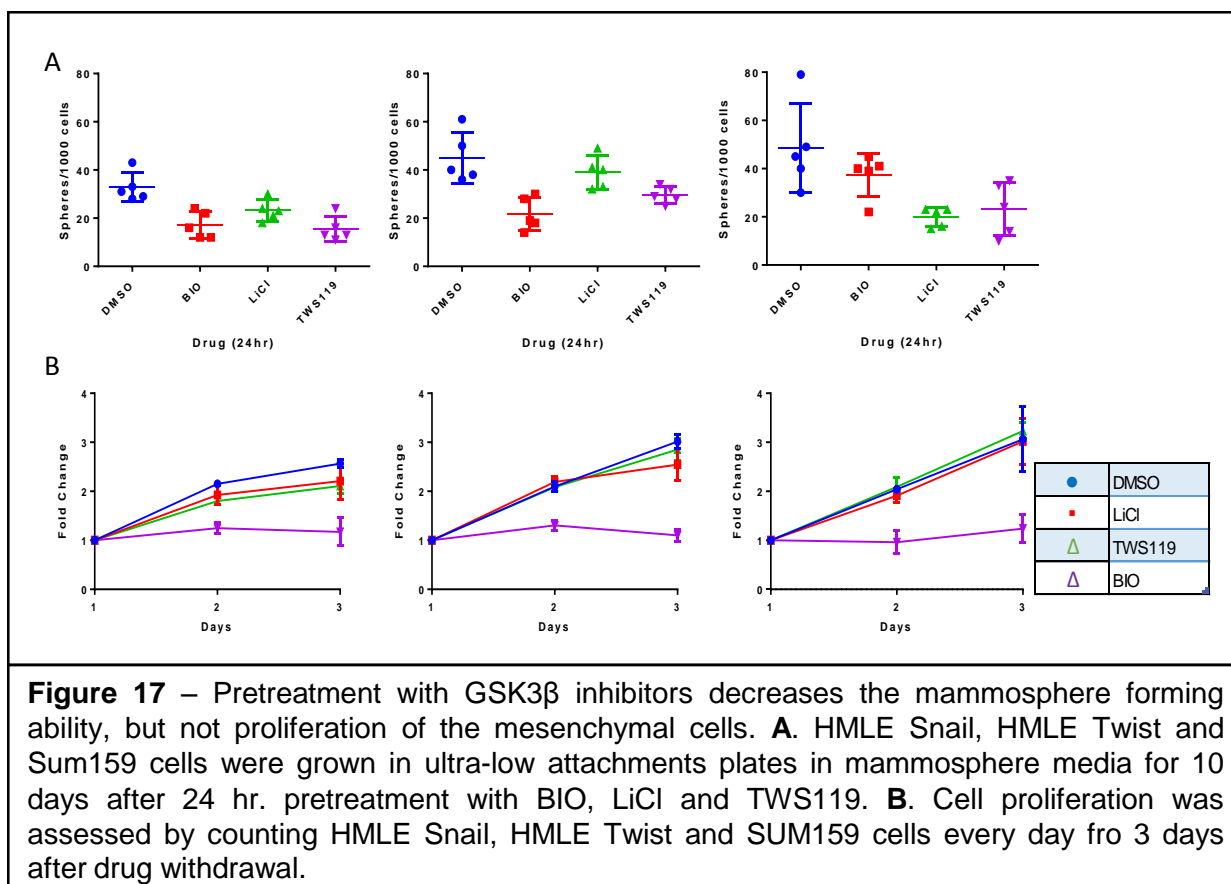
**Figure 15** – The GSK3 $\beta$  inhibitor BIO decreases mammosphere forming potential of mesenchymal cells. **A.** MDA MB 231 reporter cells were grown in ultra-low attachments plates in mammosphere media for 10 days. Number of mammospheres was counted and graphed. **B.** The heatmap summarizes the drug screen validation using mammosphere assay.

As expected BIO was able to inhibit the sphere forming potential of the MDA MB 231 reporter cells but in order to validate this observation using multiple GSK3 $\beta$  inhibitors, the effect of 3 different GSK3 $\beta$  inhibitors on the sphere forming potential of all the three mesenchymal-like human mammary cell lines, HMLE-Snail, HMLE-Twist and Sum159 was tested. The cells with mesenchymal phenotype were plated for mammosphere assay. The control wells were treated with DMSO (0.05%) and the experimental wells were treated with 3 different concentration of the 3 GSK3 $\beta$  inhibitors, BIO (0uM, 0.5uM, 1uM and 2uM), LiCl (0mM, 10mM, 20mM and 30mM) and TWS119 (0uM, 0.5uM, 1uM and 2uM). The concentration of the drug that inhibited EMT (as demonstrated in section 5B) and one concentration above and below that concentration were used for the sphere assay. The media and the drugs were replenished every 2 days and at the end of 10 days the number of mammospheres in each well were counted, plotted and analyzed using GraphPad Prism. It was observed that all the three drugs BIO, LiCl and TWS119 were capable of decreasing the mammosphere forming ability of all the three mesenchymal-like cells, HMLE-Snail, HMLE-Twist and Sum159 (Figure 16).



While all the 3 GSK3 $\beta$  inhibitors tested were able to decrease the sphere forming ability of the cells with mesenchymal properties with continuous treatment over 10 days, we had observed earlier that GSK3 $\beta$  inhibitors are capable of inhibiting EMT within only 24hr of treatment. Thus, the question arose as to whether 24hr treatment of the cells with mesenchymal phenotype was sufficient to decrease their sphere forming ability, which is a surrogate assay to quantify the EMT-

mediated CSC properties. To address this question, HMLE-Snail, HMLE-Twist and Sum159 cells were treated with BIO, LiCl and TWS119 for 24hrs. After the treatment, the viable cells were counted and plated for the mammosphere assay. 10 days following the plating, the mammospheres were quantified and plotted using GraphPad Prism. We observed that just 24hr pretreatment was sufficient to significantly decrease the sphere forming ability of HMLE-Snail and Sum159 cells (Figure 17A). The HMLE-Twist cells seem to regain their CSC properties following the withdrawal of the drugs. In order to rule out the possibility, that the decrease in the mammosphere formation is due to the decrease in the proliferation rate of the cells following treatment with GSK3 $\beta$  inhibitors, we treated all the 3 cell lines used in this study with all the 3 drugs and 10000 viable cells were plated in a 6-well plate. The proliferation rate of the cells following the withdrawal of the drugs was monitored by counting the number of cells every day for the next 3 days and generating a growth curve using this data (Figure 17B). We found that there wasn't a significant decrease in the proliferation rate of the mesenchymal-like cells lines following treatment with the inhibitors as compared to the DMSO treated cells. BIO was the only drug which decreased the proliferation rate following treatment.



## 5E. shRNA to GSK3 $\beta$ decreases the CSC properties of cells with mesenchymal attributes.

GSK3 $\beta$  inhibitors were shown to be potent inhibitors of CSC properties of cells with mesenchymal properties. Though multiple GSK3 $\beta$  inhibitors were tested for their ability to decrease the CSC properties of multiple mesenchymal-like cells, using biological methods to achieve the same goal strengthens the observations. Therefore, to examine if the biological silencing of GSK3 $\beta$  has the same effect on the stem-like properties of the mesenchymal-like cells as the GSK3 $\beta$  inhibitors, GSK3 $\beta$  was silenced in all the mesenchymal-like cells that have been consistently used in the project. HMLE-Snail, HMLE-Twist and Sum159 were transduced with the shRNA to GSK3 $\beta$  in the pGIPZ vector and the control cells were generated by transducing them with pGIPZ FF3 vector. The FF3 targets the firefly luciferase gene which is not expressed in the human cells and therefore

serves as a random target control. The transduced cells were selected based on their resistance to puromycin and stable cell lines were generated. Protein and mRNA were extracted from these cells and analyzed to see if the silencing of GSK3 $\beta$  using shRNA was successful. 2 different shRNAs were used in order to rule out the possibility of off-target effects. The expression of GSK3 $\beta$  was significantly decreased in all the cell lines tested at both the transcript and the protein level following the transduction of the shRNA (Figure 18).

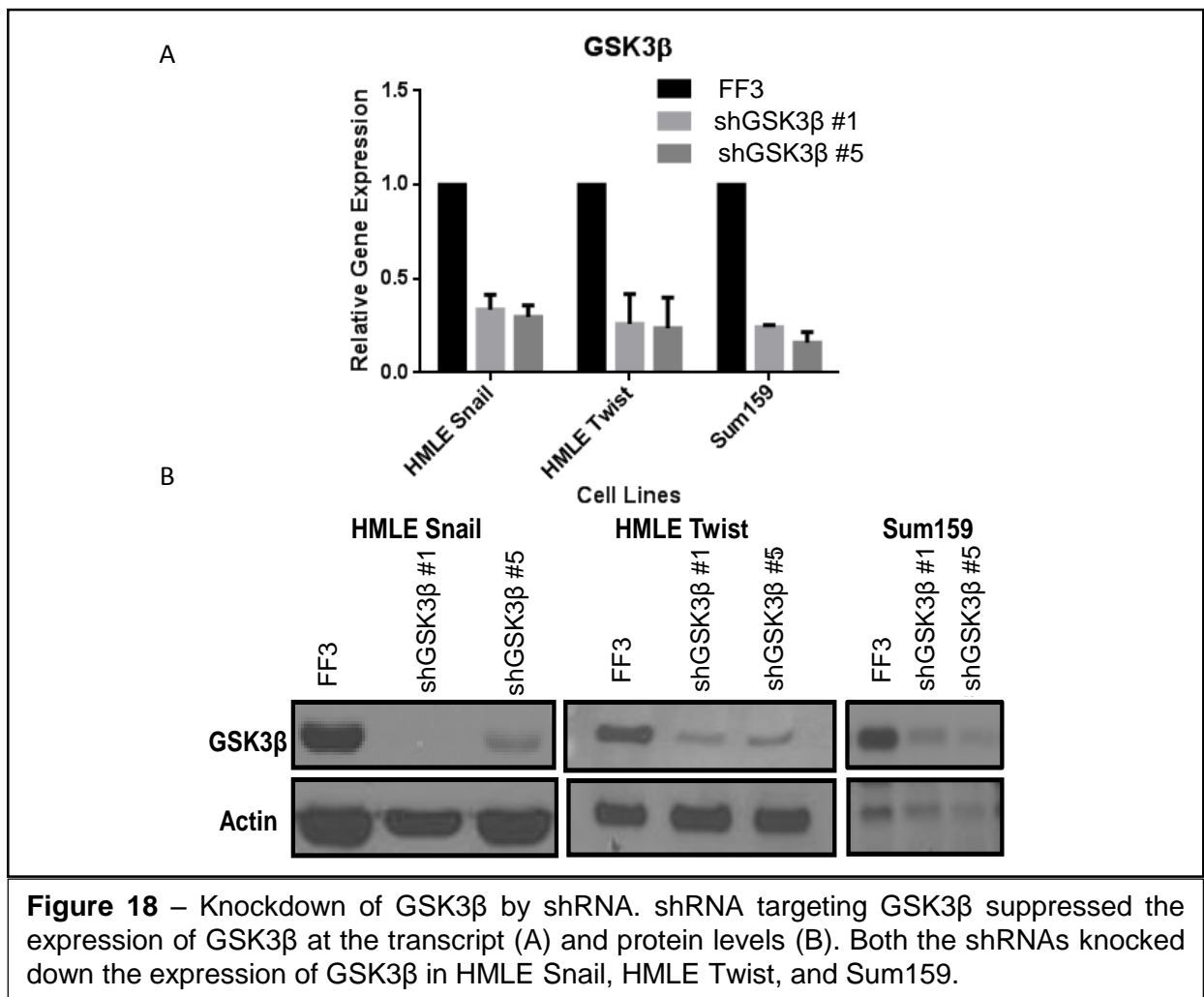
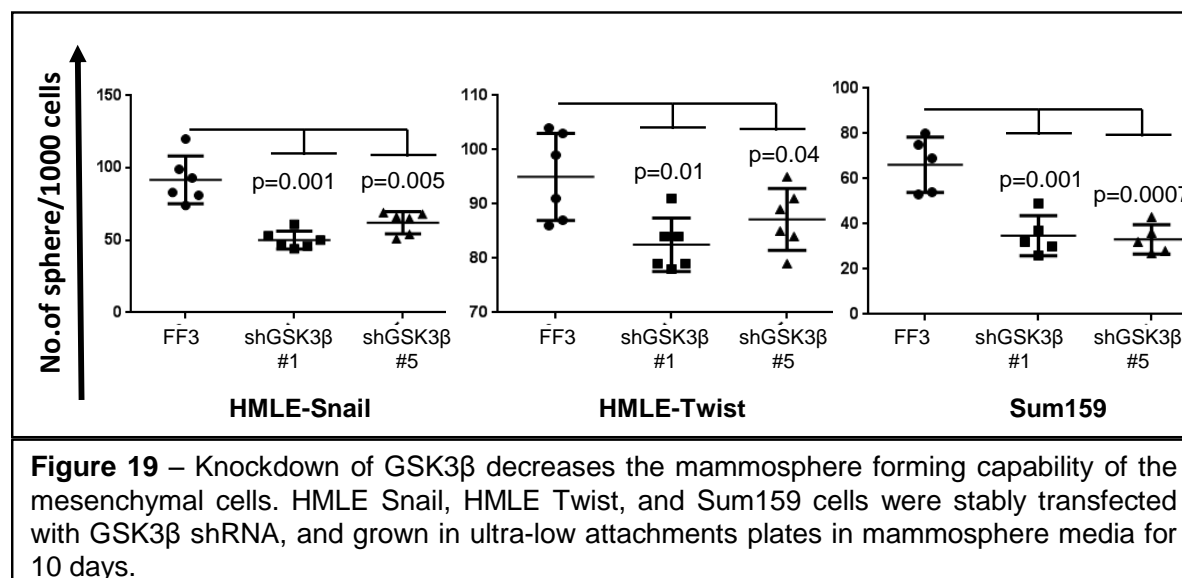


**Figure 18** – Knockdown of GSK3 $\beta$  by shRNA. shRNA targeting GSK3 $\beta$  suppressed the expression of GSK3 $\beta$  at the transcript (A) and protein levels (B). Both the shRNAs knocked down the expression of GSK3 $\beta$  in HMLE Snail, HMLE Twist, and Sum159.

The control cells and the mesenchymal-like cells with GSK3 $\beta$  shRNA were plated for the mammosphere assay. At the end of 10 days, the mammospheres were quantified and plotted using GraphPad Prism. As expected, suppressing GSK3 $\beta$  using shRNA resulted in a significant

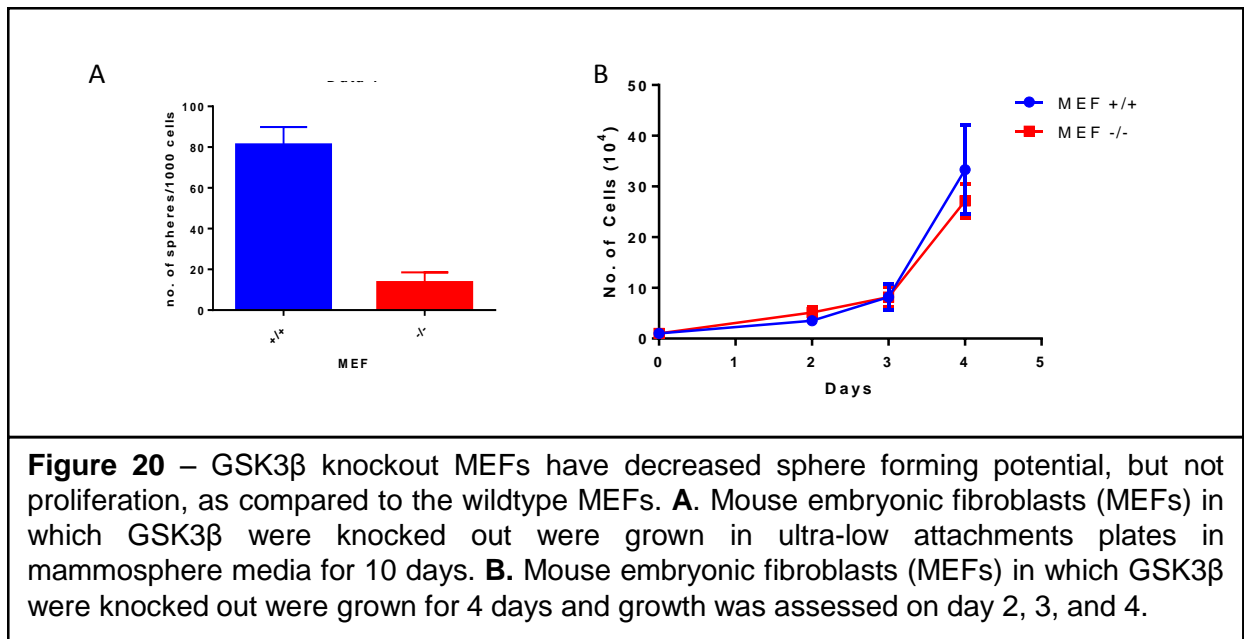
decrease in the sphere forming ability of the cells with mesenchymal and CSC properties (Figure 19).



#### 5F. GSK3 $\beta$ knock-out MEFs show decreased ability to form spheres.

In addition to using shRNA, another biological means of achieving our goal is to knock out the gene instead of suppressing its expression. Unlike shRNA which decreases the level of protein expression, knocking out the gene completely eliminates the presence of the protein. A knockout model was therefore used to assess the effect of GSK3 $\beta$  on the sphere forming ability of the mesenchymal cells as a surrogate for CSC properties. Mouse embryonic fibroblasts (MEFs) which are mesenchymal cells were used for this assay. Wild-type MEFs (MEF+/+) and MEFs with GSK3 $\beta$  knocked out (MEF-/-) were obtained as a generous gift from Dr. Sarbosov at UT MD Anderson Cancer Center. The proliferation of the 2 cell lines was assessed. Our results indicated that there was no difference in the proliferation rate of the 2 cell lines. Both these cells were then plated for the sphere-forming assay and their stem cell potential was evaluated. It was observed that although there was no significant difference in the proliferation rate between the wild-type and GSK3 $\beta$  knock-out MEFs, the knock out MEFs had significantly lower ability to form spheres suggesting that they have reduced stem cell potential (Figure 20).





## 5G. GSK3 $\beta$ inhibitors alter the CD24/44 profile of the mesenchymal-like cells

Apart from the mammosphere assay, the proportion of the stem-like cells in the mesenchymal cell lines can also be determined by assessing the CD24/44 expression profile of the mesenchymal-like cells. CD24 and CD44 are cell surface markers that are associated with more differentiated state and stem-like state, respectively [67, 239, 240]. Therefore, HMLE-Snail, HMLE-Twist and Sum159 cells were treated with all the 3 inhibitors and the control cells were treated with DMSO. Following treatment, the cells were harvested and analyzed the CD24/44 profile of the mesenchymal-like cells. Unstained mesenchymal-like cells were used to set the gates for CD24 and CD44 positivity. Cells with mesenchymal and stem-like properties are CD44 positive and CD24 negative which was observed in control treated samples. However, the treated samples displayed a marked increase in the expression of CD24 indicating an increase in the proportion of the differentiated cells in the mesenchymal-like cell lines (Figure 21).

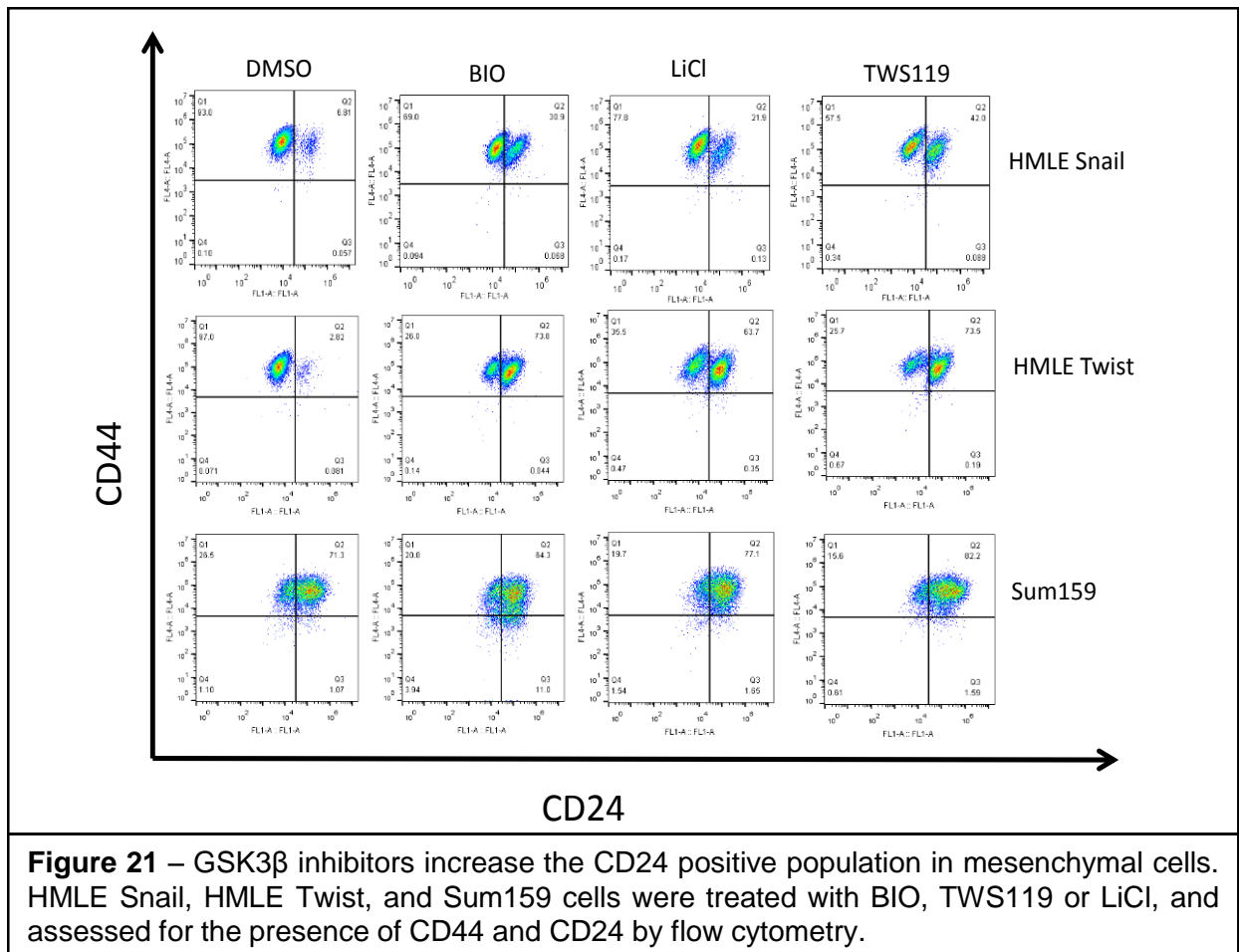
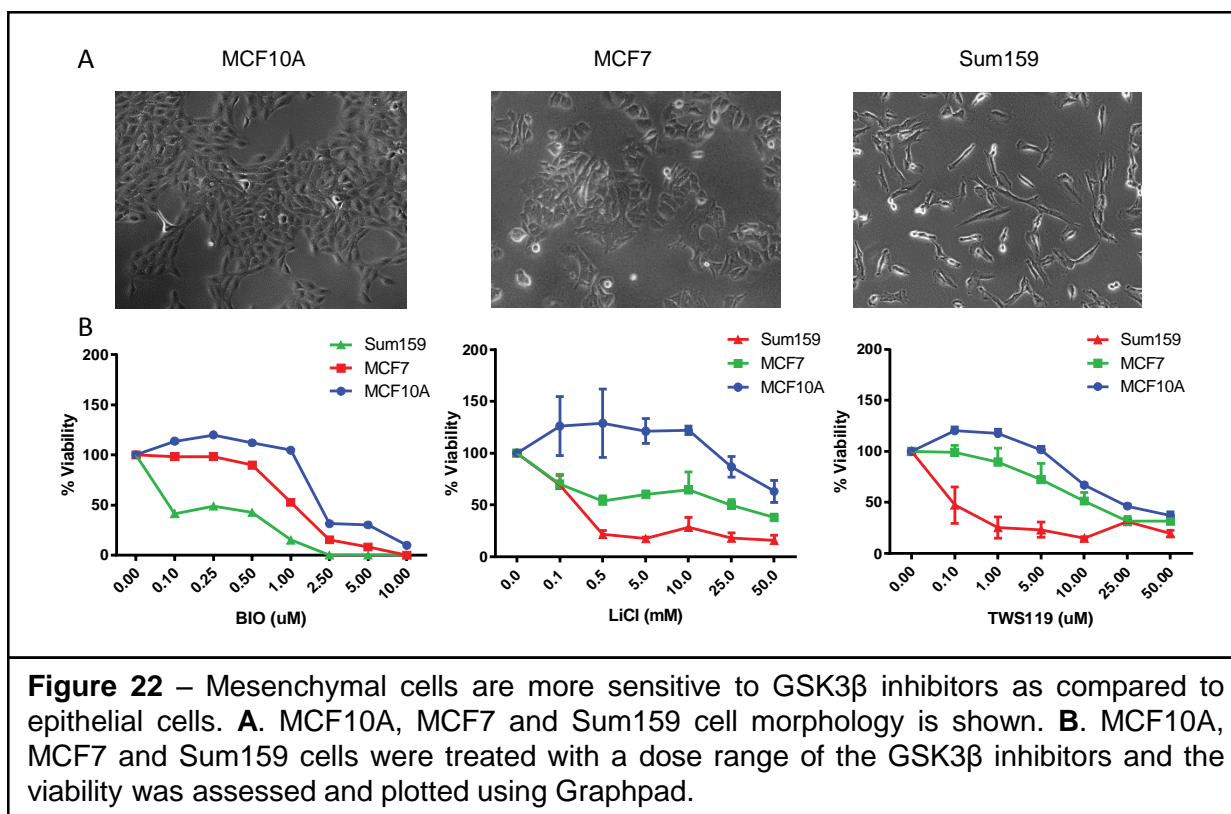


**Figure 21** – GSK3β inhibitors increase the CD24 positive population in mesenchymal cells. HMLE Snail, HMLE Twist, and Sum159 cells were treated with BIO, TWS119 or LiCl, and assessed for the presence of CD44 and CD24 by flow cytometry.

To summarize, we observed that BIO was one of the small molecule inhibitors selected in the screen that were able to inhibit the sphere forming potential of the mesenchymal-like MDA MB 231 reporter cells. Additionally, LiCl and TWS119 were also able to inhibit the sphere-forming ability of the cells with mesenchymal phenotype. Further, suppressing GSK3β expression using shRNA and GSK3β knockout MEFs elicited the same result of a significant decrease in the sphere-forming potential of these cells. Examination of the CD24/44 profile of the mesenchymal-like cells exposed to GSK3β inhibitors exhibited an increase population of CD24<sup>+</sup> expressing cells indicating the inhibition of GSK3β promotes a more differentiated phenotype in the mesenchymal-like cells.

#### 5H. Cells with mesenchymal phenotype are more sensitive to GSK3 $\beta$ as compared to their epithelial counterparts.

From our analyses, we observed that the effect of GSK3 $\beta$  overexpression on overall survival of patients was pronounced in the TNBCs. We also found a very significant upregulation of GSK3 $\beta$  in the Richardson 2 data set which predominantly had EMT/CSC enriched tumor samples. This observation suggested that there is an association between GSK3 $\beta$ , EMT and CSC properties and prompting the question of whether the mesenchymal-like cells respond differentially to the GSK3 $\beta$  inhibitors as compared to the cells with epithelial phenotype that have relatively reduced CSC properties. For this, we subjected a panel of cell lines to the GSK3 $\beta$  inhibitors. The cell lines selected for this assay were MCF10A cells (normal breast cell line), MCF7 (transformed epithelial cell line) and Sum159 (EMT/CSC enriched cell line) [241-243]. Both MCF10A and MCF7 cells share an epithelial phenotype whereas Sum159 cells clearly exhibit a mesenchymal phenotype (Figure 22A). All the cell lines were treated with a range of concentrations of BIO (0uM, 0.1uM, 0.25uM, 0.5uM, 1uM, 2.5uM, 5uM, and 10uM), LiCl (0uM, 0.1uM, 0.5uM, 5uM, 10uM, 25uM and 50uM) and TWS119 (0uM, 0.1uM, 1uM, 5uM, 10uM, 25uM and 50uM) to assess the dose response. The concentrations of the drugs were chosen such that there would be data points in all the parts of the dose response curve. The treated cells were then subjected to a MTT assay. The viability of the cells were calculated based on the absorbance of the wells treated with the vehicle (DMSO). The viability of the cells treated with the vehicle control was considered as 100% and the relative percentage viability of cells at different concentrations of the drug was calculated and plotted using GraphPad Prism. For all the three drugs tested, the mesenchymal-like cells, which possess some characteristics of basal subtype of breast cancer and TNBCs and express higher levels of mesenchymal markers, were found to be more susceptible to GSK3 $\beta$  inhibitors compared to their epithelial counterparts (Figure 22B).



In order to compare the ability of GSK3 $\beta$  inhibitors with other small molecule inhibitors (selected from the small molecule screen) to differentiate between epithelial and mesenchymal cells, we tested all the 11 drugs that were shortlisted from the screen. HMLE vector (a cell line with epithelial properties expressing the empty vector pWZL) and HMLE-Snail (a cell line with mesenchymal properties) were plated in 96 well plates and were treated with 6 different drug concentrations (0uM, 0.5uM, 1uM, 5uM, 10uM, and 100uM). The viability of the cells were assessed using the MTT assay and plotted using GraphPad Prism. We observed that including BIO, only PD168393 and CP-673451 were capable of significantly differentiating between epithelial and mesenchymal cells. However, only BIO and CP-673451 selectively killed mesenchymal cells as compared to epithelial cells (Figure 23A).

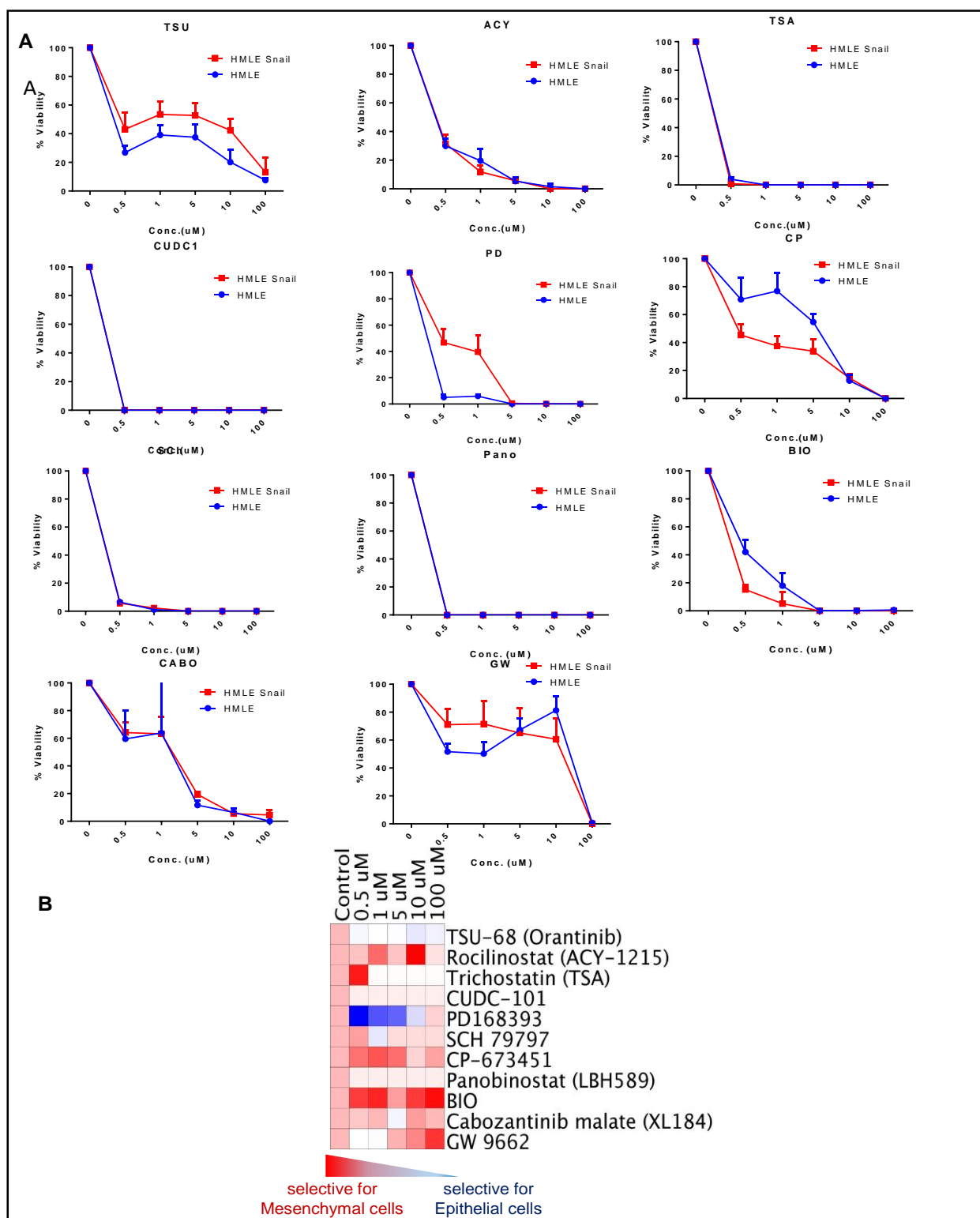
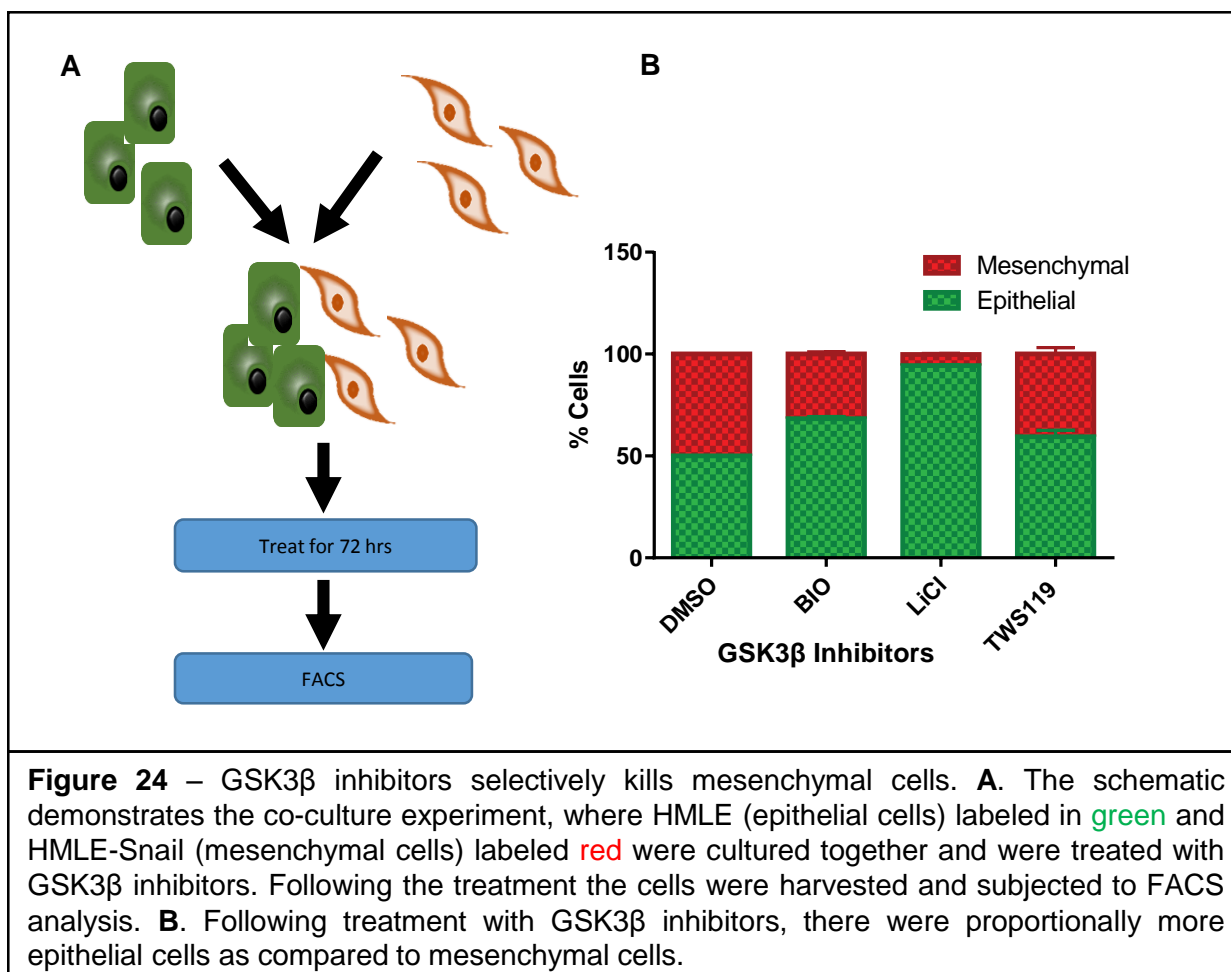


**Figure 23** – BIO and CP-673451 selectively kill mesenchymal cells whereas PD selectively kills epithelial cells. **A.** HMLE and HMLE-Snail cells were treated with a dose range of the tested inhibitors and viability was assessed by MTT assay. **B.** The heatmap summarizes the differential selectivity screen.

PD on the other hand selectively inhibited epithelial cells as compared to mesenchymal-like cells. The ratio of viability of HMLE vector to HMLE-Snail was calculated and a heatmap was generated to summarize the findings of this experiment. When the drug selectively inhibits mesenchymal cells, the viability of the epithelial HMLE vector cells is high and that of the HMLE-Snail cells is low and the ratio calculated will be high. The color red stands for high value indicating that the drug is selective for mesenchymal-like cells whereas blue stands for low value indicating that the viability of the mesenchymal-like cells is higher. As is evident from the heatmap, BIO is capable of selectively inhibiting mesenchymal-like cells as compared to their epithelial counterparts (Figure 23B).

To further test if GSK3 $\beta$  inhibitors can indeed differentiate between epithelial and mesenchymal-like cells, HMLER vector control and HMLER-Snail cells were used. HMLER cells are human mammary epithelial cells that have been immortalized and transformed and HMLER-Snail cells are HMLER cells in which Snail is overexpressed and hence these cells have mesenchymal phenotype. The mesenchymal-like cells were labeled red.  $1 \times 10^6$  cells of both red and green cells were mixed and co-cultured (Figure 24A). The cells were treated with GSK3 $\beta$  inhibitors and following treatment the proportion of viable green epithelial and red mesenchymal-like cells were assessed using flow cytometry. The percentage of cells was normalized to the percentage of red/green cells in the DMSO treated sample to account for the differences in the proliferation rate of the two cell lines. It was observed that there was a decrease in the proportion of the red mesenchymal-like cells and an increase in the proportion of the green epithelial cells indicating that the mesenchymal-like cells were selectively inhibited in the co-culture system (Figure 24B).



Summary – Aim 2: While Aim 1 established the basis of testing the potential of GSK3 $\beta$  inhibitors as targets for inhibition of EMT/CSC enriched TNBCs, observations made in experiments conducted to address Aim 2 indicate that GSK3 $\beta$  is indeed capable of inhibiting EMT and CSC properties both of which are hallmarks of TNBCs. The high throughput screen performed to select small molecules capable of inhibiting EMT in TNBC cell lines resulted in the identification of 11 candidate drugs of which one 2, CUDC-101 and BIO were validated as inhibitors of EMT. BIO, a GSK3 $\beta$  inhibitor was selected as the lead compound as CUDC-101 has multiple different targets and GSK3 $\beta$  was established as a potential target in Aim 1. In addition to BIO, 2 other GSK3 $\beta$  inhibitors, LiCl and TWS119 were also able to inhibit EMT and EMT-endowed migratory potential of the EMT/CSC-enriched cell lines. Further, GSK3 $\beta$  inhibition using small molecules, shRNA or

GSK3 $\beta$  knockout in MEFs decreased the sphere-forming ability of mesenchymal-like cells. Moreover, drugs tested also increased the expression of CD24 surface antigen on the mesenchymal-like cells. We also observed that GSK3 $\beta$  inhibitors exerted selective inhibitory effect on the mesenchymal-like cells as compared to their epithelial counterparts. Thus Aim 2 clearly demonstrates the ability of the GSK3 $\beta$  inhibitors to inhibit EMT and EMT-mediated properties in the EMT/CSC enriched cells.



## **Chapter 6 – Aim 3 – Test if GSK3 $\beta$ inhibitor can be effectively used *in vivo* to target CSC-enriched breast cancers.**

GSK3 $\beta$  inhibitor, TWS119 did not inhibit tumor size and metastatic potential of mesenchymal cells *in vivo*.

Our observations suggested that GSK3 $\beta$  inhibitors were potent inhibitors of EMT and CSC properties *in vitro*, and indeed inhibition of EMT and CSC properties has been shown to decrease the tumorigenicity and metastatic potential of cancer cells *in vivo* [60]. Therefore, we used luciferase labelled HMLER-Snail and 4T1 cells to test if GSK3 $\beta$  inhibitors were capable of inhibiting tumorigenesis and metastasis *in vivo*. In both cell lines the GSK3 $\beta$  inhibitor TWS119 decreases EMT and CSC properties *in vitro*. Both these cell lines we injected into the mammary fat pad of mice and were allowed to grow until a palpable tumor was observed. Once a palpable tumor was detected which was in ~1 week for HMLER-Snail and ~4 days for 4T1, the mice were randomized into 2 groups. One group was treated with vehicle (DMSO) and the other with 30mg/Kg of TWS119 which was administered intraperitoneally every other day. TWS119 was used for the *in vivo* experimentation as it is a highly specific drug for GSK3 $\beta$  and the dosage and route of administration was decided based work of Gattinoni et.al. [244]. Tumor progression was monitored by imaging the mice weekly for luciferase activity (Figure 25, 26). The 4T1 experiment was terminated because the tumor burden exceeded the allowed size of 2 cm in diameter prior to the completion of the experiment. HMLER-Snail experiment had to be terminated due to scarring of the site of injection that made further administration of the drug difficult.

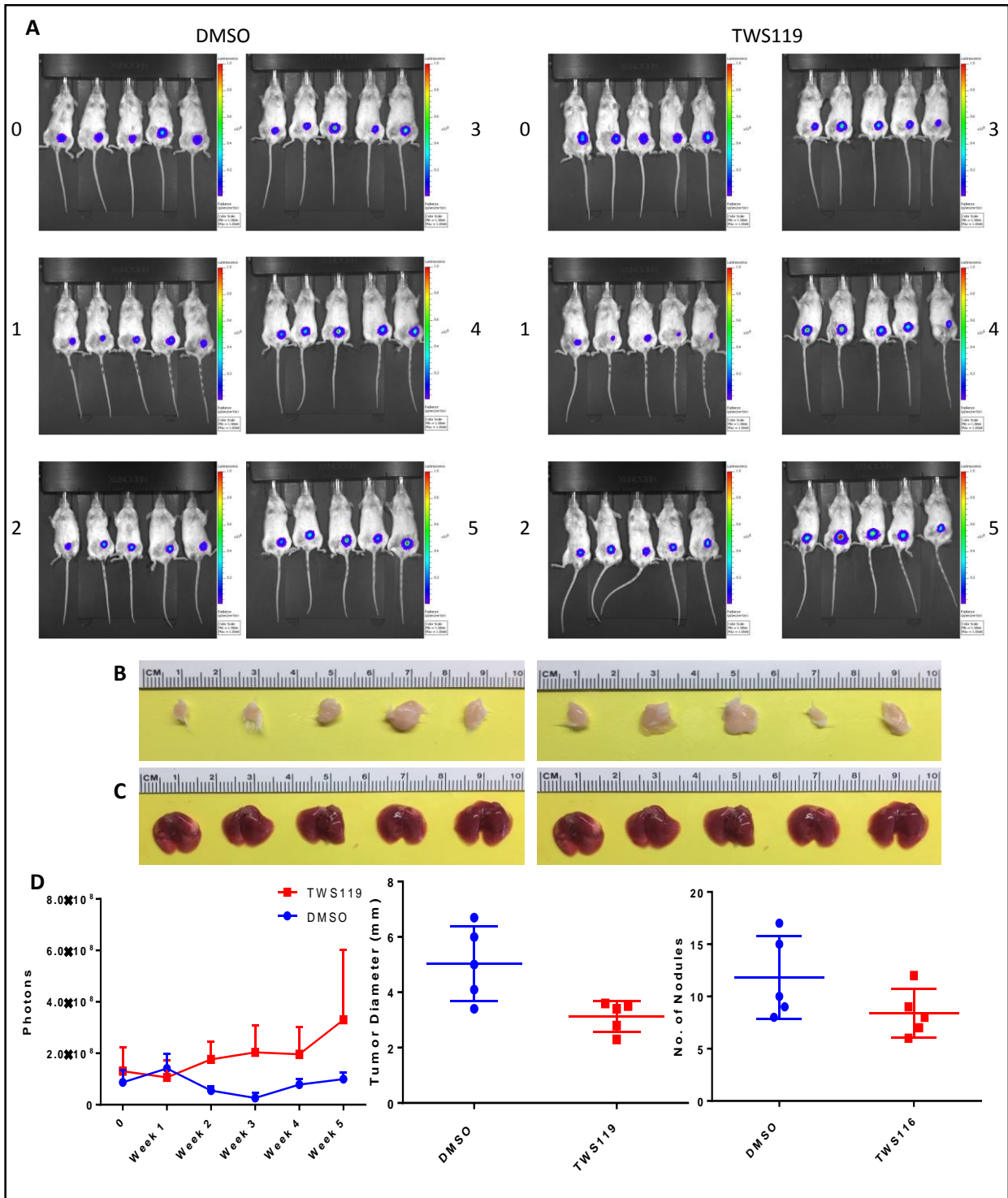


**Figure 25** – GSK3 $\beta$  inhibitor TWS119 with HMLER-Snail cells *in vivo*. **A and D.**  $1 \times 10^6$  HMLER-Snail cells were injected orthotopically and their progression in was monitored by imaging for the luciferase signal and the luminescence was assessed. **B and D.** At the end of the experiment, the animals were sacrificed and the tumors were harvested and diameter was quantified. **C and D.** At the end of the experiment, the animals were sacrificed and the lungs were harvested and nodules on the lungs were quantified.

The animals were sacrificed and the primary mammary tumor and lungs (to check for distant metastasis) were isolated and fixed for immunohistochemical analysis. The tumor size was measured and lung nodules counted. There was no significant difference in the size of tumors and the number of metastatic nodules in the lungs between the vehicle-treated set and the TWS119-treated set in both the 4T1 and the HMLER-Snail experiments (Figures 25 B,C&D, 26 B,C&D). This was in line with the observation that there was no significant difference in the photon counts between the TWS119 treated and vehicle treated mice in both these experiments (Figures 25 A&D, 26 A&D). One of the possible reasons for the inability of TWS119 to inhibit tumorigenesis and metastasis, could be that the drug did not reach the tumor. In order to test this hypothesis, immunohistochemistry (IHC) was performed to assess the expression of  $\beta$ -Catenin, FOXC2 and fibronectin. If the drug reached the target, there would be an accumulation of  $\beta$ -catenin in the nucleus indicating active Wnt signaling and inactive GSK3 $\beta$ , and if the drug was able to inhibit EMT *in vivo*, the expression of FOXC2 and fibronectin would be lower in the treated tumors as compared to the control treated tumors. The staining showed that there was no difference in the expression of  $\beta$ -catenin, FOXC2 or fibronectin between the treated and the untreated tumors indicating that the drug was unable to reach its target (Figure 27).

Summary – Aim3: Aim3 was performed to assess the efficacy of GSK3 $\beta$  inhibitors to inhibit the tumor progression of EMT/CSC-enriched breast cancer cells *in vivo*. However, due to the concentration of the drug used or due to the chosen method of application, we observed no significant decrease in the tumor size and metastatic potential of the EMT/CSC-enriched HMLER-Snail and 4T1 cells with TWS119 treatment.

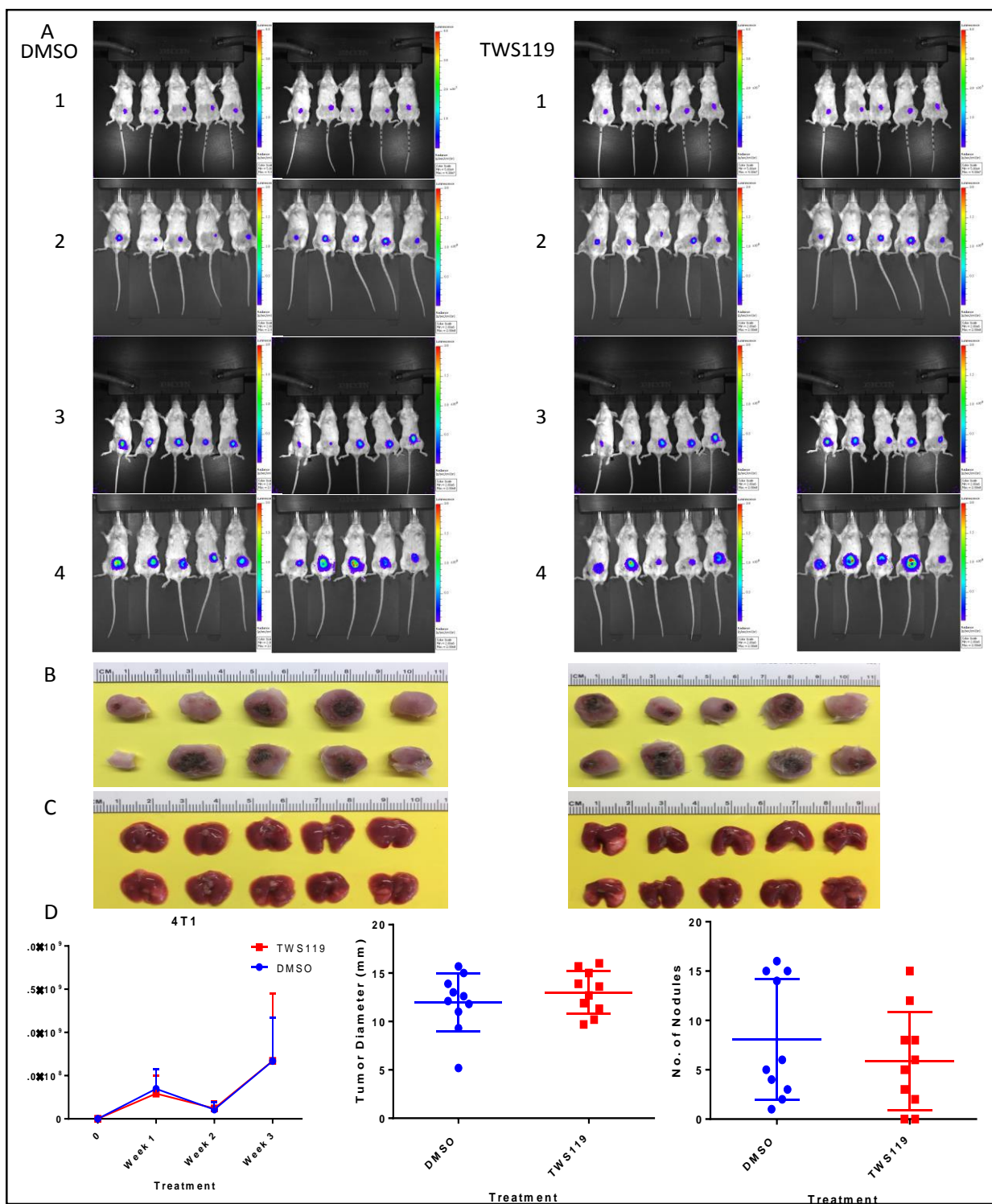


**Figure 26** – GSK3 $\beta$  inhibitor TWS119 with 4T1 cells *in vivo*. **A and D.** 10000 4T1 cells were injected orthotopically and their progression in was monitored by imaging for the luciferase signal and the luminescence was assessed. **B and D.** At the end of the experiment, the animals were sacrificed and the tumors were harvested and diameter was quantified. **C and D.** At the end of the experiment, the animals were sacrificed and the lungs were harvested and nodules on the lungs were quantified.

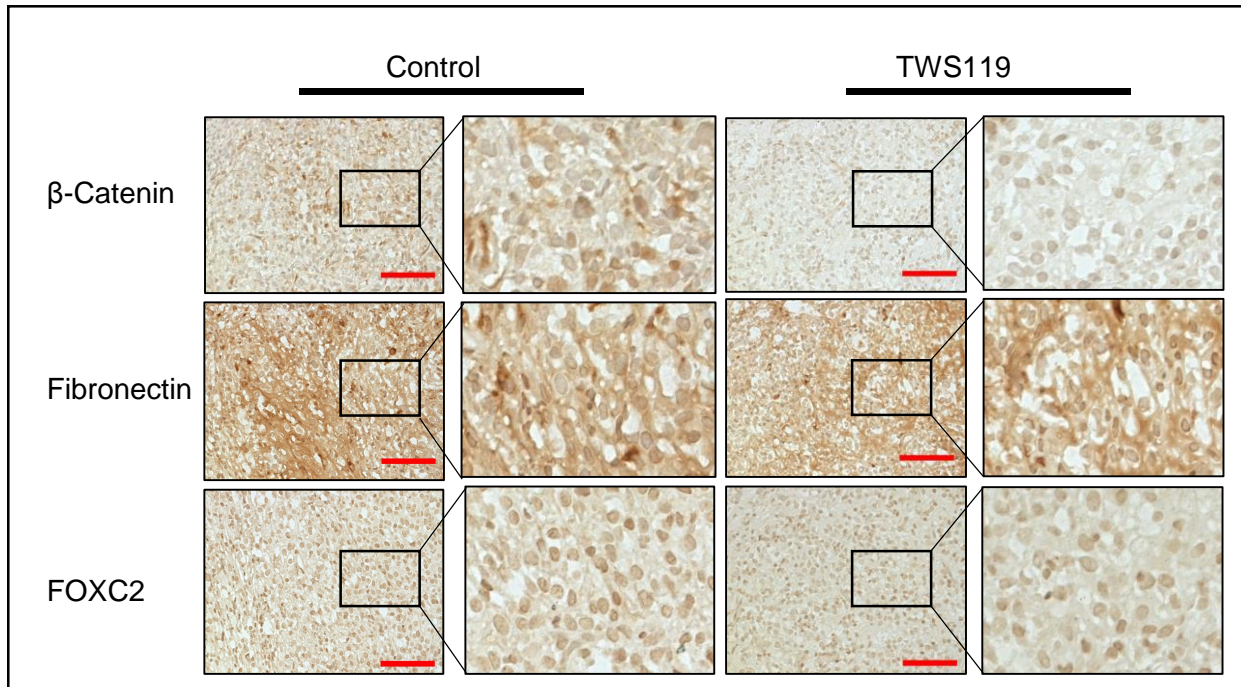


**Figure 27** – Immunohistochemistry of xenograft tumors treated with TWS119. HMLER-Snail tumors were fixed and immunohistochemistry was performed for  $\beta$ -Catenin, Fibronectin and FOXC2. We observed no difference in the expression of these proteins between the treated and the untreated tumors. Images were taken at 20x.

## Chapter 7 - Conclusions

This study was performed to investigate the role of GSK3 $\beta$  as a potential druggable target to inhibit the progression of EMT/CSC-rich TNBCs. Therefore, publicly available databases were analyzed to determine if GSK3 $\beta$  is indeed upregulated in breast cancers and the analysis revealed that GSK3 $\beta$  was significantly upregulated in breast cancer tissues as compared to the normal mammary tissues in the Ma, Richardson 2 and TCGA datasets. Besides being expressed at higher levels in breast tumors, KMPlotter analysis also demonstrated that the elevated levels of GSK3 $\beta$  in TNBCs significantly correlates with worse overall survival in these patients. These findings suggested a possible role for GSK3 $\beta$  in the progression of TNBCs.

TNBCs are EMT/CSC enriched cancers and as mentioned in Chapter 1, EMT and EMT-endowed CSCs are the cause of tumor recurrence, chemoresistance and higher metastatic potential of TNBCs. Therefore, inhibition of the EMT/CSC properties could be a feasible means of preventing TNBC-related fatality. In order to identify small molecule inhibitors capable of inhibiting EMT in TNBCs, TNBC representative cell line MDA MB 231 (modified to express Zeb1 and E-cadherin reporter) was used to perform a high-throughput drug screen. Among the ~1300 drugs tested, 11 drugs were identified as potential inhibitors of EMT. Upon validation using FACS, only 2 drugs were observed to successfully inhibit EMT in the TNBC cell line. Of the 2 drugs that were selected from the screen GSK3 $\beta$  inhibitor BIO was finalized as the lead candidate based on our analysis of the patient data and on the fact that CUDC-101 has multiple different targets. To rule out the possibility that this ability of inhibiting EMT is unique to BIO, 2 other GSK3 $\beta$  inhibitors, LiCl and TWS119 were also tested for their ability to inhibit mesenchymal properties of 3 different cell lines with EMT/CSC properties (HMLE-Snail, HMLE-Twist and Sum159). Both western blot analysis and qRT-PCR analysis demonstrated a decrease in the expression of mesenchymal markers and

increased expression of epithelial markers indicating an effective inhibition of EMT by the GSK3 $\beta$  inhibitors. GSK3 $\beta$  inhibitors were also observed to decrease the EMT-mediated migratory properties of the EMT/CSC-enriched cell lines (HMLE-Snail, HMLE-Twist and 4T1) and this effect of GSK3 $\beta$  inhibitors could be attributed to the inhibition of EMT at the wound edge in addition to the other well-established mechanisms.

It is well-known that EMT bestows CSC properties on cancer cells. As GSK3 $\beta$  inhibitors were effective in inhibiting EMT, the obvious next question was to test if GSK3 $\beta$  inhibitors were capable of inhibiting the sphere-forming potential of the TNBC cell line (MD MB 231 reporter cells). Of the 11 drugs that were selected from the drug screen, BIO was one of the drugs capable of decreasing the sphere-forming ability of the TNBC cell line. Not only BIO, but the other 2 drugs LiCl and TWS119 and shRNA to GSK3 $\beta$  were also able to decrease the sphere-forming potential of the mesenchymal-like cells. Additionally, MEFs in which GSK3 $\beta$  was knocked out also lost their ability to form spheres. Further, the 3 GSK3 $\beta$  inhibitors tested were also able to increase the proportion of CD24 expressing cells in the mesenchymal-like cell lines. All these observations taken together indicate that GSK3 $\beta$  inhibitors decrease the CSC properties and increase the proportion of differentiated population of the mesenchymal-like cell lines.

As the GSK3 $\beta$  inhibitors were shown to inhibit EMT and EMT-mediated CSC properties, which are characteristic of the mesenchymal-like cell lines, it was intriguing to test if the GSK3 $\beta$  inhibitors exerted selective inhibitory effect on EMT/CSC enriched cells as compared to their epithelial counterparts. Of the 11 drugs isolated in the screen, BIO was one of the 2 drugs capable of more potently inhibiting mesenchymal-like HMLE-Snail cells as compared to the epithelial HMLE-vector cells. All 3 GSK3 $\beta$  inhibitors (BIO, LiCl and TWS119) selectively inhibited mesenchymal-like cells



(Sum159) as compared to epithelial (MCF7) or normal-like (MCF10A) breast cell lines. In addition, in co-culture experiments, all 3 GSK3 $\beta$  inhibitors selectively inhibited mesenchymal-like (HMLER-Snail) cells as compared to the epithelial (HMLER) cells.

Based on our *in vitro* observations that GSK3 $\beta$  inhibitors effectively inhibited EMT, and EMT-mediated enhanced migratory and sphere-forming potential and selectively inhibited mesenchymal-like cells, we decided to test GSK3 $\beta$ -specific inhibitor (TWS119) *in vivo*. However, at the dosage used and with the route used to administer the drugs, no inhibitory effect was observed on the tumor size and metastatic potential of EMT/CSC-enriched cell lines. IHC analysis indicated that there was no inhibition of GSK3 $\beta$  based on the observation that there was no difference in the level of expression and localization of  $\beta$ -catenin between the treated and the untreated tumors. Therefore, the drug dosage and administration has to be modified to ensure that the drug is able to effectively inhibit GSK3 $\beta$  *in vivo*.



## Chapter 8 – Discussion and future directions

Since the discovery of Wnt signaling and its role in cancer, there has been an extraordinary emphasis on the association of the Wnt signaling with EMT, CSC properties and consequently on metastasis of cancers. However, this eclipses the roles played by other equally important players in the field. In this study we focused on the role of GSK3 $\beta$  and its importance as a prognostic factor and therapeutic target in breast cancer.

In our study, we found that high expression of GSK3 $\beta$  correlated with the poor survival of breast cancer patients. This was surprising as GSK3 $\beta$  is a negative regulator of Wnt signaling and therefore the presence of high levels of GSK3 $\beta$  would indicate an inactive Wnt signaling which would be considered as a good prognostic factor, considering the known effect of Wnt signaling on CSCs. Data mining also revealed that GSK3 $\beta$  is indeed expressed in elevated levels in breast tumor samples as compared to normal breast tissue.

Using multiple small molecule inhibitors of GSK3 $\beta$ , we have demonstrated that inhibition of GSK3 $\beta$  significantly decreased the expression of FOXC2 and fibronectin, both of which are robust markers of the mesenchymal phenotype. The decrease in expression of FOXC2 protein clearly explains the loss of CSC properties in the mesenchymal-like cells, as it has been previously illustrated that FOXC2 is essential for the CSC properties of cancer cells [67]. Additionally, under certain circumstances, GSK3 $\beta$  is known to be a positive regulator of NF $\kappa$ B, which in turn, has been demonstrated to promote FOXC2 expression and function [245, 246]. Therefore, pharmacological inhibition of GSK3 $\beta$  also promises to downregulate NF $\kappa$ B-mediated upregulation of FOXC2, thereby providing the means of targeting multiple pathways of tumor progression and metastasis [208]. In depth understanding of how GSK3 $\beta$  functions and is regulated sheds light on

how complex this protein is. For example, when we treat with a small molecule inhibitor, there is no way of pinpointing the pool of GSK3 $\beta$  that is majorly affected or if the overall function of GSK3 $\beta$  in all the pools is uniformly inhibited. There is also a dearth of knowledge regarding the flux of GSK3 $\beta$  between the different pools. Therefore, it is impossible to predict if one pool of GSK3 $\beta$  is maintained at the cost of the other pools thus allowing certain functions of GSK3 $\beta$  to proceed uninterrupted while compromising on the functions that are less vital to the cell in a particular context. Therefore, while it is easy to just examine the role of a molecule with regard to a single signaling pathway or cell type, looking at the bigger picture is essential to give context to the findings.

Again contrary to the expectations, we found that inhibition of GSK3 $\beta$  clearly inhibited the CSC properties of the mesenchymal-like cells, which is evident in both the increase in the expression of differentiation-related cell surface marker CD24 and the decrease in the stem cell-related sphere forming ability of the cells. This emphasizes the fact that these effects of GSK3 $\beta$  inhibition could be due to the effect of the inhibitors on the Wnt-independent activity of the GSK3 $\beta$ . GSK3 $\beta$  is a highly versatile kinase with several targets involved in different pathways which regulate each other and thus making GSK3 $\beta$  a pivotal player in regulating the different pathways. Therefore, the effect elicited by GSK3 $\beta$  inhibitors need not primarily be equivalent to the activation of Wnt signaling pathway. The different pathways that could be affected depend upon the regulation of the downstream molecules which determine the direction of flow of information.

Along with the inhibition of the CSC properties, the GSK3 $\beta$  inhibitors also significantly decrease the migration of the mesenchymal-like cells, which indicates a reduction in the aggressive metastatic potential of these cells. There have been other publications demonstrating that

inhibition of GSK3 $\beta$  inhibits the migratory properties of the cells and this effect of GSK3 $\beta$  has been attributed to its effects on molecules such as Rac and Rock [236]. However, we show additional means by which GSK3 $\beta$  could alter the migration of the cells. In HMLE cells, we show that migration of the cells is accompanied by the upregulation of FOXC2 at the migratory front of the cells. In the presence of the GSK3 $\beta$  inhibitors, this upregulation of FOXC2 is prevented which adds to the inhibitory effect of GSK3 $\beta$  inhibitors.

One of the main challenges in this study was the fact that shRNAs to GSK3 $\beta$  were not able to recapitulate the downregulation of mesenchymal markers effected by the small molecule inhibitors. This could be attributed to the fact the small molecule inhibitors inhibit GSK3 $\beta$  to a greater extent than the inhibition by the shRNA, and that the inhibition by the shRNA was enough to affect the sphere forming ability of the cells, but not sufficient to suppress the expression of the mesenchymal markers. In order to address this issue, GSK3 $\beta$  knockout MEFs were used and we were able to demonstrate a decrease in the expression of FOXC2, but it was difficult to use fibroblasts to study alterations in EMT. Another means of testing could be to use CRISPR technology to delete GSK3 $\beta$  which would be superior because it would deletion of the GSK3 $\beta$  gene resulting in the abrogation of the protein. We have not yet tested this approach. While both knockdown of GSK3 $\beta$  as in the MEF and the use of CRISPR are good means for identifying the role of GSK3 $\beta$  in cell lines, this method will be hard to achieve in patients. Also GSK3 $\beta$  is a multifunctional molecule with many reported (apparently unrelated) functions. Another explanation for this discrepancy could be the fact that the small molecule inhibitors inhibit both GSK3 $\beta$  and GSK3 $\alpha$ , which have some redundant functions. However, attempts to create double knockdowns failed as cells most likely did not survive in the absence of such vital kinases. It is interesting to note that shRNA to GSK3 $\beta$  did significantly decrease the CSC properties of the cells without affecting their EMT properties. This leads to another interesting theory that GSK3 $\beta$  could

be the point of bifurcation between EMT and CSC properties which are currently considered to be the 2 sides of the same coin. The ultimate goal of this study is to find a means of targeting tumor progression and metastasis. Due to the importance of Wnt signaling in tumor progression and metastasis, efforts are ongoing to design Wnt inhibitors that can effectively inhibit metastasis. However, these studies are in their infancy and have to overcome several obstacles to be successful anticancer drugs.

The most striking finding in this study is that the GSK3 $\beta$  inhibitors have a potent inhibitory effect on mesenchymal-like cells (Sum159) but not on epithelial (MCF7) or normal-like (MCF10A) breast cancer cell lines. It will be important for future studies to decipher the molecular mechanism underlying this differential activity. One way to address this issue would be to perform a microarray to compare the changes in the gene expression profile of the cells following treatment with GSK3 $\beta$  inhibitors. This could provide insight into which pathways are differentially altered between the normal-like, epithelial and mesenchymal-like breast cancer cell lines.

On the other hand the GSK3 $\beta$  inhibitors have been widely used in the treatment of psychiatric disorders and their effect and side effects have been well documented. GSK3 $\beta$  is a vital molecule that serves as a hub for several signaling pathways. Therefore, the small molecule inhibitors of GSK3 $\beta$  can be used to efficiently target and modulate several different pathways and significantly hinder the proliferation and metastasis of cancer cells. Despite the existence of controversial literature suggesting a potential role of GSK3 $\beta$  as a tumor suppressor in breast cancer based on *in vitro* studies, there is paucity of *in vivo* data to substantiate this claim [192, 247, 248]. Knowing how diverse and heterogeneous cancer is, even breast cancer cannot be classified as a single disease. Therefore, it would be unwise to classify a ubiquitous and multifunctional kinase such as

GSK3 $\beta$  as a tumor promoter or suppressor. Additionally the strong correlation between the expression of GSK3 $\beta$  and poor prognosis in breast cancer patients is in itself a strong proponent of the therapeutic use of GSK3 $\beta$  inhibitors in addition to the standard-of-care treatment currently available for the treatment of breast cancers. One of the other main concerns is that inhibition of GSK3 $\beta$  in patients would lead to the activation of Wnt, a tumor promoter and hyperactivation of Wnt signaling pathway in breast cancer is a well-established fact. Therefore, inhibition of GSK3 $\beta$  cannot further activate the already activated system. Therefore, treating breast cancers with hyperactivated Wnt signaling should manifest no effect on the Wnt signaling pathway but on the other pathways in which GSK3 $\beta$  is involved. There are also reports to show that there is no evidence of increased tumor incidence in patients chronically treated with lithium for their psychiatric disorders [249].

Contrary to expectation, our *in vivo* experiments to test the efficacy of the GSK3 $\beta$  inhibitors were not conclusive regarding the efficacy of the drug. It is possible that the injected drug did not reach the intended target. Therefore, we performed IHC to test if this hypothesis is true. The tumors and the lungs isolated from the animals were fixed and embedded and stained to determine if GSK3 $\beta$  was indeed inhibited in the tumors or if the drugs did not reach the target. The HMLER-Snail tumor sections were stained for  $\beta$ -Catenin, FOXC2 and fibronectin. If the drug successfully reached the target and inhibited GSK3 $\beta$ , we would expect to see a significant increase in the expression and nuclear localization of  $\beta$ -Catenin and based on the *in vivo* experiments, a decrease in the expression of FOXC2 and fibronectin. However, we observed no difference in the levels of expression of  $\beta$ -Catenin between the GSK3 $\beta$  inhibitor treated and the control treated tumors indicating that the drug did not reach its target or did not exert its effect on the tumor cells. Therefore, the experiment did not give the expected results. Additionally, our observations with regards to the 4T1 experiment indicate that continued treatment could have attenuated the ability

of the breast cancer cells to metastasize. However, this could not be tested due to the morbid tumor volumes in case of 4T1 cell lines and due to the toxic effect of DMSO at the site of injection.

One of the main challenges is the lack of *in vivo* studies using TWS119. As a result, there is not enough published data available to determine the correct dosage and treatment regime. Therefore, more pharmacological studies are required to optimize the treatment plan for testing the efficacy of the drug to inhibit tumorigenesis and metastasis of breast cancer. Considering the ability of GSK3 $\beta$  inhibitors to specifically target mesenchymal-like cells with CSC properties, the GSK3 $\beta$  inhibitors may be better suited for combination treatments.

A key future direction is to identify chemotherapeutic agents whose efficacy can be improved by the addition of GSK3 $\beta$  inhibitors to the treatment regimen. As the GSK3 $\beta$  inhibitor from Eli Lilly (LY2090314) is FDA approved and in clinical trial, we have decided to add this drug to our studies [200]. LY2090314 has been shown to increase the potency of platinum drugs [200]. Therefore, platinum drugs will be one of the primary candidates to be tested for combination treatment with GSK3 $\beta$  inhibitors in TNBCs. The next step will be to determine the dosage and test the efficacy of the drug *in vivo*. In case of LY2090314, there have been several *in vivo* studies performed in melanoma models [250]. Therefore as the treatment parameters have been well established, it could therefore serve as the starting platform to test this drug *in vivo*. Based on these new data, we aim to design combination treatment regimens for treating orthotopic TNBC mouse models. Additionally, we have access to several TNBC patient-derived xenograft (PDX) models through our collaborators and these will serve as perfect models to test the combination treatments as they are truer representatives of the disease heterogeneity than cell lines. The subsequent goal would be to study the pathways that are differentially altered between the epithelial and

mesenchymal-like cells following treatment with GSK3 $\beta$  inhibitors using microarray or RNAseq techniques.

The primary goal of this study was to identify novel druggable targets to treat TNBCs which currently lack targeted therapies. This study serves as a preliminary indicator that there is more promise in using GSK3 $\beta$  inhibitors if close consideration is given to the pleiotropic signaling cascades it influences rather than as a mere modulator of a single signaling cascade which is the Wnt signaling pathway. Our goal is to continue our efforts to establish a probable mechanism of action for the effect to GSK3 $\beta$  inhibitors in the inhibition of EMT and CSCs and to define a viable and potent combination treatment for TNBCs.

## References

1. N, H., et al., *SEER Cancer Statistics Review, 1975-2011*. 2014.
2. Criscitiello, C., et al., *Understanding the biology of triple-negative breast cancer*. Annals of Oncology, 2012. **23**(suppl 6): p. vi13-vi18.
3. Lehmann, B.D., et al., *Identification of human triple-negative breast cancer subtypes and preclinical models for selection of targeted therapies*. The Journal of Clinical Investigation. **121**(7): p. 2750-2767.
4. Bianchini, G., et al., *Triple-negative breast cancer: challenges and opportunities of a heterogeneous disease*. Nat Rev Clin Oncol, 2016. **13**(11): p. 674-690.
5. *Comprehensive molecular portraits of human breast tumours*. Nature, 2012. **490**(7418): p. 61-70.
6. Kreike, B., et al., *Gene expression profiling and histopathological characterization of triple-negative/basal-like breast carcinomas*. Breast Cancer Research, 2007. **9**(5): p. R65.
7. Kreike, B., et al., *Gene Expression Profiles of Primary Breast Carcinomas from Patients at High Risk for Local Recurrence after Breast-Conserving Therapy*. Clinical Cancer Research, 2006. **12**(19): p. 5705-5712.
8. Turner, N., et al., *Integrative molecular profiling of triple negative breast cancers identifies amplicon drivers and potential therapeutic targets*. Oncogene, 2010. **29**(14): p. 2013-2023.
9. Swanson, J.O. and R.C. Richie, *Breast Cancer: A Review of the Literature*. Journal of Insurance medicine, 2003. **35**: p. 85-101.
10. Ahmad, A., *Pathways to Breast Cancer Recurrence*. ISRN Oncology, 2013. **2013**: p. 16.
11. Moody, S.E., et al., *The transcriptional repressor Snail promotes mammary tumor recurrence*. Cancer Cell, 2005. **8**(3): p. 197-209.
12. Mitra, A., L. Mishra, and S. Li, *EMT, CTCs and CSCs in tumor relapse and drug-resistance*. Oncotarget, 2015. **6**(13): p. 10697-10711.
13. Wang, Y., et al., *A retrospective study of breast cancer subtypes: the risk of relapse and the relations with treatments*. Breast Cancer Research and Treatment, 2011. **130**(2): p. 489.
14. Yersal, O. and S. Barutca, *Biological subtypes of breast cancer: Prognostic and therapeutic implications*. World Journal of Clinical Oncology, 2014. **5**(3): p. 412-424.
15. Lowery, A.J., et al., *Locoregional recurrence after breast cancer surgery: a systematic review by receptor phenotype*. Breast Cancer Research and Treatment, 2012. **133**(3): p. 831-841.
16. Meng, X., et al., *A new hypothesis for the cancer mechanism*. Cancer and Metastasis Reviews, 2012. **31**(1): p. 247-268.
17. Li, Y., et al., *Implications of Cancer Stem Cell Theory for Cancer Chemoprevention by Natural Dietary Compounds*. The Journal of nutritional biochemistry, 2011. **22**(9): p. 799-806.
18. Valastyan, S. and Robert A. Weinberg, *Tumor Metastasis: Molecular Insights and Evolving Paradigms*. Cell. **147**(2): p. 275-292.
19. Gupta, G.P. and J. Massagué, *Cancer Metastasis: Building a Framework*. Cell, 2006. **127**(4): p. 679-695.
20. Nguyen, D.X., P.D. Bos, and J. Massague, *Metastasis: from dissemination to organ-specific colonization*. Nat Rev Cancer, 2009. **9**(4): p. 274-284.
21. TSENG, L.M., et al., *Distant metastasis in triple-negative breast cancer*. Neoplasm, 2013. **60**(3): p. 290-294.
22. Dent, R., et al., *Pattern of metastatic spread in triple-negative breast cancer*. Breast Cancer Research and Treatment, 2009. **115**(2): p. 423-428.
23. Bissell, M.J. and W.C. Hines, *Why don't we get more cancer? A proposed role of the microenvironment in restraining cancer progression*. Nat Med, 2011. **17**(3): p. 320-329.



24. Hu, M., et al., *Regulation of In Situ to Invasive Breast Carcinoma Transition*. Cancer cell, 2008. **13**(5): p. 394-406.
25. Levental, K.R., et al., *Matrix Crosslinking Forces Tumor Progression by Enhancing Integrin Signaling*. Cell, 2009. **139**(5): p. 891-906.
26. Friedl, P. and K. Wolf, *Tumour-cell invasion and migration: diversity and escape mechanisms*. Nat Rev Cancer, 2003. **3**(5): p. 362-374.
27. Pal, S.K., B.H. Childs, and M. Pegram, *Triple negative breast cancer: unmet medical needs*. Breast cancer research and treatment, 2011. **125**(3): p. 627-636.
28. Giampieri, S., et al., *Localised and reversible TGF $\beta$  signalling switches breast cancer cells from cohesive to single cell motility*. Nature cell biology, 2009. **11**(11): p. 1287-1296.
29. Gupta, G.P., et al., *Mediators of vascular remodelling co-opted for sequential steps in lung metastasis*. Nature, 2007. **446**(7137): p. 765-770.
30. Carmeliet, P. and R.K. Jain, *Molecular mechanisms and clinical applications of angiogenesis*. Nature, 2011. **473**(7347): p. 298-307.
31. Douma, S., et al., *Suppression of anoikis and induction of metastasis by the neurotrophic receptor TrkB*. Nature, 2004. **430**(7003): p. 1034-1039.
32. Schafer, Z.T., et al., *Antioxidant and oncogene rescue of metabolic defects caused by loss of matrix attachment*. Nature, 2009. **461**(7260): p. 109-113.
33. Hur, E.-M. and F.-Q. Zhou, *GSK3 signalling in neural development*. Nat Rev Neurosci, 2010. **11**(8): p. 539-551.
34. Joyce, J.A. and J.W. Pollard, *Microenvironmental regulation of metastasis*. Nat Rev Cancer, 2009. **9**(4): p. 239-252.
35. Padua, D., et al., *TGF $\beta$  Primes Breast Tumors for Lung Metastasis Seeding through Angiopoietin-like 4*. Cell, 2008. **133**(1): p. 66-77.
36. Qian, B.-Z., et al., *CCL2 recruits inflammatory monocytes to facilitate breast-tumour metastasis*. Nature, 2011. **475**(7355): p. 222-225.
37. Psaila, B. and D. Lyden, *The metastatic niche: adapting the foreign soil*. Nat Rev Cancer, 2009. **9**(4): p. 285-293.
38. Erler, J.T., et al., *Hypoxia-induced lysyl oxidase is a critical mediator of bone marrow cell recruitment to form the pre-metastatic niche*. Cancer cell, 2009. **15**(1): p. 35-44.
39. Zhang, X.H.F., et al., *Latent bone metastasis in breast cancer tied to Src-dependent survival signals*. Cancer cell, 2009. **16**(1): p. 67-78.
40. Barkan, D., et al., *Inhibition of Metastatic Outgrowth From Single Dormant Tumor Cells by Targeting the Cytoskeleton*. Cancer research, 2008. **68**(15): p. 6241-6250.
41. Shibue, T. and R.A. Weinberg, *Integrin  $\beta$ (1)-focal adhesion kinase signaling directs the proliferation of metastatic cancer cells disseminated in the lungs*. Proceedings of the National Academy of Sciences of the United States of America, 2009. **106**(25): p. 10290-10295.
42. Barkan, D., et al., *Metastatic Growth from Dormant Cells Induced by a Col-I Enriched Fibrotic Environment*. Cancer research, 2010. **70**(14): p. 5706-5716.
43. McAllister, S.S., et al., *Systemic Endocrine Instigation of Indolent Tumor Growth Requires Osteopontin*. Cell, 2008. **133**(6): p. 994-1005.
44. Hiratsuka, S., et al., *C-X-C receptor type 4 promotes metastasis by activating p38 mitogen-activated protein kinase in myeloid differentiation antigen (Gr-1)-positive cells*. Proceedings of the National Academy of Sciences of the United States of America, 2011. **108**(1): p. 302-307.
45. Chambers, A.F., A.C. Groom, and I.C. MacDonald, *Metastasis: Dissemination and growth of cancer cells in metastatic sites*. Nat Rev Cancer, 2002. **2**(8): p. 563-572.
46. Hart, I.R. and I.J. Fidler, *Role of Organ Selectivity in the Determination of Metastatic Patterns of B16 Melanoma*. Cancer Research, 1980. **40**(7): p. 2281-2287.

47. Kang, Y., et al., *A multigenic program mediating breast cancer metastasis to bone*. Cancer Cell, 2003. **3**(6): p. 537-549.
48. Minn, A.J., et al., *Genes that mediate breast cancer metastasis to lung*. Nature, 2005. **436**(7050): p. 518-524.
49. Bos, P.D., et al., *Genes that mediate breast cancer metastasis to the brain*. Nature, 2009. **459**(7249): p. 1005-1009.
50. Tabaries, S., et al., *Claudin-2 is selectively enriched in and promotes the formation of breast cancer liver metastases through engagement of integrin complexes*. Oncogene, 2011. **30**(11): p. 1318-1328.
51. Lamouille, S., J. Xu, and R. Derynck, *Molecular mechanisms of epithelial–mesenchymal transition*. Nat Rev Mol Cell Biol, 2014. **15**(3): p. 178-196.
52. Kalluri, R. and R.A. Weinberg, *The basics of epithelial-mesenchymal transition*. The Journal of Clinical Investigation. **119**(6): p. 1420-1428.
53. Steinestel, K., et al., *Clinical significance of epithelial-mesenchymal transition*. Clinical and Translational Medicine, 2014. **3**: p. 17-17.
54. Burgess, D.J., *Breast cancer: Circulating and dynamic EMT*. Nat Rev Cancer, 2013. **13**(3): p. 148-149.
55. Yu, M., et al., *Circulating Breast Tumor Cells Exhibit Dynamic Changes in Epithelial and Mesenchymal Composition*. Science (New York, N.Y.), 2013. **339**(6119): p. 580-584.
56. Davis, F.M., et al., *Targeting EMT in cancer: opportunities for pharmacological intervention*. Trends in Pharmacological Sciences. **35**(9): p. 479-488.
57. Sarrió, D., et al., *Epithelial-Mesenchymal Transition in Breast Cancer Relates to the Basal-like Phenotype*. Cancer Research, 2008. **68**(4): p. 989.
58. Prat, A., et al., *Phenotypic and molecular characterization of the claudin-low intrinsic subtype of breast cancer*. Breast Cancer Research, 2010. **12**(5): p. R68.
59. Mani, S.A., et al., *The epithelial-mesenchymal transition generates cells with properties of stem cells*. Cell, 2008. **133**.
60. Hollier, B.G., et al., *FOXC2 expression links epithelial-mesenchymal transition and stem cell properties in breast cancer*. Cancer research, 2013. **73**(6): p. 1981-1992.
61. Hazan, R.B., et al., *Cadherin Switch in Tumor Progression*. Annals of the New York Academy of Sciences, 2004. **1014**(1): p. 155-163.
62. Briehner, W.M. and A.S. Yap, *Cadherin junctions and their cytoskeleton(s)*. Current Opinion in Cell Biology, 2013. **25**(1): p. 39-46.
63. Hansen, S.M., V. Berezin, and E. Bock, *Signaling mechanisms of neurite outgrowth induced by the cell adhesion molecules NCAM and N-Cadherin*. Cellular and Molecular Life Sciences, 2008. **65**(23): p. 3809-3821.
64. Yilmaz, M. and G. Christofori, *EMT, the cytoskeleton, and cancer cell invasion*. Cancer and Metastasis Reviews, 2009. **28**(1): p. 15-33.
65. Huang, R.Y.-J., P. Guilford, and J.P. Thiery, *Early events in cell adhesion and polarity during epithelial-mesenchymal transition*. Journal of Cell Science, 2012. **125**(19): p. 4417-4422.
66. Peinado, H., D. Olmeda, and A. Cano, *Snail, Zeb and bHLH factors in tumour progression: an alliance against the epithelial phenotype?* Nat Rev Cancer, 2007. **7**(6): p. 415-428.
67. Mani, S.A., et al., *The epithelial-mesenchymal transition generates cells with properties of stem cells*. Cell, 2008. **133**.
68. Nieto, M.A., *The snail superfamily of zinc-finger transcription factors*. Nat Rev Mol Cell Biol, 2002. **3**(3): p. 155-166.
69. Manzanares, M., A. Locascio, and M.A. Nieto, *The increasing complexity of the Snail gene superfamily in metazoan evolution*. Trends in Genetics, 2001. **17**(4): p. 178-181.

70. Lin, T., et al., *Requirement of the Histone Demethylase LSD1 in Snai1-mediated Transcriptional Repression during Epithelial-Mesenchymal Transition*. *Oncogene*, 2010. **29**(35): p. 4896-4904.
71. Dong, C., et al., *G9a interacts with Snail and is critical for Snail-mediated E-cadherin repression in human breast cancer*. *The Journal of Clinical Investigation*, 2012. **122**(4): p. 1469-1486.
72. Dong, C., et al., *Interaction with Suv39H1 is Critical for Snail-mediated E-cadherin Repression in Breast Cancer*. *Oncogene*, 2013. **32**(11): p. 1351-1362.
73. Herranz, N., et al., *Polycomb Complex 2 Is Required for E-cadherin Repression by the Snail1 Transcription Factor*. *Molecular and Cellular Biology*, 2008. **28**(15): p. 4772-4781.
74. Tong, Z.T., et al., *EZH2 supports nasopharyngeal carcinoma cell aggressiveness by forming a co-repressor complex with HDAC1/HDAC2 and Snail to inhibit E-cadherin*. *Oncogene*, 2012. **31**(5): p. 583-594.
75. Peinado, H., et al., *Snail Mediates E-Cadherin Repression by the Recruitment of the Sin3A/Histone Deacetylase 1 (HDAC1)/HDAC2 Complex*. *Molecular and Cellular Biology*, 2004. **24**(1): p. 306-319.
76. Zhou, B.P., et al., *Dual regulation of Snail by GSK-3[beta]-mediated phosphorylation in control of epithelial-mesenchymal transition*. *Nat Cell Biol*, 2004. **6**(10): p. 931-940.
77. McCubrey, J.A., et al., *Roles of GSK-3 and microRNAs on epithelial mesenchymal transition and cancer stem cells*. *Oncotarget*, 2016. **8**: p. 14221-14250.
78. Yook, J.I., et al., *A Wnt-Axin2-GSK3[beta] cascade regulates Snail1 activity in breast cancer cells*. *Nat Cell Biol*, 2006. **8**(12): p. 1398-1406.
79. Wu, Y., et al., *Stabilization of Snail by NF- $\kappa$ B Is Required for Inflammation-Induced Cell Migration and Invasion*. *Cancer cell*, 2009. **15**(5): p. 416-428.
80. Sahlgren, C., et al., *Notch signaling mediates hypoxia-induced tumor cell migration and invasion*. *Proceedings of the National Academy of Sciences of the United States of America*, 2008. **105**(17): p. 6392-6397.
81. Wu, Y., B.M. Evers, and B.P. Zhou, *Small C-terminal Domain Phosphatase Enhances Snail Activity through Dephosphorylation*. *The Journal of Biological Chemistry*, 2009. **284**(1): p. 640-648.
82. Yang, Z., et al., *Pak1 Phosphorylation of Snail, a Master Regulator of Epithelial-to-Mesenchyme Transition, Modulates Snail's Subcellular Localization and Functions*. *Cancer Research*, 2005. **65**(8): p. 3179-3184.
83. Zhang, K., et al., *Lats2 kinase potentiates Snail1 activity by promoting nuclear retention upon phosphorylation*. *The EMBO Journal*, 2012. **31**(1): p. 29-43.
84. Du, C., et al., *Protein Kinase D1 Suppresses Epithelial-to-Mesenchymal Transition through Phosphorylation of Snail*. *Cancer Research*, 2010. **70**(20): p. 7810-7819.
85. Sanchez-Tillo, E., et al., *ZEB1 represses E-cadherin and induces an EMT by recruiting the SWI/SNF chromatin-remodeling protein BRG1*. *Oncogene*, 2010. **29**(24): p. 3490-3500.
86. Xu, J., S. Lamouille, and R. Derynck, *TGF- $\beta$ -induced epithelial to mesenchymal transition*. *Cell research*, 2009. **19**(2): p. 156-172.
87. Park, S.-M., et al., *The miR-200 family determines the epithelial phenotype of cancer cells by targeting the E-cadherin repressors ZEB1 and ZEB2*. *Genes & Development*, 2008. **22**(7): p. 894-907.
88. Mani, S.A., et al., *The epithelial-mesenchymal transition generates cells with properties of stem cells*. *Cell*, 2008. **133**(4): p. 704-715.
89. Mani, S.A., et al., *Mesenchyme Forkhead 1 (FOXC2) plays a key role in metastasis and is associated with aggressive basal-like breast cancers*. *Proceedings of the National Academy of Sciences*, 2007. **104**(24): p. 10069-10074.
90. Craene, B.D. and G. Berx, *Regulatory networks defining EMT during cancer initiation and progression*. *Nat Rev Cancer*, 2013. **13**(2): p. 97-110.

91. Kang, Y., C.-R. Chen, and J. Massagué, *A Self-Enabling TGF $\beta$  Response Coupled to Stress Signaling*. Molecular Cell. **11**(4): p. 915-926.
92. Yang, F., et al., *SET8 promotes epithelial-mesenchymal transition and confers TWIST dual transcriptional activities*. The EMBO Journal, 2012. **31**(1): p. 110-123.
93. Yang, M.-H., et al., *Direct regulation of TWIST by HIF-1[alpha] promotes metastasis*. Nat Cell Biol, 2008. **10**(3): p. 295-305.
94. Kondoh, H. and Y. Kamachi, *SOX-partner code for cell specification: Regulatory target selection and underlying molecular mechanisms*. The International Journal of Biochemistry & Cell Biology, 2010. **42**(3): p. 391-399.
95. Bresnick, E.H., et al., *GATA Switches as Developmental Drivers*. The Journal of Biological Chemistry, 2010. **285**(41): p. 31087-31093.
96. Valles, A.M., et al., *Alpha 2 beta 1 integrin is required for the collagen and FGF-1 induced cell dispersion in a rat bladder carcinoma cell line*. Cell Adhes Commun, 1996. **4**(3): p. 187-99.
97. Billottet, C., et al., *Modulation of several waves of gene expression during FGF-1 induced epithelial-mesenchymal transition of carcinoma cells*. J Cell Biochem, 2008. **104**(3): p. 826-39.
98. Grotegut, S., et al., *Hepatocyte growth factor induces cell scattering through MAPK/Egr-1-mediated upregulation of Snail*. Embo j, 2006. **25**(15): p. 3534-45.
99. Savagner, P., K.M. Yamada, and J.P. Thiery, *The zinc-finger protein slug causes desmosome dissociation, an initial and necessary step for growth factor-induced epithelial-mesenchymal transition*. J Cell Biol, 1997. **137**(6): p. 1403-19.
100. Kim, H.J., et al., *Constitutively active type I insulin-like growth factor receptor causes transformation and xenograft growth of immortalized mammary epithelial cells and is accompanied by an epithelial-to-mesenchymal transition mediated by NF-kappaB and snail*. Mol Cell Biol, 2007. **27**(8): p. 3165-75.
101. Canonici, A., et al., *Insulin-like growth factor-I receptor, E-cadherin and alpha v integrin form a dynamic complex under the control of alpha-catenin*. Int J Cancer, 2008. **122**(3): p. 572-82.
102. Graham, T.R., et al., *Insulin-like growth factor-I-dependent up-regulation of ZEB1 drives epithelial-to-mesenchymal transition in human prostate cancer cells*. Cancer Res, 2008. **68**(7): p. 2479-88.
103. Lu, Z., et al., *Downregulation of caveolin-1 function by EGF leads to the loss of E-cadherin, increased transcriptional activity of beta-catenin, and enhanced tumor cell invasion*. Cancer Cell, 2003. **4**(6): p. 499-515.
104. Ahmed, N., et al., *Molecular pathways regulating EGF-induced epithelial-to-mesenchymal transition in human ovarian surface epithelium*. Am J Physiol Cell Physiol, 2006. **290**(6): p. C1532-42.
105. Yang, L., C. Lin, and Z.R. Liu, *P68 RNA helicase mediates PDGF-induced epithelial to mesenchymal transition by displacing Axin from beta-catenin*. Cell, 2006. **127**(1): p. 139-55.
106. Lamouille, S., J. Xu, and R. Derynck, *Molecular mechanisms of epithelial-mesenchymal transition*. Nat Rev Mol Cell Biol, 2014. **15**(3): p. 178-96.
107. Schnaper, H.W., et al., *TGF- $\beta$  signal transduction and mesangial cell fibrogenesis*. American Journal of Physiology - Renal Physiology, 2003. **284**(2): p. F243-F252.
108. Gressner, A.M., et al., *Roles of TGF-beta in hepatic fibrosis*. Front Biosci, 2002. **7**: p. d793-807.
109. Willis, B.C. and Z. Borok, *TGF- $\beta$ -induced EMT: mechanisms and implications for fibrotic lung disease*. American Journal of Physiology - Lung Cellular and Molecular Physiology, 2007. **293**(3): p. L525-L534.
110. Zeisberg, E.M., et al., *Endothelial-to-mesenchymal transition contributes to cardiac fibrosis*. Nat Med, 2007. **13**(8): p. 952-961.
111. Kalluri, R. and R.A. Weinberg, *The basics of epithelial-mesenchymal transition*. J Clin Invest, 2009. **119**.

112. Feng, X.H. and R. Derynck, *Specificity and versatility in tgf-beta signaling through Smads*. Annu Rev Cell Dev Biol, 2005. **21**: p. 659-93.
113. Massagué, J., *TGFβ signalling in context*. Nature reviews. Molecular cell biology, 2012. **13**(10): p. 616-630.
114. Miyazono, K., P. ten Dijke, and C.H. Heldin, *TGF-beta signaling by Smad proteins*. Adv Immunol, 2000. **75**: p. 115-57.
115. Morita, T., T. Mayanagi, and K. Sobue, *Dual roles of myocardin-related transcription factors in epithelial-mesenchymal transition via slug induction and actin remodeling*. The Journal of Cell Biology, 2007. **179**(5): p. 1027-1042.
116. Thuault, S., et al., *Transforming growth factor-beta employs HMGA2 to elicit epithelial-mesenchymal transition*. J Cell Biol, 2006. **174**(2): p. 175-83.
117. Ozdamar, B., et al., *Regulation of the polarity protein Par6 by TGFbeta receptors controls epithelial cell plasticity*. Science, 2005. **307**(5715): p. 1603-9.
118. Bhowmick, N.A., et al., *Transforming Growth Factor-β1 Mediates Epithelial to Mesenchymal Transdifferentiation through a RhoA-dependent Mechanism*. Molecular Biology of the Cell, 2001. **12**(1): p. 27-36.
119. Bakin, A.V., et al., *Phosphatidylinositol 3-kinase function is required for transforming growth factor beta-mediated epithelial to mesenchymal transition and cell migration*. J Biol Chem, 2000. **275**(47): p. 36803-10.
120. Chaudhury, A., et al., *TGF-beta-mediated phosphorylation of hnRNP E1 induces EMT via transcript-selective translational induction of Dab2 and ILEI*. Nat Cell Biol, 2010. **12**(3): p. 286-93.
121. Gordon, K.J., et al., *Bone morphogenetic proteins induce pancreatic cancer cell invasiveness through a Smad1-dependent mechanism that involves matrix metalloproteinase-2*. Carcinogenesis, 2009. **30**(2): p. 238-48.
122. Zeisberg, M., A.A. Shah, and R. Kalluri, *Bone morphogenic protein-7 induces mesenchymal to epithelial transition in adult renal fibroblasts and facilitates regeneration of injured kidney*. J Biol Chem, 2005. **280**(9): p. 8094-100.
123. Clevers, H. and R. Nusse, *Wnt/β-Catenin Signaling and Disease*. Cell, 2012. **149**(6): p. 1192-1205.
124. Yu, Q.C., E.M. Verheyen, and Y.A. Zeng, *Mammary Development and Breast Cancer: A Wnt Perspective*. Cancers, 2016. **8**(7): p. 65.
125. Howe, L.R. and A.M. Brown, *Wnt signaling and breast cancer*. Cancer Biol Ther, 2004. **3**(1): p. 36-41.
126. Bergstein, I. and A.M.C. Brown, *WNT Genes and Breast Cancer*, in *Breast Cancer: Molecular Genetics, Pathogenesis, and Therapeutics*, A.M. Bowcock, Editor. 1999, Humana Press: Totowa, NJ. p. 181-198.
127. Kirikoshi, H., Sekihara, H., & Katoh, M., *Expression of WNT14 and WNT14B mRNAs in human cancer, up-regulation of WNT14 by IFNγ and up-regulation of WNT14B by β-estradiol*. International Journal of Oncology, 2001. **19**: p. 1221-1225.
128. Pohl, S.-G., et al., *Wnt signaling in triple-negative breast cancer*. Oncogenesis, 2017. **6**: p. e310.
129. Xu, J., et al., *beta-Catenin is required for the tumorigenic behavior of triple-negative breast cancer cells*. PLoS One, 2015. **10**(2): p. e0117097.
130. Mohammed, M.K., et al., *Wnt/beta-catenin signaling plays an ever-expanding role in stem cell self-renewal, tumorigenesis and cancer chemoresistance*. Genes Dis, 2016. **3**(1): p. 11-40.
131. Shubbar, E., et al., *Elevated cyclin B2 expression in invasive breast carcinoma is associated with unfavorable clinical outcome*. BMC Cancer, 2013. **13**: p. 1.
132. Khramtsov, A.I., et al., *Wnt/beta-catenin pathway activation is enriched in basal-like breast cancers and predicts poor outcome*. Am J Pathol, 2010. **176**(6): p. 2911-20.

133. Lin, S.-Y., et al.,  *$\beta$ -Catenin, a novel prognostic marker for breast cancer: Its roles in cyclin D1 expression and cancer progression*. Proceedings of the National Academy of Sciences, 2000. **97**(8): p. 4262-4266.
134. Ryo, A., et al., *Pin1 regulates turnover and subcellular localization of [beta]-catenin by inhibiting its interaction with APC*. Nat Cell Biol, 2001. **3**(9): p. 793-801.
135. Jönsson, M., et al., *Involvement of adenomatous polyposis coli (APC)/ $\beta$ -catenin signalling in human breast cancer*. European Journal of Cancer. **36**(2): p. 242-248.
136. Borg, J.-P., et al., *Deregulation of the non-canonical pathway in triple-negative breast cancer*. The FASEB Journal, 2013. **27**(1 Supplement): p. 610.1.
137. Rangel, M.C., et al., *Developmental signaling pathways regulating mammary stem cells and contributing to the etiology of triple-negative breast cancer*. Breast Cancer Res Treat, 2016. **156**(2): p. 211-26.
138. Kaidanovich-Beilin, O. and J. Woodgett, *GSK-3: Functional Insights from Cell Biology and Animal Models*. Frontiers in Molecular Neuroscience, 2011. **4**(40).
139. Pandey, M.K. and T.R. DeGrado, *Glycogen Synthase Kinase-3 (GSK3) - Targeted Therapy and Imaging*. Theranostics, 2016. **6**(4): p. 571-593.
140. Embi, N., D.B. Rylatt, and P. Cohen, *Glycogen synthase kinase-3 from rabbit skeletal muscle. Separation from cyclic-AMP-dependent protein kinase and phosphorylase kinase*. Eur J Biochem, 1980. **107**(2): p. 519-27.
141. Ali, A., K.P. Hoeflich, and J.R. Woodgett, *Glycogen synthase kinase-3: properties, functions, and regulation*. Chem Rev, 2001. **101**(8): p. 2527-40.
142. Rylatt, D.B., et al., *Glycogen synthase from rabbit skeletal muscle. Amino acid sequence at the sites phosphorylated by glycogen synthase kinase-3, and extension of the N-terminal sequence containing the site phosphorylated by phosphorylase kinase*. Eur J Biochem, 1980. **107**(2): p. 529-37.
143. Woodgett, J.R., *Molecular cloning and expression of glycogen synthase kinase-3/factor A*. Embo j, 1990. **9**(8): p. 2431-8.
144. Hanks, S.K. and T. Hunter, *Protein kinases 6. The eukaryotic protein kinase superfamily: kinase (catalytic) domain structure and classification*. Faseb j, 1995. **9**(8): p. 576-96.
145. Mukai, F., et al., *Alternative splicing isoform of tau protein kinase I/glycogen synthase kinase 3 $\beta$* . J Neurochem, 2002. **81**(5): p. 1073-83.
146. Pandey, M.K. and T.R. DeGrado, *Glycogen Synthase Kinase-3 (GSK-3)-Targeted Therapy and Imaging*. Theranostics, 2016. **6**(4): p. 571-593.
147. ter Haar, E., et al., *Structure of GSK3[ $\beta$ ] reveals a primed phosphorylation mechanism*. Nat Struct Mol Biol, 2001. **8**(7): p. 593-596.
148. Beurel, E., S.F. Grieco, and R.S. Jope, *Glycogen synthase kinase-3 (GSK3): regulation, actions, and diseases*. Pharmacology & therapeutics, 2015. **0**: p. 114-131.
149. Sutherland, C., I.A. Leighton, and P. Cohen, *Inactivation of glycogen synthase kinase-3  $\beta$  by phosphorylation: new kinase connections in insulin and growth-factor signalling*. Biochem J, 1993. **296** ( Pt 1): p. 15-9.
150. Sutherland, C. and P. Cohen, *The alpha-isoform of glycogen synthase kinase-3 from rabbit skeletal muscle is inactivated by p70 S6 kinase or MAP kinase-activated protein kinase-1 in vitro*. FEBS Lett, 1994. **338**(1): p. 37-42.
151. Iitaka, C., et al., *A Role for Glycogen Synthase Kinase-3 $\beta$  in the Mammalian Circadian Clock*. Journal of Biological Chemistry, 2005. **280**(33): p. 29397-29402.
152. Bijur, G.N. and R.S. Jope, *Glycogen synthase kinase-3  $\beta$  is highly activated in nuclei and mitochondria*. Neuroreport, 2003. **14**(18): p. 2415-9.

153. King, T.D., G.N. Bijur, and R.S. Jope, *Caspase-3 activation induced by inhibition of mitochondrial complex I is facilitated by glycogen synthase kinase-3 $\beta$  and attenuated by lithium*. Brain Res, 2001. **919**(1): p. 106-14.
154. Grimes, C.A. and R.S. Jope, *The multifaceted roles of glycogen synthase kinase 3 $\beta$  in cellular signaling*. Prog Neurobiol, 2001. **65**(4): p. 391-426.
155. Jope, R.S. and G.V. Johnson, *The glamour and gloom of glycogen synthase kinase-3*. Trends Biochem Sci, 2004. **29**(2): p. 95-102.
156. Sutherland, C., *What Are the bona fide GSK3 Substrates?* International Journal of Alzheimer's Disease, 2011. **2011**: p. 505607.
157. Franca-Koh, J., et al., *The regulation of glycogen synthase kinase-3 nuclear export by Frat/GBP*. J Biol Chem, 2002. **277**(46): p. 43844-8.
158. Happel, N., et al., *M phase-specific phosphorylation of histone H1.5 at threonine 10 by GSK-3*. J Mol Biol, 2009. **386**(2): p. 339-50.
159. Gupta, C., J. Kaur, and K. Tikoo, *Regulation of MDA-MB-231 cell proliferation by GSK-3 $\beta$  involves epigenetic modifications under high glucose conditions*. Exp Cell Res, 2014. **324**(1): p. 75-83.
160. Bardai, F.H. and S.R. D'Mello, *Selective toxicity by HDAC3 in neurons: regulation by Akt and GSK3 $\beta$* . J Neurosci, 2011. **31**(5): p. 1746-51.
161. Cernotta, N., et al., *Ubiquitin-dependent degradation of HDAC4, a new regulator of random cell motility*. Mol Biol Cell, 2011. **22**(2): p. 278-89.
162. Chen, S., et al., *HDAC6 regulates mitochondrial transport in hippocampal neurons*. PLoS One, 2010. **5**(5): p. e10848.
163. De Sarno, P., X. Li, and R.S. Jope, *Regulation of Akt and glycogen synthase kinase-3  $\beta$  phosphorylation by sodium valproate and lithium*. Neuropharmacology, 2002. **43**(7): p. 1158-64.
164. Meares, G.P. and R.S. Jope, *Resolution of the nuclear localization mechanism of glycogen synthase kinase-3: functional effects in apoptosis*. J Biol Chem, 2007. **282**(23): p. 16989-7001.
165. Taelman, V.F., et al., *Wnt signaling requires sequestration of glycogen synthase kinase 3 inside multivesicular endosomes*. Cell, 2010. **143**(7): p. 1136-48.
166. Takahashi-Yanaga, F. and T. Sasaguri, *GSK-3 $\beta$  regulates cyclin D1 expression: A new target for chemotherapy*. Cellular Signalling, 2008. **20**(4): p. 581-589.
167. Malumbres, M. and M. Barbacid, *To cycle or not to cycle: a critical decision in cancer*. Nat Rev Cancer, 2001. **1**(3): p. 222-31.
168. Matsuoka, M., et al., *Activation of cyclin-dependent kinase 4 (cdk4) by mouse MO15-associated kinase*. Molecular and Cellular Biology, 1994. **14**(11): p. 7265-7275.
169. *GSK-3 $\beta$ : A Bifunctional Role in Cell Death Pathways*. International Journal of Cell Biology, 2012. **2012**: p. 11.
170. Watcharasil, P., et al., *Glycogen synthase kinase-3 $\beta$  (GSK3 $\beta$ ) binds to and promotes the actions of p53*. J Biol Chem, 2003. **278**(49): p. 48872-9.
171. Turenne, G.A. and B.D. Price, *Glycogen synthase kinase3  $\beta$  phosphorylates serine 33 of p53 and activates p53's transcriptional activity*. BMC Cell Biology, 2001. **2**(1): p. 12.
172. Martins, D.F., et al., *The Antinociceptive Effects of AR-A014418, a Selective Inhibitor of Glycogen Synthase Kinase-3  $\beta$ , in Mice*. The Journal of Pain, 2011. **12**(3): p. 315-322.
173. Watcharasil, P., et al., *Direct, activating interaction between glycogen synthase kinase-3 $\beta$  and p53 after DNA damage*. Proceedings of the National Academy of Sciences, 2002. **99**(12): p. 7951-7955.
174. Youle, R.J. and A. Strasser, *The BCL-2 protein family: opposing activities that mediate cell death*. Nat Rev Mol Cell Biol, 2008. **9**(1): p. 47-59.
175. Lessene, G., P.E. Czabotar, and P.M. Colman, *BCL-2 family antagonists for cancer therapy*. Nat Rev Drug Discov, 2008. **7**(12): p. 989-1000.

176. Sun, T., M. Rodriguez, and L. Kim, *Glycogen synthase kinase 3 in the world of cell migration*. Development, Growth & Differentiation, 2009. **51**(9): p. 735-742.
177. Kurokawa, K., et al., *Mechanism and role of localized activation of Rho-family GTPases in growth factor-stimulated fibroblasts and neuronal cells*. Biochem Soc Trans, 2005. **33**(Pt 4): p. 631-4.
178. Pertz, O., et al., *Spatiotemporal dynamics of RhoA activity in migrating cells*. Nature, 2006. **440**(7087): p. 1069-72.
179. Settleman, J., et al., *Association between GTPase activators for Rho and Ras families*. Nature, 1992. **359**(6391): p. 153-4.
180. Brouns, M.R., et al., *The adhesion signaling molecule p190 RhoGAP is required for morphogenetic processes in neural development*. Development, 2000. **127**(22): p. 4891-903.
181. Brouns, M.R., S.F. Matheson, and J. Settleman, *p190 RhoGAP is the principal Src substrate in brain and regulates axon outgrowth, guidance and fasciculation*. Nat Cell Biol, 2001. **3**(4): p. 361-7.
182. Cicchetti, P., et al., *3BP-1, an SH3 domain binding protein, has GAP activity for Rac and inhibits growth factor-induced membrane ruffling in fibroblasts*. Embo j, 1995. **14**(13): p. 3127-35.
183. Yoon, H.Y., et al., *ARAP2 effects on the actin cytoskeleton are dependent on Arf6-specific GTPase-activating-protein activity and binding to RhoA-GTP*. J Cell Sci, 2006. **119**(Pt 22): p. 4650-66.
184. Wittmann, T. and C.M. Waterman-Storer, *Cell motility: can Rho GTPases and microtubules point the way?* J Cell Sci, 2001. **114**(Pt 21): p. 3795-803.
185. Morfini, G., et al., *Glycogen synthase kinase 3 phosphorylates kinesin light chains and negatively regulates kinesin-based motility*. Embo j, 2002. **21**(3): p. 281-93.
186. Jimbo, T., et al., *Identification of a link between the tumour suppressor APC and the kinesin superfamily*. Nat Cell Biol, 2002. **4**(4): p. 323-7.
187. Broussard, J.A., D.J. Webb, and I. Kaverina, *Asymmetric focal adhesion disassembly in motile cells*. Curr Opin Cell Biol, 2008. **20**(1): p. 85-90.
188. Deakin, N.O. and C.E. Turner, *Paxillin comes of age*. J Cell Sci, 2008. **121**(Pt 15): p. 2435-44.
189. Bianchi, M., et al., *Regulation of FAK Ser-722 phosphorylation and kinase activity by GSK3 and PP1 during cell spreading and migration*. Biochem J, 2005. **391**(Pt 2): p. 359-70.
190. Brown, A.M., *Wnt signaling in breast cancer: have we come full circle?* Breast Cancer Research, 2001. **3**(6): p. 351.
191. McCubrey, J.A., et al., *GSK-3 as potential target for therapeutic intervention in cancer*. Oncotarget, 2014. **5**(10): p. 2881-2911.
192. Farago, M., et al., *Kinase-inactive glycogen synthase kinase 3beta promotes Wnt signaling and mammary tumorigenesis*. Cancer Res, 2005. **65**(13): p. 5792-801.
193. Sokolosky, M., et al., *Inhibition of GSK-3beta activity can result in drug and hormonal resistance and alter sensitivity to targeted therapy in MCF-7 breast cancer cells*. Cell Cycle, 2014. **13**(5): p. 820-33.
194. Bachelder, R.E., et al., *Glycogen synthase kinase-3 is an endogenous inhibitor of Snail transcription: implications for the epithelial-mesenchymal transition*. The Journal of Cell Biology, 2005. **168**(1): p. 29-33.
195. Zhou, B.P., et al., *Dual regulation of Snail by GSK-3beta-mediated phosphorylation in control of epithelial-mesenchymal transition*. Nat Cell Biol, 2004. **6**(10): p. 931-40.
196. Kao, S.H., et al., *GSK3beta controls epithelial-mesenchymal transition and tumor metastasis by CHIP-mediated degradation of Slug*. Oncogene, 2014. **33**(24): p. 3172-82.
197. Quintayo, M.A., et al., *GSK3β and cyclin D1 expression predicts outcome in early breast cancer patients*. Breast Cancer Research and Treatment, 2012. **136**(1): p. 161-168.
198. Ugolkov, A., et al., *GSK-3 inhibition overcomes chemoresistance in human breast cancer*. Cancer Letters, 2016. **380**(2): p. 384-392.



199. Shin, S., et al., *Glycogen synthase kinase-3[beta] positively regulates protein synthesis and cell proliferation through the regulation of translation initiation factor 4E-binding protein 1*. *Oncogene*, 2014. **33**(13): p. 1690-1699.
200. Gray, J.E., et al., *A first-in-human phase I dose-escalation, pharmacokinetic, and pharmacodynamic evaluation of intravenous LY2090314, a glycogen synthase kinase 3 inhibitor, administered in combination with pemetrexed and carboplatin*. *Invest New Drugs*, 2015. **33**(6): p. 1187-96.
201. Masuda, H., et al., *Differential Response to Neoadjuvant Chemotherapy Among 7 Triple-Negative Breast Cancer Molecular Subtypes*. *Clinical Cancer Research*, 2013. **19**(19): p. 5533-5540.
202. Ding, S., et al., *Synthetic small molecules that control stem cell fate*. *Proceedings of the National Academy of Sciences of the United States of America*, 2003. **100**(13): p. 7632-7637.
203. Ma, X.J., et al., *A two-gene expression ratio predicts clinical outcome in breast cancer patients treated with tamoxifen*. *Cancer Cell*, 2004. **5**(6): p. 607-16.
204. Richardson, A.L., et al., *X chromosomal abnormalities in basal-like human breast cancer*. *Cancer Cell*, 2006. **9**(2): p. 121-132.
205. The Cancer Genome Atlas, N., *Comprehensive molecular portraits of human breast tumors*. *Nature*, 2012. **490**(7418): p. 61-70.
206. Györfy, B., et al., *An online survival analysis tool to rapidly assess the effect of 22,277 genes on breast cancer prognosis using microarray data of 1,809 patients*. *Breast Cancer Res Treat*, 2010. **123**(3): p. 725-31.
207. J Werden, S., et al., *Phosphorylation of serine 367 of FOXC2 by p38 regulates ZEB1 and breast cancer metastasis, without impacting primary tumor growth*. Vol. 35. 2016.
208. Sarkar, T.R., et al., *GD3 Synthase regulates epithelial-mesenchymal transition and metastasis in breast cancer*. *Oncogene*, 2015. **34**(23): p. 2958-2967.
209. Taube, J.H., et al., *Epigenetic silencing of microRNA-203 is required for EMT and cancer stem cell properties*. *Sci Rep*, 2013. **3**: p. 2687.
210. Stewart, S.A., et al., *Lentivirus-delivered stable gene silencing by RNAi in primary cells*. *Rna*, 2003. **9**(4): p. 493-501.
211. Pietila, M., et al., *FOXC2 regulates the G2/M transition of stem cell-rich breast cancer cells and sensitizes them to PLK1 inhibition*. *Sci Rep*, 2016. **6**: p. 23070.
212. Werden, S.J., et al., *Phosphorylation of serine 367 of FOXC2 by p38 regulates ZEB1 and breast cancer metastasis, without impacting primary tumor growth*. *Oncogene*, 2016. **35**(46): p. 5977-5988.
213. Paranjape, A.N., et al., *Inhibition of FOXC2 restores epithelial phenotype and drug sensitivity in prostate cancer cells with stem-cell properties*. *Oncogene*, 2016. **35**(46): p. 5963-5976.
214. Dhanasekaran, S.M., et al., *Delineation of prognostic biomarkers in prostate cancer*. *Nature*, 2001. **412**(6849): p. 822-826.
215. ; Available from: <http://www.selleckchem.com/products/TWS119.html>.
216. Györfy, B., et al., *An online survival analysis tool to rapidly assess the effect of 22,277 genes on breast cancer prognosis using microarray data of 1,809 patients*. *Breast Cancer Research and Treatment*, 2010. **123**(3): p. 725-731.
217. Rich, J.T., et al., *A PRACTICAL GUIDE TO UNDERSTANDING KAPLAN-MEIER CURVES*. *Otolaryngology--head and neck surgery : official journal of American Academy of Otolaryngology-Head and Neck Surgery*, 2010. **143**(3): p. 331-336.
218. M. J. Toneff, A.S., A. Tinnirello, P. Den Hollander, S. Habib, S. Li, M. J. Ellis, L. Xin, S. A. Mani and J. M. Rosen, *The Z-cad dual fluorescent sensor detects dynamic changes between the epithelial and mesenchymal cellular states*. *BMC Biology*, 2016. **14**.

219. Lai, C.-J., et al., *CUDC-101, a Multitargeted Inhibitor of Histone Deacetylase, Epidermal Growth Factor Receptor, and Human Epidermal Growth Factor Receptor 2, Exerts Potent Anticancer Activity*. Cancer Research, 2010. **70**(9): p. 3647-3656.
220. Schech, A., et al., *Histone Deacetylase Inhibitor Entinostat Inhibits Tumor-Initiating Cells in Triple-Negative Breast Cancer Cells*. Mol Cancer Ther, 2015. **14**(8): p. 1848-57.
221. Tate, C.R., et al., *Targeting triple-negative breast cancer cells with the histone deacetylase inhibitor panobinostat*. Breast Cancer Research, 2012. **14**(3): p. R79.
222. DAMASKOS, C., et al., *Histone Deacetylase Inhibitors: An Attractive Therapeutic Strategy Against Breast Cancer*. Anticancer Research, 2017. **37**(1): p. 35-46.
223. Min, A., et al., *Histone deacetylase inhibitor, suberoylanilide hydroxamic acid (SAHA), enhances anti-tumor effects of the poly (ADP-ribose) polymerase (PARP) inhibitor olaparib in triple-negative breast cancer cells*. Breast Cancer Research, 2015. **17**(1): p. 33.
224. Capasso, A., et al., *HDAC and PD-1 inhibition in humanized triple-negative breast cancer xenografts*. Journal of Clinical Oncology, 2017. **35**(15\_suppl): p. e14604-e14604.
225. Meijer, L., et al., *GSK-3-Selective Inhibitors Derived from Tyrian Purple Indirubins*. Chemistry & Biology, 2003. **10**(12): p. 1255-1266.
226. Ribas, J., et al., *7-Bromoindirubin-3[prime]-oxime induces caspase-independent cell death*. Oncogene, 2006. **25**(47): p. 6304-6318.
227. Jope, R.S., C.J. Yuskaitis, and E. Beurel, *Glycogen Synthase Kinase-3 (GSK3): Inflammation, Diseases, and Therapeutics*. Neurochemical research, 2007. **32**(4-5): p. 577-595.
228. De Sarno, P., X. Li, and R.S. Jope, *Regulation of Akt and glycogen synthase kinase-3 $\beta$  phosphorylation by sodium valproate and lithium*. Neuropharmacology, 2002. **43**(7): p. 1158-1164.
229. Li, X., et al., *Lithium Regulates Glycogen Synthase Kinase-3 $\beta$  in Human Peripheral Blood Mononuclear Cells: Implication in the Treatment of Bipolar Disorder*. Biological Psychiatry. **61**(2): p. 216-222.
230. Zhang, F., et al., *Inhibitory Phosphorylation of Glycogen Synthase Kinase-3 (GSK-3) in Response to Lithium: EVIDENCE FOR AUTOREGULATION OF GSK-3*. Journal of Biological Chemistry, 2003. **278**(35): p. 33067-33077.
231. Chalecka-Franaszek, E. and D.-M. Chuang, *Lithium activates the serine/threonine kinase Akt-1 and suppresses glutamate-induced inhibition of Akt-1 activity in neurons*. Proceedings of the National Academy of Sciences, 1999. **96**(15): p. 8745-8750.
232. Cohen, P. and M. Goedert, *GSK3 inhibitors: development and therapeutic potential*. Nat Rev Drug Discov, 2004. **3**(6): p. 479-487.
233. Huang, R.-Y., et al., *Use of lithium and cancer risk in patients with bipolar disorder: population-based cohort study*. The British Journal of Psychiatry, 2016.
234. LSC, M., *Lithium Not Associated With Increased Cancer Risk in Bipolar Disorder*, in *Lithium treatment and cancer incidence in bipolar disorder: a large nationwide Swedish register study*, L. Stiles, Editor. 2017: PsychiatryAdvisor.
235. Yoeli-Lerner, M., et al., *THE AKT/PKB AND GSK-3 $\beta$  SIGNALING PATHWAY REGULATES CELL MIGRATION THROUGH THE NFAT1 TRANSCRIPTION FACTOR*. Molecular cancer research : MCR, 2009. **7**(3): p. 425-432.
236. Sun, T., M. Rodriguez, and L. Kim, *Glycogen synthase kinase 3 in the world of cell migration*. Dev Growth Differ, 2009. **51**(9): p. 735-42.
237. Heppner, G.H., et al., *Heterogeneity in drug sensitivity among tumor cell subpopulations of a single mammary tumor*. Cancer Res, 1978. **38**(11 Pt 1): p. 3758-63.
238. Heppner, G.H., F.R. Miller, and P.M. Shekhar, *Nontransgenic models of breast cancer*. Breast Cancer Res, 2000. **2**(5): p. 331-4.

239. Al-Hajj, M., et al., *Prospective identification of tumorigenic breast cancer cells*. Proceedings of the National Academy of Sciences, 2003. **100**(7): p. 3983-3988.
240. Ponti, D., et al., *Isolation and in vitro propagation of tumorigenic breast cancer cells with stem/progenitor cell properties*. Cancer Res, 2005. **65**(13): p. 5506-11.
241. Soule, H.D., et al., *Isolation and characterization of a spontaneously immortalized human breast epithelial cell line, MCF-10*. Cancer Res, 1990. **50**(18): p. 6075-86.
242. Sidi, Y., et al., *Growth inhibition and induction of phenotypic alterations in MCF-7 breast cancer cells by an IMP dehydrogenase inhibitor*. Br J Cancer, 1988. **58**(1): p. 61-3.
243. Forozan, F., et al., *Molecular cytogenetic analysis of 11 new breast cancer cell lines*. Br J Cancer, 1999. **81**(8): p. 1328-1334.
244. Gattinoni, L., et al., *Wnt signaling arrests effector T cell differentiation and generates CD8(+) memory stem cells*. Nature medicine, 2009. **15**(7): p. 808-813.
245. Sarkar, T.R., et al., *GD3 synthase regulates epithelial-mesenchymal transition and metastasis in breast cancer*. Oncogene, 2014. **0**.
246. Demarchi, F., et al., *Glycogen synthase kinase-3 beta regulates NF-kappa B1/p105 stability*. J Biol Chem, 2003. **278**(41): p. 39583-90.
247. Beurel, E., et al., *Glycogen synthase kinase-3 inhibitors augment TRAIL-induced apoptotic death in human hepatoma cells*. Biochemical Pharmacology, 2009. **77**(1): p. 54-65.
248. Armanious, H., et al., *Clinical and biological significance of GSK-3beta inactivation in breast cancer-an immunohistochemical study*. Hum Pathol, 2010. **41**(12): p. 1657-63.
249. Huang, R.-Y., et al., *Use of lithium and cancer risk in patients with bipolar disorder: population-based cohort study*. The British Journal of Psychiatry, 2016. **209**(5): p. 393.
250. Atkinson, J.M., et al., *Activating the Wnt/ $\beta$ -Catenin Pathway for the Treatment of Melanoma – Application of LY2090314, a Novel Selective Inhibitor of Glycogen Synthase Kinase-3*. PLOS ONE, 2015. **10**(4): p. e0125028.

## **Vita**

Geraldine Vidhya Raja was born in Tamil Nadu, India on June 6, 1986. She received her Bachelor's degree in Biotechnology from D.Y.Patil Institute of Biotechnology and Bioinformatics, India in 2008. She pursued her Master's degree in Biotechnology at the State University of New York at Buffalo (University at Buffalo). As a part of her Master's thesis, she studied the importance of sialylation of TF-antigen for tumor progression in Dr.Kate Rittenhouse-Olson's lab and graduated in May 2010. She gained admission to The University of Texas Health Science Center at Houston Graduate School for Biomedical Sciences in January 2011 for her doctoral training and completed her doctoral dissertation under the guidance of Dr.Sendurai Mani at MD Anderson Cancer Center, Houston, Texas, to earn a doctorate degree in Cancer Biology in August 2017.